

# **Seismic Vulnerability of Bridges Using Simplified Models**

C. Gómez Soberón  
S. Oller  
A. H. Barbat

**Monografías de Ingeniería Sísmica**

Editor A. H. Barbat

**Seismic Vulnerability of  
Bridges Using Simplified  
Models**

C. Gómez Soberón  
S. Oller  
A. H. Barbat

CENTRO INTERNACIONAL DE MÉTODOS NUMÉRICOS EN INGENIERÍA  
Edificio C1, Campus Norte UPC  
Gran Capitán s/n  
08034 Barcelona, Spain

**MONOGRAFÍAS DE INGENIERÍA SÍSMICA**  
Editor A. H. Barbat

ISSN: 1134-3249

**SEISMIC VULNERABILITY OF BRIDGES USING SIMPLIFIED MODELS**  
Monografía CIMNE IS47  
© Los autores

ISBN: 84-89925-96-8  
Depósito legal: B-11220-2002

## **Acknowledgement**

This research was partially supported by E.C. Environmental Programme RTD Project ENV4-CT.-97-0574 "Advanced Methods for Assessing the Seismic Vulnerability of Bridges" and by Formation of Researchers Programme (FI) of the Generalitat of Catalonia. This support is gratefully acknowledged. The authors wish to thank ARSENAL Research (Austria), Joint Research Center (JRC), Ispra (Italy), SETRA (France), Universidade do Porto (Portugal), International Center of Theoretical Physics (Italy), and ISMES S. P. A. (Italy) for their collaboration.



## Notation

$\alpha$	: Mean energy difference of two seismic records
$\alpha_{DI}, \beta_{DI}$	: Parameters of adjust of a Miranda damage index
$\alpha_{skew}, \alpha_i, \alpha_f$	: Total, beginning and final skew angle of a bridge
$\alpha_{sl}$	: Significance level
$\beta$	: Beta parameter of the Newmark's algorithm
$\beta_I$	: Weight factors
$\gamma$	: Gamma parameter of the Newmark's algorithm
$\gamma_c, \gamma_v$	: Density in pier and girder elements
$\gamma_G, \gamma_{G\ max}$	: Global and maximum drift
$\delta_{r,max}$	: Maximum top displacement of a structure
$\delta_{r,y}$	: Yield top displacement of a structure
$\delta(\cdot)$	: Dirac delta function
$\Delta \mathbf{v}$	: Incremental maximum displacement vector of a section
$\Delta \mathbf{F}$	: Out of balance load vector of a section
$\Delta t$	: Time increment
$\Delta M(\cdot)$	: Residual moment of a pier
$\varepsilon$	: Strain tensor in a point
$\varepsilon^{cc}$	: Undamaged compression strain of the unconfined concrete
$\theta_i$	: Weight factor depending of the state of stress in a point
$\theta_{max}, \theta_u$	: Maximum and ultimate curvature of an element
$\lambda$	: Empirical parameter of a Park et al. damage index
$\mu$	: Mean of a probabilistic variable
$\mu_G$	: Global ductility of an element
$\xi(t)$	: Amplitude of the modulating function of a seismic signal
$\xi^*(t)$	: Amplitude of the modulating function of a seismic modified signal
$\sigma$	: Standard deviation of a statistical variable
$\sigma(x_1, \dots, x_N)$	: Standard deviation of a statistical sample
$(\sigma_{low}, \sigma_{up})_{95\%}$	: 95% confidence interval for the standard deviation of a statistical sample
$\sigma_0^1, \sigma_0^3$	: Maximum and minimum principal stresses in a point
$\sigma$	: Stress tensor in a point
$\sigma_0$	: Elastic stress tensor in a point
$\sigma_0^c$	: Undamaged compression stress of the unconfined concrete
$\sigma_i$	: Inelastic stress tensor in a point
$\tau$	: Equivalent stress tensor in a point
$v_\theta, v_p$	: Maximum displacements of pier $i$ due to rotation of its base and due to external actions
$\mathbf{v}(t), \dot{\mathbf{v}}(t), \ddot{\mathbf{v}}(t)$	: Maximum displacement, velocity and acceleration vectors of the bridge piers
$\varphi$	: Phase angle

---

$\varphi_i^{i-1} \varphi_i^{i+1}$	: Rotation of girders left and right to pier $i$
$\chi^2$	: Statistic of the chi-square goodness of fit test
$\chi(\cdot)$	: Curvature function of a pier
$\omega_i$	: Frequency of the $I$ mode shape
$A$	: Bearings height
$a_i$	: Ground acceleration associated to the degree of freedom $i$
$a_{max}, PGA$	: Peak ground acceleration
$A$	: Parameter of the isotropic damage model
$ADT$	: Average daily traffic of a bridge
$A_c, A_b, A_a$	: Total cross section area, cross section area of concrete and cross-section area of steel in piers
$A_{IEL}$	: Percentage of the Value-Added-Lost per month
$A_{LF}, B_{LF}, C_{LF}$	: Classification of loss of function of Chinese bridges
$A_c^d(\cdot)$	: Damaged area of piers
$A_c^{d(j)}$	: Damaged area of a $j$ subsection of piers
$A_v, A_p$	: Cross section area of girders and bearings elements
$b$	: Dimension of the cross section of piers at base
$BVR$	: Base Vulnerability Rating of a bridge
$B_{IEL}$	: National Economic Value Added
$c_i$	: Correlation coefficients
$C$	: Capacity of a structure
$C_c$	: Convergence criterion
$C_{IEL}$	: Percentage of population affected by earthquake hazard
$COV$	: Coefficient of variation of a statistical variable
$CVR$	: Vulnerability piers rating
$C/D$	: Capacity demand ratio
$\mathbf{C}$	: Damping matrix of a structural system
$d, D$	: Damage or degradation in a point
$DL$	: Detour length
$DMG$	: Central damage factor of a damage state
$DPM$	: Damage probability matrix
$DS$	: Damage state
$D_b, DP_i$	: Pier damage indices
$D_{IEL}$	: Monthly Gross National Product
$D_{K-S}$	: Statistic of the Kolmogorov-Smirnov goodness of fit test
$D_m$	: Global mean damage index of a bridge
$D_p$	: Global functional damage index of a bridge
$D_a$	: Global mean damage index of DiPasquale y Cakmak
$\mathbf{D}$	: Amplitude vector
$\mathbf{D}_0$	: Elastic constitutive tensor in a point
$ER$	: Correction factor of an importance index of a bridge
$E_i$	: Expected frequency of a statistical sample
$E_c^0$	: Initial Young's modulus of piers
$E_c^d$	: Young's modulus for the damaged piers
$E_c, E_b, E_a$	: Young's modulus of reinforced concrete, concrete and reinforced steel materials
$E(y/x)$	: Conditional mean of two statistical variables
$f$	: Cyclic frequencies of the system
$F'_c, f_t$	: Uniaxial compression and tensile strength of concrete
$f(\cdot)$	: Damage function
$f_X(x)$	: Marginal probability distribution

---

$\mathbf{f}_e$	: Effective forces vector
$F$	: Force acting in a structure
$F_e$	: Top external force of a pier
$F_i$	: Inertial force in pier $i$
$F_i^{i-1} F_i^{i+1}$	: Elastic forces in pier $i$ by the rotation of adjoins girders
$F_{i-1}^i F_{i+1}^i$	: Elastic forces in piers $i-1$ and $i+1$ by the rotation of adjoin girders
$F(\tau, r)$	: Damage criterion in a point
$F(x_i)$	: Theoretical accumulated distribution function
$Fn(x_i)$	: Empirical accumulated distribution function
$g$	: Gravitational acceleration
$g_t, g_c$	: Specific dissipated energies in uniaxial tension and compression
$G(x)$	: Logistic transformation of $k$ independent variables
$G$	: Shear modulus of bearings elements
$G_f$	: Fracture energy in a point
$G(\cdot)$	: Monotonic scalar function
$GD(t)$	: Gradient of deterioration of an element
$h$	: Height of the cross section of piers
$h_a$	: Distance in plan between bearings
$H$	: Height of piers
$H_0$	: Null hypothesis of a statistical goodness of fit test
$H_a$	: Alternative hypothesis of a statistical goodness of fit test
$I$	: Transversal inertial moment of piers
$IEL$	: Indirect Economic Lost index
$II$	: Importance index of a bridge
$I_e$	: Intensity of the seismic action
$I^d(\cdot)$	: Inertial of the damaged cross section of piers
$I_T^d(\cdot)$	: Global inertia of damaged piers
$k$	: Bending stiffness of a pier
$k_h, k_a$	: Proportion of concrete and steel cross section area in piers
$k_1, k_2$	: Parameters of the constitutive concrete law
$K-S$	: Statistical Kolmogorov-Smirnov goodness of fit test
$K^S$	: Equivalent rotational stiffness at base in piers
$\mathbf{K}$	: Stiffness matrix of a structural system
$\mathbf{K}_e$	: Equivalent stiffness matrix
$l$	: Number of classes of a statistical sample
$l^*$	: Characteristic length of an element
$l_c^{(j)}$	: Distance between global neutral axis and $j$ subsection neutral axis
$L$	: Girder length or bridge length
$L_f$	: Likelihood function
$L_{max}$	: Maximum bridge length in a database
$L_p$	: Pier length
$m_i$	: Mass associated to the degree of freedom $i$
$M$	: Order of a polynomial fitting function for generated artificial signals
$MDOF$	: Multiple degree of freedom system
$MMI$	: Modified Mercalli Intensity
$M_s, M_{sy}$	: Section and yield moment of an element
$M(\cdot)$	: Moment equation for each pier
$M_e(\cdot)$	: External moment equation of a pier



---

$M_{int}(\cdot)$	: Internal moment equation of a pier
$\mathbf{M}$	: Mass matrix of a structural system
$n$	: Compressive strength – tensile strength ratio
$n_c$	: Number of critical sections in a structure
$n_p$	: Number of piers of the bridge
$n_s$	: Number of structures of analysis
$nm$	: Number of materials in a structure
$n(i)$	: Number of sample points less than $x_i$
$NT$	: Factor representing critically of traffic congestion
$N$	: Number of elements in a statistical sample
$N_1, N_2, N_3$	: Numbers of affected regions, economic sectors and moths used to estimate the indirect economic loss
$N_d$	: Reference support length
$N_{ds}$	: Number of damage state
$N_{joints}$	: Number of joints in a bridge
$N_{span}$	: Number of spans in a bridge
$O_i$	: Observed frequency of class $i$
$P_i$	: Associated name of each pier of the bridge
$P_f, P_{fi}$	: Probability of failure of a structure and of structural elements
$P_{g(h)}$	: Generalised probability of failure of structures with different materials
$P_S$	: Percentage of the main reinforcing steel of piers
$q$	: Distributed mass in pier $i$
$r$	: Damage threshold in a point
$r^*$	: Initial threshold value (material property) in a point
$R$	: Percentage of restoration of a structure
$RC$	: Reinforced concrete
$RT$	: Factor of nature of a bridge route
$RV$	: Bridge length of the longest bridge in a database ratio
$R_c$	: Curvature ration of a bridge
$R_e$	: Resistance of an structure
$R_i$	: Total force in pier $i$ due to girders rotation
$RC_j$	: Residual capacity of a structure
$S$	: Continuous minimum bearing support length
$SDOF$	: Single degree of freedom system
$t$	: Time
$t_1, t_2, t_3, t_4$	: Thickness of the box cross section of bridge piers
$T$	: Fundamental period of the system
$T_o$	: Initial period of each mode shape
$T_f$	: Final period of each mode shape
$T_R$	: Restoration time associated to a central damage factor
$TOL$	: Tolerance
$VI$	: Vulnerability index of a bridge
$Var(x_1, \dots, x_N)$	: Variance of a statistical sample
$\bar{x}$	: Statistical mean of variable $x$
$x_i$	: Element $i$ of variable $x$
$x_{min}, x_{max}$	: Minimum and maximum values of variable $x$
$(x_{low}, x_{up})_{95\%}$	: 95% confidence interval of the mean value
$x_1, x_2, x_3$	: Reference system
$X_1^{CG}, X_2^{CG}$	: Coordinates of the neutral axis of the section of piers
$Y_i$	: Parameters of a vulnerability index of a bridge
$Y_{cur}$	: Curvature angle of a bridge

# Content

ACKNOWLEDGEMENT .....	II
NOTATION .....	I
CONTENT .....	V
<b>CHAPTER 1</b>	
INTRODUCTION .....	I
1.1 - SEISMIC BEHAVIOUR OF BRIDGES DURING THE LAST SEVERE EARTHQUAKES .....	1
1.1.1- Loma Prieta .....	1
1.1.2- Northridge .....	2
1.1.3- Hyogoken-Nanbu (Kobe) .....	2
1.2 - OBJECTIVES .....	3
<b>CHAPTER 2</b>	
SEISMIC VULNERABILITY OF STRUCTURES. THEORETICAL BACKGROUND .....	4
2.1. SOURCES OF DATA .....	4
2.2. EVALUATION METHODS .....	5
2.2.1. According to the employed technique .....	5
2.2.1.1. Direct techniques .....	5
2.2.1.2 Indirect techniques .....	6
2.2.1.3 Conventional techniques .....	7
2.2.1.4 Hybrid techniques .....	7
2.2.2. According to input, method and output .....	7
2.3. DAMAGE PROBABILITY MATRICES AND FRAGILITY CURVES .....	9
<b>CHAPTER 3</b>	
VULNERABILITY INDICES .....	10
3.1           PARAMETERS .....	10
3.2           PROPOSED MODELS .....	16
3.2.1. Procedure of the ATC 6-2 .....	16
3.2.2. Model of Pezeshk et al. ....	20
3.2.3. Seong Kim model .....	21
3.2.4. Maldonado et al. model .....	26

## CHAPTER 4

<b>SEISMIC MODELS OF BRIDGES .....</b>	<b>28</b>
4.1. SINGLE-DEGREE-OF-FREEDOM EQUIVALENT MODEL (SDOF) .....	28
4.2. MODEL OF HRISTOVSKI AND RISTIC.....	29
4.3. SEISMIC CAPACITY ASSESSMENT FOR BRIDGE PIERS .....	30
4.4. QUANTIFICATION OF BEHAVIOUR COEFFICIENTS FOR CURVED RC BRIDGES .....	31
4.4.1. <i>Estimation of the vulnerability function</i> .....	32
4.4.2. <i>Example of application</i> .....	34
4.5. SEISMIC FRAGILITY CURVES OF BRIDGES USING A FINITE ELEMENT MODEL .....	35
4.5.1. <i>Hypothesis of the analysis</i> .....	35
4.5.2. <i>Fragility curves</i> .....	36
4.5.3. <i>- Example</i> .....	38

## CHAPTER 5

<b>MODELS BASED ON EXPERT'S JUDGEMENT .....</b>	<b>40</b>
5.1. DATA INVENTORY .....	40
5.2. DAMAGE PROBABILITY MATRICES (DPM) OF THE ATC-13 .....	40
5.3. LOSS OF FUNCTION AND RESTORATION TIMES .....	41
5.4. FRAGILITY CURVES .....	42
5.5. DIRECT DAMAGE .....	43
5.6. INDIRECT ECONOMIC LOSSES.....	45
5.7. RECENT RESEARCHES ON LOSS ASSESSMENT.....	46

## CHAPTER 6

<b>MODELS BASED ON STATISTICS OF REAL DAMAGE DATA .....</b>	<b>48</b>
6.1. DPM FOR TRANSPORTATION SYSTEMS AFTER TANGSHAN EARTHQUAKE.....	48
6.2. EVALUATION OF BRIDGE DAMAGE DATA FROM THE LOMA PRIETA AND NORTHRIDGE EARTHQUAKES.....	49
6.2.1. <i>Database characteristics</i> .....	50
6.2.2. <i>Classification of bridges. Data sets</i> .....	50
6.2.3. <i>Correlation studies</i> .....	50
6.2.4. <i>Results</i> .....	51
6.2.4.1. <i>Loma Prieta earthquake</i> .....	51
6.2.4.2. <i>Northridge earthquake</i> .....	53
6.3. FRAGILITY CURVES OF BRIDGES BASED ON REPORTED DAMAGES AFTER KOBE EARTHQUAKE .....	55
6.4. HYPOTHESIS TESTING AND CONFIDENCE INTERVALS FOR EMPIRICAL FRAGILITY CURVES FOR BRIDGES.....	56
6.4.1. <i>Empirical fragility curves for bridges affected by the Northridge earthquake</i> .....	56
6.4.2. <i>Hypothesis testing and confidence intervals</i> .....	58

## CHAPTER 7

<b>SIMPLIFIED ELASTIC MODEL.....</b>	<b>60</b>
7.1 SIMPLIFIED ELASTIC FORMULATION OF THE BRIDGE.....	61
7.1.1. <i>Evaluation of transversal stiffness of bridge in a mode i</i> .....	62
7.1.2. <i>Transversal stiffness of a pier for a mode i</i> .....	65
7.1.3. <i>Pier-girder equation of equilibrium</i> .....	67
7.2. APPLICATION OF THE PROPOSED MODEL TO STUDY THE BEHAVIOUR OF THE WARTH BRIDGE .....	70
7.2.1. <i>Description of the structure</i> .....	70

7.2.2 Experimental test.....	71
7.2.3 Simplified finite element model.....	72
7.2.4 Proposed model.....	72
7.2.5 Elastic analysis.....	73

## CHAPTER 8

<b>DAMAGE CHARACTERIZATION USING THE SIMPLIFIED MODEL.....</b>	<b>76</b>
8.1 PROPOSED METHODOLOGY.....	76
8.1.1 Top displacement due to the seismic action.....	77
8.1.2 Maximum external moment.....	77
8.1.3 Damaged state of the structure.....	78
8.2. DAMAGE FUNCTION.....	80
8.3 DETERMINATION OF THE DAMAGED INERTIA.....	81
8.4 PIER DAMAGE AND GLOBAL DAMAGE INDICES.....	82
8.5 COMPARISON BETWEEN THE RESULTS OBTAINED BY MEANS OF THE SIMPLIFIED MODEL AND A FINITE ELEMENTS MODEL.....	83
8.6 EXAMPLE.....	85

## CHAPTER 9

<b>SEISMIC HAZARD OF THE WARTH BRIDGE SITE.....</b>	<b>88</b>
9.1. FIRST SEISMIC SCENARIO.....	88
9.1.1. Determination of the amplitude modulating function, $\xi(t)$ .....	89
9.1.2. Determination of a model for the frequency modulating function,.....	90
9.1.3. Definition of a nonstationary record.....	92
9.1.4. Improvement of the signal.....	92
9.2. SECOND SEISMIC SCENARIO.....	92

## CHAPTER 10

<b>PROBABILISTIC DAMAGE ANALYSIS OF THE WARTH BRIDGE.....</b>	<b>93</b>
10.1. INTRODUCTION.....	93
10.2. FRAGILITY CURVES FOR WARTH BRIDGE.....	94
10.2.1 Input random variables.....	94
10.2.2 Statistical analysis.....	96
10.2.3 Examples.....	98
10.2.3.1 Influence of random structural parameters and deterministic seismic action. First seismic scenario.....	99
10.2.3.2 Influence of random structural parameters and simulated accelerograms. First seismic scenario.....	103
10.2.3.3 Influence of random mechanical parameters and simulated accelerograms. First seismic scenario.....	106
10.2.3.4 Influence of random mechanical parameters and modified simulated accelerograms. First seismic scenario.....	107
10.2.3.5 Influence of random mechanical parameters, simulated accelerograms and the possibility of pier rotation at its base. First seismic scenario.....	107
10.2.3.6 Influence of random structural parameters and deterministic accelerograms. Second seismic scenario.....	115

<b>APPENDIX A. NEWARK'S ALGORITHM.....</b>	<b>119</b>
--	------------

**APPENDIX B. ISOTROPIC DAMAGE MODEL .....121**

**REFERENCES .....124**

# Chapter 1

## Introduction

Currently, numerous existing bridges can suffer damage of different considerations when subjected to seismic actions of certain magnitude. The failure of these systems can be the origin of enormous economical losses (direct and indirect) that can collapse economic activities. Therefore, simplified and reliable evaluation tools of the current state of these structures are necessary for the subsequent decision making on rehabilitation and damage mitigation plans (Chang et al., 1998).

Studies on the seismic vulnerability of bridges are still far from the standard reached for buildings, and more research in this field is necessary. The future researches should include standard procedures, easy to be applied, close to the reality, and thus, more rigorous. In subsequent researches, the attention should be directed especially to damage detection and evaluation techniques.

### 1.1 - Seismic behaviour of bridges during the last severe earthquakes

During the Loma Prieta (1989, M=7.1), Northridge (1994, M=6.7) and Hyogoken-Nanbu (1995, M=6.9) earthquakes, important damages and considerable economic losses occurred in different transportation systems, in spite of the fact that these earthquakes are sometimes designated as "moderate magnitude". These earthquakes also caused the collapse and partial failure of many highway bridges. Some of the reported damage in bridges are summarised below for each one of these events (Moehle 1995, Nakajima 1996, and O'Rourke 1996).

#### 1.1.1- Loma Prieta

The 1989, October 17, earthquake (maximum Modified Mercalli Intensity MMI=IX) caused damage and collapse of bridges in an area of 60 miles away from the epicentre, located in the Santa Cruz Mountains. Sixty-two lives were lost during this earthquake, including forty-one deaths from the collapse of the Cypress Viaduct, and one death from the partial failure of the San Francisco-Oakland Bay Bridge.

The impact of the earthquake includes, also, significant economical losses; for example due to out of service of the Bay Bridge or closed to traffic of five viaducts of the San Francisco Freeway System. The earthquake required an economical spending for more than \$6000 millions, \$1800 million of which were used in the transportation system. The total damage in the state bridges system totalised about \$300 million, most of them for structures on soft soil (Basöz and Kiremidjian 1998, Basöz and Kiremidjian 1995, EQE International 1989, and Miranda 1996).

About 5% of all the bridges that were affected by the earthquake sustained damage, the majority localised in the San Francisco Bay area. Thirteen of the state-owned bridges in the Bay area suffered major damage and were closed to traffic following the earthquake. In the highway system were reported three important bridges collapsed. In addition to these

structures, ten bridges were closed by structural damage; four of them presented damage at the San Francisco Freeway system, principally for shear fracture and/or shear failure of columns and knee joints or connectors.

### *1.1.2- Northridge*

Most of the Los Angeles metropolitan transportation systems survived the earthquake (January 17, 1994, maximum MMI=IX) with minimal or easily repairable damage. However, extensive damage or collapse of several highway bridge structures, designed and built between last half of the sixties and the firsts half of the seventies, caused widespread disruption after the earthquake. The damaged bridges are mostly state bridges in Los Angeles and Ventura Counties, where the highest peak ground acceleration were recorded.

The repair cost for the six collapsed bridges totalised \$132.08 millions. All of them were of concrete box girder type with multiple spans, constructed with pre-1971 design standards. Despite the relative low level of ground shaking, high skew, irregularity in substructure stiffness and inadequate seat width in some cases caused the collapse of these bridges.

The behaviour of bridges during the earthquake indicates that great part of the damage would be avoided with the current design requirements. In summary, portions of the four regional-greater highways were closed during several months due to seismic damages. This system interruption produced traffic collapse and economic losses. Among 1200 bridges of the Northridge zone, seven had severe damages and 230 required moderate or small repairs, according to the report of Housner and Thiel (1995).

A complete information above the reported damages can be consulted in: DesRoches and Fenves (1998), Housner and Thiel (1995), Moehle (1995), Olshansky (1997), Thomas et al. (1998), Priestley et al. (1994), and Gómez et al. 1999a 1999b.

### *1.1.3- Hyogoken-Nanbu (Kobe)*

The Kobe city suffered an important earthquake (intensity 7 of the Japanese scale) the January 17<sup>th</sup>, 1995. The earthquake has been officially named Hyogo-ken Nambu earthquake, but it is also referred to as the Great Hanshin earthquake or simply the Kobe earthquake.

Damage to the transportation system was severe and widespread. This damage occasioned the rupture of the communication between Osaka and Kobe, only re-established in precarious conditions three weeks after the 17<sup>th</sup> of January. The main causes of damage of the transportation system has been attributed to the high vicinity of the structures to the fault line, important vertical components of the ground movements, severe ground settlements, and the inadequate detailing (R/C confinement/shear reinforcement, connection between substructure and superstructure) comparing to the current practice (EQE International 1995, Pinto 1999, and Sánchez-Sánchez 1996). The combination of steel and concrete piers has been used in elevated roads, apparently without specific criteria. In addition, the single pier is the most common solution of these elevated structures. The mixture of materials and the lack of redundancy contributed also to the damage (Pinto 1999).

All of the highways and expressways transportation systems between Nishinomiya and Kobe were severely damaged during the earthquake. The damage statistics reported 320 bridges with damage, 27% from those suffered greater structural damage. The type of damages in bridges consisted of: cracking, spalling and buckling of rebars in RC piers leading to excessive top deformations an causing the deck to fall down. In the epicentral zone, the Hanshin Highway suffered considerable damage in almost 28 kilometres of its Routes 3 and 5. On Route 3, constructed between thirty and twenty years ago, two spans of simply-

supported steel girders fell off their pier caps because of the large displacement on the girders. Several steel piers could not support the dead load and were literally torn apart because the local buckling. On Route 5, opened to traffic in 1994, the Nishinomiya Harbour Bridge collapsed in a segment and had several piers damaged.

## 1.2 - Objectives

The effects of last important earthquakes are an example of the damage that can be expected in zones with important urban areas. Entire collapse of the communication systems, the infrastructures and the social and economical life may be expected from strong and moderate earthquakes. Nevertheless, the advances in the earthquake engineering have essentially contributed to the upgrading of new designs codes and have not yet been applied to retrofitting programs of existing structures, thus explaining the degree of damage. Thus, strong efforts must be put in the retrofitting of existing structures vulnerable to earthquakes. Research in this area leading to definition of simple guidelines is urgently needed.

As known, different methodological paths to define the current state of structures are available. In previous publications (Gómez et al. 1999a and Gómez et al. 1999b), the characteristics of the principal methodologies for estimating the seismic vulnerability of highway bridges were discussed with detail. Among these, in this research work we opted to explore the use of analytical models, mainly considering simplified and reliable schemes for the definition of possible damage in bridges.

This work is divided in two principal sections. The first section includes six chapters where the state-of-the-art of the seismic vulnerability of bridges is discussed. Thus, in chapter two the theoretical background of the evaluation methods to obtain the vulnerability of structures is commented. In addition, chapters three to six describe in detail the existing methodologies to evaluate the vulnerability of bridges, classifying as: (1) vulnerability index, (2) mathematical analyses, (3) experts and statistical evaluations, and (4) statistical evaluations of the observed damages.

In the second section of this work a simplified methodology to estimate the seismic vulnerability of reinforced concrete bridges with simple pier bent and elastic girders is proposed and evaluated. The methodology is applied to a real bridge, built 30 years ago. This second section is subdivided in four chapters. In the firsts two, the elastic and the non-linear procedures of evaluation are discussed. The non-linear procedure includes an analytical methodology to estimate the local pier damage, using a continuous damage model, and the global bridge damage. Thereinafter, an analytical process to consider the generation of artificial seismic actions compatible with the velocity spectrum of deterministic records is described in chapter nine, considering thus the uncertain nature of the seismic action. Finally, in chapter ten, the application of the proposed analytical procedure to estimate the seismic vulnerability of the real bridge is included. The obtained damage results show that the studied bridge would suffer only a minor damage when subjected to a seismic action similar to that of the considered seismic scenario.

The proposed methodology was compared with previous experimental and analytical results obtained from commercial codes. It is shown that the simplified methodology is less computational time consuming and can provide reliable values of the maximum damage suffered by the bridge piers.



## **Chapter 2**

### **Seismic vulnerability of structures. Theoretical background**

The analysis of bridges subjected to possible seismic action has grown in interest in the last years, principally due to the poor behaviour that these structures had during the earthquakes of Northridge in 1994 and Kobe in 1995. This growing interest produced numerous studies focused on the evaluation of the impact of various seismic actions in different types of structures.

To evaluate the seismic risk of any structure it is necessary to use a vulnerability model. There are several available models proposed for different structures, whose quantitative or qualitative results provide the possible damage of the system submitted to seismic action. The existing models have different levels of complication. Usually, simple vulnerability models use statistical analysis and the more complex ones make use of structural and probabilistic analyses.

In spite of the huge interest that the seismic behaviour of the bridges has produced in the last years and of the large number of bridges designed with old codes, only a few studies have been aimed to determine generic models for the seismic vulnerability of bridges. The few existing general projects use a number of simple models starting from calibration and analysis of data and the possible damage ranges.

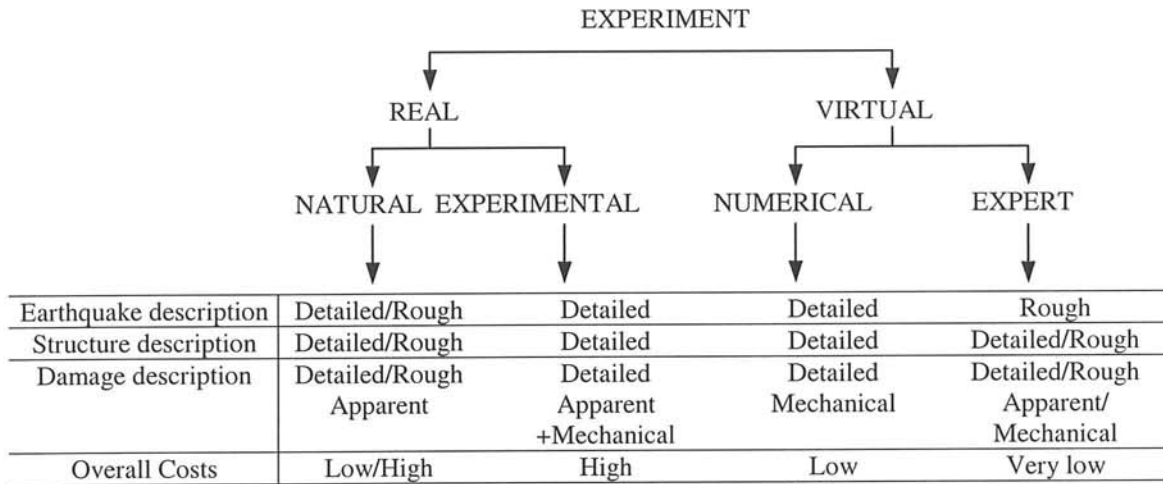
In this chapter, the principal characteristics of the techniques for evaluating the vulnerability of bridges will be commented, making emphasis on the principal existing applications in next chapters.

#### **2.1. Sources of data**

The general objective of any vulnerability analysis is to predict the physical damage with as few as possible number of uncertainties. An ideal analysis has sufficient available damage data obtained through inspection after earthquakes and makes thereafter a regression analysis for similar systems.

In risk studies, it is necessary to make use of the available information by means of different types of forecast experiments to evaluate the damage produced by earthquake. These experiments can be real, that is performed in real structures or specimens, or virtual, based on numerical analysis or experts opinion. The selection of a given type of experiment is a function of the description of the external action, structural type, damage level and overall cost, as it can be observed in figure 2.1 (Dolce 1997)

The experiments in real structures provide huge results, but need equipment for data recording and therefore tend to be expensive. The laboratory experiments give detailed information, but in occasions turn out to be very expensive and can be not repeated in many structures, the information is being thus deterministic. Furthermore, most of the models are scaled prototypes and they do not reproduce exactly the behaviour of the real systems.



**Figure 2.1** Experiments for damage prediction

The numerical experiments are convenient due to their lower cost and the quantity of information they provide, though the results are dependent on the accuracy level considered in the structural and action model. The expert experiments (figure 2.1) are based on the opinion of different professionals, starting from their experience and knowledge on a given area. This type of experiments is of low-cost and can be reliable.

To estimate the damages, one can combine different types of experiments; for example, the numerical experiments are often completed with calibrations or laboratory validations. In each case, within the estimate of the vulnerability, one should perform those experiments that provide the best possible estimation with the lowest costs.

## 2.2. Evaluation methods

### 2.2.1. According to the employed technique

Several criteria have been used in the past to classify the different methodologies for vulnerability evaluations. One of the most complete has been recently proposed by Petrini and Corsarnegro (describing in Dolce et al. 1994 and Dolce 1997), in which they classify the methodologies as direct, indirect, conventional and hybrid.

#### 2.2.1.1. Direct techniques

Direct techniques provide in a single step the prediction of the damage caused by a given earthquake; the most frequently used are the typological and the mechanical methods, which can be described as follows.

1. The *typological methods* consider constructions as samples of classes, which are defined by materials and techniques and by some other factors that can affect the seismic response. The vulnerability is expressed by the conditional probability that a structure of a certain type will suffer a damage level for a given earthquake intensity. The evaluation of the probability distributions is based on the damage observed in past earthquakes. These techniques require quite simple field researches, but are valid only in a statistical sense and cannot be applied to single constructions.

The typological methods are generally supported by the characteristics of the database and the information about the structural behaviour to select degrees of qualitative vulnerability as, for example, moderate damage, severe damage or collapse. The degrees of vulnerability are assigned as intervals of values of the damage index, which evaluates a series of parameters that, to the judgement of the authors, are determinant for the seismic response of the systems. The selection of the parameters of each model is made considering the knowledge of the response of the structural typology before earthquakes. Additionally, different categories are associated to each parameter, for example, if the parameter selected is the material that composes the system, the categories can be steel, reinforced concrete, wood, etc. For each category, values that fix the vulnerability are obtained; so, a steel category will have a greater value and a smaller vulnerability than a wood category.

In these vulnerability models, the database plays an important role. If the available data are scarce or confusing, the degree of reliability obtained in the modelling can be misleading. In some occasions, these databases are not available and some statistic vulnerability models are performed through statistics regression or simplified experimental expressions.

The typological methods are common in the creation of models for buildings, but very scarce for other type of structures. The existing models of vulnerability of bridges include as important parameters for the behaviour of the structure variables such as: year of construction, span between piers, support soil, construction material type, foundation type, etc.

2. The *mechanical methods* for seismic vulnerability estimation predict the seismic effects by means of suitable mechanical models of structures. Usually, very simple models, like single-degree-of-freedom systems with limited ductility, are used. The damage can be expressed by an index, which is often the ratio of the plastic deformation undergone by the model and the maximum deformation capacity, while the seismic action is characterised by its acceleration. This method is similar to the usual engineering approach for the evaluation of the structural safety and can be applied to both individual construction and urban ones. However, its effectiveness is limited to constructions whose seismic behaviour can be easily described by simple models. Examples of these methods for buildings can be observed in Gülkan et al., 1996, and Singhal and Kiremidjian, 1997.

When the databases for a region are scarce or not reliable, or when low seismicity zones are studied, the mechanical methods are the best tool. As a counterpart, these methods are more expensive than the statistic ones and will have the reliability of the structural models, of the definition of the damage indices and of the selection of the seismic excitation for the analyses.

### 2.2.1.2 Indirect techniques

The indirect techniques determine a vulnerability index in a first step and a relationship between damage and seismic intensity in a second step. This evaluation technique is of usefulness in the seismic analysis of large structural groups.

### 2.2.1.3 Conventional techniques

The conventional techniques are essentially heuristic and introduce a vulnerability index independently of the damage prediction. They are used to compare different constructions belonging to the same area, based on some factors whose contribution to the seismic resistance is calibrated by experts. The indices give a relative measure of vulnerability in a given area and are difficult to compare for different types of constructions (e.g. masonry versus RC structures) because of the differences in the factors considered in the evaluations.

The reliability of the results of conventional methods is determined by the quality of the estimated physical characteristic and by the capacity/demand models that are used. The models less reliable qualify the capacity through empirical equations and the demand through simplified dynamical or static analysis (Dolce et al. 1994, Dolce 1997, Yépez et al. 1995, and Yépez 1996).

### 2.2.1.4 Hybrid techniques

These techniques combine elements of the previous methods with expert's opinion. The hybrid techniques are developed taking those aspects of each technique that are useful to solve a particular problem.

## 2.2.2. According to input, method and output

A different method of classification could examine separately each of the three fundamental steps that characterise the methodological path and qualify a vulnerability analysis: *input*, *method* and *output*. The *input* indicates the type of available data, the *method* is the technique used to evaluate the seismic vulnerability of the structures and *output* represents the obtained results.

Updating such type of classification requires just adding new classes in any of the three steps that turn out to be incomplete. In the research of Dolce (1997) five classes of *input*, three classes of *method* and two classes of *output* have been considered, as can be observed in figure 2.2. In this figure, the absolute and the relative vulnerability are comprehended as:

- *Absolute vulnerability*. Vulnerability functions (fragility curves) which represent the average damage as a function of the seismic intensity, or, alternatively, conditional distribution of damage given the seismic intensity (damage probability matrices). Due to the great application of these concepts and their usefulness, they are described in the following paragraph in detail.
- *Relative vulnerability*. Heuristic/empirical or experimentally drawn vulnerability indices, for which no correlation with damage and seismic intensity is available; they only permit to classify the constructions according to their seismic vulnerability.

According to the above classification, the methods to evaluate the seismic vulnerability described in the previous section are classified by Dolce et al. (1997) as indicated in table 2.1. As it can be observed in this table, the direct methods use earthquake data and the qualitative and geometric information on the structures, use statistical techniques and the results are expressed as the absolute vulnerability.

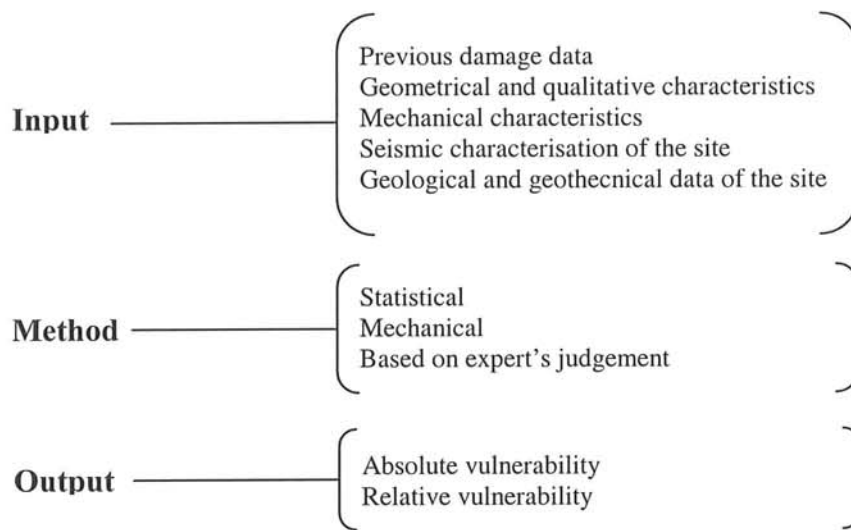


Figure 2.2 Classes of input, method and output proposed by Dolce

Input	Method	Output
<b>Direct typological techniques</b>		
1) Damage	1) Statistical	1) Absolute vulnerability
2) Geometrical/qualitative data	-	-
3) Seismic characterisation	-	-
<b>Direct mechanical techniques</b>		
3) Mechanical characteristics	2) Mechanical	1) Absolute vulnerability
4) Seismic characterisation	-	2) Relative vulnerability
<b>Conventional techniques</b>		
2) Geometrical/qualitative data	3) Expert judgement	2) Relative vulnerability
<b>Indirect techniques</b>		
1) Damage	1) Statistical	1) Absolute vulnerability
2) Geometric/qualitative data, relative vulnerability	-	-
4) Seismic characterisation	-	-

Table 2.1 Different methodological paths for seismic vulnerability estimation

The mechanical methods require as input the mechanical characteristics, use mechanical methods and obtain as result the absolute vulnerability. In the case of conventional techniques, the process starts from geometric/qualitative characteristics, it is based on expert's judgement and the result obtained is the relative vulnerability. Finally, the indirect methods use the same path that the direct methods. Nevertheless, in this case, the qualitative characteristics are treated in such a way to obtain the relative vulnerability index (as in the conventional method) and the relationship between damage, vulnerability and the intensity index.

Independently of the methodology used, the estimation of the vulnerability depends on the quality of the available data, on the accuracy of the method used and on the reliability of the damage prediction. The selection of one specific way to be followed depends on many aspects such as: available data, quality of the desired results, type of the system to be

---

evaluated, seismic hazard of the zone, available tools, importance of the system, economic availability, etc.

### **2.3. Damage probability matrices and fragility curves**

As commented previously, the absolute vulnerability can be defined using two concepts: damage probability matrices and/or fragility curves. The damage probability matrices (DPM) are discrete expressions of the conditional probabilities  $P[D=j/i]$ , which means the probability of obtaining a damage equal to  $j$ , due to an excitation of size equal to  $i$ . For example, from statistical methods the average probability damage ( $j$ ) for structures having different typologies can be obtained, for an earthquake of intensity ( $i$ ). The DPM can be obtained by means of any of the techniques described in the previous paragraph and they should consider the uncertainties that govern its evaluation. For buildings, there are many researches, which evaluate the vulnerability of structures in different areas. These researches include, in many cases, practically exhaustive statistical evaluations and representations by means of DPM and continuous curves. Examples of this type of matrices can be found in the ATC-13 (1985) for many structural typologies.

Another way of obtaining the damage index is by means of the fragility curves, which are graphic relationships or functions that express in a continuous form the vulnerability of the structure in function of the size of the earthquake. For example, such curves could relate the average damage of a specific structural typology and different seismic intensities. Some vulnerability functions in bridges evaluated with data provided by ATC-13 will be shown later.

It is fundamental the selection of the parameter that expresses the size of the seismic excitation in obtaining the damage probability matrices or the fragility curves. Generally speaking, in research projects is common to characterize the ground motion by means of macroseismic intensity scale, mainly due to the lack of other data. The use of the seismic intensity as a measure of the seismic hazard has sometimes a subjective character; it is recommend instead the use of instrumental measures. However, currently few of the seismic vulnerability projects include this type of measures.

## Chapter 3

### Vulnerability indices

One of the ways to determine the seismic vulnerability of bridges is the assignment of the overall seismic rating of the structures in study. This evaluation procedure is based on the subjective assignation of values, from different parameters that characterise the seismic behaviour of the structures or the influence of these in its environment, to add a representative global value of its fragility. The selection of the component parameters of each model is based on the experience acquired by the analysis of the damages produced by past earthquakes and the professional experience of the designers of models.

The parameters selected in this type of evaluation are configured, normally, in three principal groups, such as structural parameters, importance of the structure, and foundation and site characteristics. The structural parameters have as objective to distinguish the structural aspects that make systems more or less vulnerable, while the characterisation of the structure as a lifeline (whose operation is primordial after an earthquake) is considered through the parameters included in the importance group. Finally, the foundation and site characteristic parameters have as objective to distinguish the different foundation effects and the influence of the seismicity of the area. Each one of the selected parameters of the evaluation model is divided in one or several categories, also distinguishing aspects more or less vulnerable. Summarising, to higher is the overall seismic rating; to more vulnerable is the bridge.

Currently, various models of evaluation of the vulnerability of bridges, by assignment of the overall seismic rating, have been proposed. As a rule, the selection of the parameters considered as primordial, its division in categories and the assignment of the values to each category differentiate such proposals. In this chapter will be commented the principal evaluation models of the vulnerability of bridges, before the description of the principal parameters used by them.

#### 3.1 Parameters

The principal parameters used in the currently models to evaluate the vulnerability index of bridges subjected to seismic action are:

- ***Year of built.*** Most bridges defects are found in older bridges rather than ones, which reflect the state-of-the-art design. Though, a bridge built with current design codes is not a guarantee of adequate seismic performance, it is sure that an old bridge has greater probabilities of severe damages.
- ***Superstructure type.*** This parameter indicates the influence of the superstructure type in the bridge behaviour. Bridges with continuous superstructures and supports that can withstand large translational deformations usually remain serviceable with minor

repairs. However, bridges with discontinuous superstructure and/or brittle supporting members are usually severely damaged because of the liquefaction phenomenon.

- **Alignment of the bridge.** When a bridge is subjected to dynamic load, the superstructure of an irregular section can suffer important amplifications. To analyse this parameter the skew and curvature angles are used, defined the skew angle as the angle between the support centreline and a line perpendicular to the bridge centreline. Right and much curved superstructures are associated to the less and the most vulnerable bridges, respectively (Ren and Gaus 1993).
- **Number of expansion joints.** Superstructure discontinuities, such as expansion joints, will affect the overall stability of the bridge. The superstructure will provide any redundancy if it is possible the collapse of the bridge.
- **Bearing type.** The vulnerability rating for bearings reflect the susceptibility of the bridge to a bearing failure. There are, basically, four types of bearings used in bridge constructions (ATC-6 1981). One type, the rocker bearing, is generally constructed of steel and rolls on a curved surface. It is the most seismically vulnerable of the bridge bearings because it usually has a large vertical dimension, is difficult to restrain and can become unstable after a limited movement. Another type of bearing, the roller bearing (usually of steel) is stable during an earthquake, except that it can become misaligned and horizontally displaced. The third type is the elastomeric bearing pad (constructed of natural or synthetic elastomer and relies on the distortion of this material) is very stable during an earthquake, although it has been known to "walk out" under severe shaking. The last bearing type is the sliding bearing (relies on the sliding of one surface over another) which consist of asbestos sheet placed between two concrete surfaces.

In vulnerable structures, serious failure usually is due to loss of support resulting from large relative transverse or longitudinal movement at the bearings. The expected movement at a bearing is dependent on many factors and can be not easily analysed. Because it is difficult to predict relative movement, the minimum support length, given by Seismic Codes, may be used as the basis for checking the adequacy of longitudinal support lengths.

- **Classification.** The studied bridge can be classified as regular and irregular. A bridge is called irregular if differential stiffness, differential pier heights, or large elevation changes exist. An irregular bridge could sustain more damage than a regular structure.
- **Piers type.** Most of the possible damage than a bridge can suffer is related with the typology, configuration, height, union type and reinforcements of its piers. Some of the currently models define this parameter conform to the form of the cross section and disposition of the piers; others consider the material and union of pier with the rest structural elements. The most commons types of bridge piers are multicolumn, single and hammer piers. Between these, the single pier type is the most vulnerable.
- **Substructure material.** A better behaviour of bridges with steel substructures has been reported in past earthquakes. Then, this kind of bridges is the less vulnerable.



- **Minimum support length.** The minimum support lengths for bearings seat must be greater than the actual support length. Otherwise, during an earthquake there is a chance that the bearing seat will lose support, resulting in failure of the superstructure.
- **Abutment type.** Abutments failures during earthquakes do not usually result in total collapse of the bridge. Therefore, the abutment vulnerability rating should be based on damage that would temporarily prevent access to the bridge. One of the mayor problems observed in past earthquakes has been the settlement or fill at the abutment, principally due to superior construction or fills, the absence of water and the generally wider and better-retained bridge approaches (ATC-6 1981). Additional abutment fill settlements are possible in the case of abutment failures due to excessive seismic earth pressures or seismic forces transferred from the superstructure.
- **Foundation type.** Many structures have failed in spite of having a satisfactory design, mainly due to problems in its foundation and the surrender soil. This parameter tries to evaluate the geological and topographic conditions of the soil of support, the type of foundation and the material of it. Deeper and less dense soils are associated to conditions that are more vulnerable.
- **Liquefaction potential.** This parameter determines the most significant type of ground instability of the soil, although other types, such as slope instability or fills settlement, can result in bridge damage during an earthquake. The ground and foundations displacements induced by the liquefaction effect have been a major cause of bridge damage during past earthquakes. Therefore, lateral spread displacements caused failures and, in some cases, collapsed of bridges during the Alaskan (U.S.A.), Limon (Costa Rica) and Kobe (Japan) earthquakes. Nearly all of the bridge damages by liquefaction was at rivers or other water crossing, where delicately sloping alluvial or fill deposits liquefied and spread laterally. These types of deposits (loose, saturated, granular sediment beneath gently sloping ground or near incised channels) are highly vulnerable to liquefaction and lateral spread.

The value of this parameter is normally based on a qualitative assessment of liquefaction susceptibility. Considering the lack of easy methodologies for evaluate the liquefaction effect at bridge sites, Youd (1998) proposes a systematic application of standard criteria for assessing liquefaction susceptibility at bridge site. In his method, Youd evaluate ground displacement potential and assess the vulnerability of bridges to damage induced by liquefaction. With this first evaluation, the bridges with low hazard are classified easily and bridges with significant hazard are suggested for a more detailed study. If the available bridge-site information is insufficient to complete the liquefaction hazard analysis, then Youd utilised simplified seismic, topographic, geologic, and hydrologic criteria to prioritise the site for further investigation.

The principal steps and logic path for the Youd screening procedure are listed in figure 3.1. In the assessing liquefaction hazard, the recommended procedure is to start at the top of the path, perform the required analysis for each step, and finalized with bridge classification. As can be observed in figure 3.1, the Youd procedure is divided in the following steps:

- The first step of the screening procedure is the regional evaluation of liquefaction susceptibility. This step includes analysis such as: prior evaluation, geologic analysis, seismic hazard evaluation and water table

evaluation. In each one of these aspects, if the evaluation indicate very low liquefaction hazard, the bridge site is classified as low hazard and low priority for further investigation, and the evaluation for that site is complete. If the geologic criteria indicate a higher susceptibility rating, the site is classified as possible liquefiable, and the screening proceeds to the next step.

- The second general step in the screening procedure analyses situations where is present a lack of confidence information or where regional evaluations do not consider low susceptibility to liquefaction. Within this step are evaluated the screening for extra sensitive clays, the soil classification and the analysis of penetration test (standard penetration and cone penetration tests) to prove the possibility of liquefaction in the interested site.
- Liquefaction by itself is not a cause of bridge damage. Structural damage occurs when liquefaction induces intolerable ground displacements or deformations or loss of foundation bearing strength. Then, this final general step estimates the ground displacement hazard, analyzing the possibility of embankment or slope instability, slope deformations, lateral spread displacement, ground settlement, and bearing capacity.

The detailed procedures to complete the above steps can be consulted en Youd (1992). Summarising, application of the screening procedure of Youd analysed the principal effects that can produce liquefaction at bridge site. Starting from these analyses, the soils are classified in one of the following four possible outcomes:

- Confirmed high liquefaction hazard. These sites should be given very high priority for additional investigation and development of possible mitigation measures. Prioritisation at this level should consider the importance of the bridge, the age of bridges, its vulnerability, and the current state of the structure.
- Confirmed liquefaction susceptibility, but unknown hazard. Sites with confirmed surface liquefiable sediments or sensitive clay layers, but unknown ground failure hazard, should be given high priority for further investigation. Bridges involved water crossing should be given priority for further investigation.
- Insufficient information to assess liquefaction resistance or strength-loss potential. Where insufficient information is available, additional site investigations will be required to fully evaluate liquefaction hazard. These investigations include additional laboratory and experimental testing. Sites with water crossing are more vulnerable. Sites with geologic conditions indicative of liquefaction susceptibility should be given priority over sites assessed as having moderate and lesser susceptibility.
- Low hazard and low priority for further investigation. Sites categorized as low priority for further investigation do not need further studies.

- **Maintenance state.** With the time, any structural system can see diminished its resistance by the action of external loads. The application of maintenance programs can detect and remedy the structural damage. A structure that has rehabilitate recently can be considered less fragile that other of similar type, of the same age and without changes (Maldonado et al 2000a).
- **Construction procedure.** This parameter analyses the importance of the constructive procedure in the seismic response of the system, for the superstructure and for the substructure.
- **Non-structural elements.** This parameter analyses the effects that external elements can have in the bridge behaviour and the performance of other vital lines that are transported through of it.
- **Importance of the bridge as a vital transportation line.** The importance of a bridge is a difficult attribute to quantify and although there have been many attempts to do so; there is a little consensus about a preferred methodology. Some of the models that evaluate the vulnerability index of bridges use the estimation of the importance of a bridge as a necessary parameter. The importance of a bridge is evaluated, in these researches, by means of subjective analysis of characteristics such as the *Average Daily Traffic* (ADT), the presence of other facilities, the quantity of affected persons by the structural failure or the relationship and connection with other structures.

Generally, more rigorous methodologies to evaluate the importance of highway bridges include traffic volume, detour length, the presence or absence of utilities and some form of functional classification, for example emergency route and/or defence route. Few or the methodologies, if any, considers network redundancy and socio-economic issues, both of which are even more difficult to quantify than the early set of attributes.

In the U.S.A. coterminous, almost every state uses a different methodology to evaluate the importance of bridges. In some of these methodologies are implicated subjective assignments; while in others are used statistical expressions. In any way, the existing methodologies are based on the assignment of an importance or critical value; the structures with a greater value will be classified as more important and pondered for investigations that are more detailed or for future retrofitting programs (Thomas et al. 1998). The more common variables used in these models are:

- The quantity of traffic that crosses the structure during a given period of time, usually the ADT.
- The detour length, used to arrive to the nearest bridge to the structure of analysis, evaluating thus the possibility of alternate routes when the failure of the system is presented.
- The index that identify the bridge and route nature, distinguishing between principal arteries, emergency routes or defence routes, streets, railroad and secondary routes.
- The index that identifies the utility of the route of the bridge and the one that crosses it, classifying as essential or little useful.

- Total length of the bridge and, in some cases, the width of the girder.
- The index that identifies the importance of the facilities that are crossed by the bridge, usually to divide residences and offices or stores and parking zones. In addition, when a bridge crosses a river or a railroad is analysed.

Equation 3.1 is an example of the proposed empirical expressions for to obtain the importance index of bridges (*II*). This equation is the result of comparative analyses of the principal methods used in the United State and of statistic studies based on expert's surveys (Thomas et al. 1998).

$$II = ER \left\{ \left[ (RT_{carry}) (DL_{carry} \times NT_{carry}) \right] + 0.6 [RT_{cross} \times NT_{cross}] + \right. \\ \left. 0.34 \left[ (ADT_{carry} / Ave ADT) (L)^{0.25} + RV_{cross} \right] \right\} \quad (3.1)$$

where:

"*carry*" indicates the critical route, "*cross*" indicates the critical route under the bridge

$ER = 1.1$  and  $1.0$  for confirmed emergency route and others, respectively

$RT_{carry} =$  Factor for nature of route:  $1.1$  for Interstate route or principal artery and  $0.9$  for all other routes and railroad bridges

$DL_{carry} =$  Factor representing criticality of detour length:

$= 1.2$ , for detour length (DL)  $>155$  km,

$= 1.0$ , for  $80 \text{ km} < DL \leq 155 \text{ km}$ ,

$= 0.9$ , for  $15 \text{ km} < DL \leq 80 \text{ km}$ ,

$= 0.8$ , for  $5 \text{ km} < DL \leq 15 \text{ km}$ ,

$= 0.7$ , for  $DL \leq 5 \text{ km}$ ,

$= 1.0$ , for bridges carrying railroads.

$NT_{carry} =$  Factor representing criticality of traffic congestion:

$= (ADT_{carry} / Ave ADT)^{0.25}$  and  $0.8$  for bridges carrying railroads

$ADT_{carry} =$  Average Daily Traffic on the bridge

$L =$  bridge length (m)

$RT_{cross} =$  Factor for nature of route

$= 0.8$  for all routes and  $0.0$  for no route or structure under the bridge

$NT_{cross} =$  Factor representing criticality of traffic congestion

$= (ADT_{cross} / Ave ADT)^{0.25}$

$RV_{cross} =$  Ratio of bridge length to longest bridge in the database  $= L / L_{max}$

$Ave ADT =$  Average  $ADT_{carry}$  in the classification database

$L_{max} =$  Maximum bridge length (m) in the classification database

The bridges ranked by means of equation 3.1 were designated as "critical", "essential" and "others" A bridge was defined as critical if its rank is major than the 95<sup>th</sup> of the bridge rank percentiles. In the same way, essential bridges have a rank major than the 65<sup>th</sup> of the bridge rank percentiles and bridges with a rank letter than these 65<sup>th</sup> values are defined as others.

In some models as analysis parameter is included the seismic hazard of the zone, through the macroseismic intensity or by means of the peak ground acceleration. However, as these methods are applied to evaluate the vulnerability of structures of a specific zone, not always its evaluation is determinant.

### 3.2 Proposed models

#### 3.2.1. Procedure of the ATC 6-2

One of the first procedures to define the seismic vulnerability of bridges was developed by the ATC (ATC-6 1981 and ATC-6-2 1983) and represents the initial step in taking measures for retrofitting this type of structures. The ATC 6-2 applies hybrid techniques, a combination of statistical methods and conventional techniques. The evaluation of the vulnerability is based on three main conditions: structural characteristics needed to determine the vulnerability index, seismicity on the bridge site and importance of the structure as a vital transportation link. The seismic rating of a bridge is accomplished by making independent ratings of the bridges in each one of these areas. The scores are added to arrive at an overall seismic rating according to the following procedure.

1. *Vulnerability rating* - Vulnerability ratings assume any value between 0 and 10. In general, a 0 value means a very low vulnerability; a value of 5 means moderate collapse vulnerability or a high loss of function vulnerability; and a value of 10 means high collapse vulnerability.

Although the performance of a bridge is based on the interaction of all its components, it has been observed during past earthquakes that certain bridge components are more vulnerable to damage. These are the bearings, piers and footings, abutments and foundations. Among these, bearings seem to be the most economically retrofitted. For this reason, the seismic vulnerability rating is determined by examining the bearings separately from the other structural members. The vulnerability ratings of the remainder of the structure may be determined as the greatest of the vulnerability ratings of each of the others components that are vulnerable to failure. The vulnerable features of each of these components and methods for calculating their vulnerability ratings are:

**Bearings.** A suggested step-by-step method for obtaining the vulnerability rating of the bearings is the following:

- Determine if the bridge has non-vulnerable bearing details. Such bridges would include: (1) continuous structures; (2) continuous structures whose skew is less than  $20^\circ$ , or the skew is greater than  $20^\circ$  but less than  $40^\circ$  and the length-to-width ratio of the bridge deck is less 1.5; (3) the bearing seat on the abutment is continuous in the transverse direction and the bridge has in excess of three girders; and, (4) the support length is equal to or greater than one half the minimum required support length. If the bearing details are non-vulnerable, a vulnerability rating of 0 can be assigned and the remainder steps for bearings omitted.
- Determine the vulnerability to structural collapse or loss of bridge access due to transverse movement. When transverse restraint is subject to failure, girders are vulnerable to collapse if either of the following condition exists: (1) individual girders are supported on individual pedestals or piers; and (2) the exterior girder in

a 2- or 3- girder bridge is near the edge of a continuous bearing support. In either of these cases, the vulnerability rating should be 10. When bearings are vulnerable to a falling over failure but structure collapse is unlikely, the vulnerability rating should be 5.

- Determine the vulnerability of the structure to collapse or loss of accessibility due to excessive longitudinal movement. If the longitudinal support length measured in a direction perpendicular to the support is less than one, but greater than a half of the required longitudinal support length, the vulnerability rating shall be assigned a value of 5, unless in addition rocker bearings are vulnerable to toppling, in which case a value of 10 should be used. If the longitudinal support length is less than a half of the required longitudinal support length, then a vulnerability rating of 10 should be assigned.

**Piers and foundations.** The following step-by-step procedure may be used to determine the vulnerability of piers and footings:

- Assign a pier and footing vulnerability rating of 0 to bridges localised in zones of moderate seismicity (with an acceleration coefficient less than 0.29 for the USA case).
- Assign vulnerability rating of 0 if bearing keeper plates or anchor bolts are assumed to fail, eliminating the transfer of load to piers or footings.
- If piers and footings have adequate transverse steel as required by Seismic Codes, assign pier vulnerability rating of 0.
- Calculate the Base Vulnerability Rating (*BVR*), which is an indicator of the vulnerability of a pier to sudden shear failure. The *BVR* shall be assigned according to the following equation:

$$BVR = 13 - 6 \left( \frac{L_p}{P_s F b} \right) \quad (3.2)$$

where:  $L_p$  is the effective pier length, in feet;  $P_s$  is the percent of the main reinforcing steel;  $F$  is a framing factor (1 for multiple pier bents fixed at one end; 2 for multiple pier bents fixed in both extremes, 1.5 for single pier bent fixed at the top and bottom-box girders; and, 1.25 for single pier bent fixed in both extremes and a girder with not box section); and  $b$  is the transverse pier dimension, in feet.

The vulnerability of piers rating, *CVR*, will be between 0 and 10, it will be taken equal to *BVR* minus the points shown for each one of the following conditions:

1. Peak ground acceleration  $a_{max} < 0.4$  (three points).
2. Right structure. Skew  $< 20^\circ$  (two points).

3. Continuous structures with diaphragm abutments of approximately equal stiffness, in which the length-to-width ratio of the deck is less than four (one point).
4. Grade 40, or below, reinforcement (one point).

The maximum value that can be subtracted from *BVR* is of four points, unless larger *CVR* are calculated in the following point.

Values of *CVR* less than zero or greater than 10 should be assigned values of 0 and 10, respectively. For single-pier bents supported on pile footings unreinforced for uplift, or poorly confined foundations, the *CVR* is function of the peak ground acceleration.

**Abutments.** The model of the ATC 6-2 uses the following systematic procedure for determining the vulnerability rating for the abutments, except in unusual cases; the maximum abutment vulnerability rating will be 5:

- Determine the vulnerability of the structure to abutment fill settlement. When fill settlement are estimated to be greater than six inches (0.15 m), assign vulnerability rating for the abutment of 5.
- For bridges with earth retaining abutments with skews greater than 40° and where the distance between the seat and the bottom of the foundation footing exceeds 3.05 meters a vulnerability rating of 5 should be assigned.

**Liquefaction.** The procedure is based on the following steps:

- Determine the susceptibility of foundation soils to liquefaction. High susceptibility is associated with: (1) foundation soil providing lateral support to piles or vertical support to footings like average saturated loose sands, silty sands, non plastic silts; and, (2) similar soils underlay abutments fills. Moderate susceptibility is associated with similar conditions where average soil conditions may be described as medium dense. Low susceptibility is associated with dense soils.
- Determine the potential extent of liquefaction related damage where susceptible soil conditions exist.
- In general, bridges subjected to severe liquefaction related damage shall be assigned a vulnerability rating of 10. This rating may be reduced to 5 for single span bridges with skew less than 20° or rigid box culverts with floors.
- Bridges subjected to major liquefaction related damage shall be assigned a vulnerability rating of 10. This rating may be reduced to between 5 and 9 for single-span bridges with skew less than 40° rigid box culverts with floors, and continuous multi-span bridges with skew less than 20° provided with:
  1. Reinforced concrete piers are continuous with the superstructure and have a *CVR* less than 5 and height in excess of 25 feet (7.63 m).

2. Steel piers are in excess of 25 feet high (7.63 m).
  3. Discontinuous piers with the superstructure and shifting of the superstructure will no result in instability.
    - Bridges subjected to moderate liquefaction related damage should have a vulnerability rating of 5. This rating should be increased to between 6 and 10 if the vulnerability rating for the bearings is greater than or equal to 5.
2. An evaluation of the local *seismicity* will provide values between zero and ten for this characteristic.
  3. For this last characteristic, the bridges are classified in two groups. The first include the essential structures by means of Social/Survival and Security/Defence requirements. The second classification is for all other bridges. Bridges classified as essential may have assigned ratings between 6 and 10, while the remainders may have ratings between 0 and 5. The evaluation of these ratings are subjective, conform to the bridge traffic, the presence of other facilities, the quantity of affected persons by the structural failure and the relationship and connection with other structures.

The model of the ATC 6-2 estimates the total vulnerability of the structure adding the values of each one of the three characteristics by assigned weights. The weights, in percentage, can be equal (33.3%) for all the characteristics or different in function of their importance. For example, if the structures to analyse are within a region with similar seismicity, the weights for this characteristic is zero and the remaining weights are modified to reach the 100%. If the two remaining characteristics are rating equal, the weights are 50% for vulnerability of the structure and 50% for its importance. Thus, as a result, the model provides ratings between 0 and 10.

For structures more complex or for more detailed evaluations of an existing bridge, the ATC 6-2 proposes to evaluate the fragility of the bridges through a hybrid technique, combination between the previous statistic studies and applications of conventional techniques, by means of the determination of Capacity/Demand ( $C/D$ ) ratios. These expressions are the relation between the available capacity of structures before an earthquake and the demand to support external action. The available capacity is obtained, in global form or for particular elements, through analysis that can be elastic or non-linear. The basic equation to determine the seismic  $C/D$  relationships is:

$$C/D = \frac{R_C - \sum Q_i}{Q_{EQ}} \quad (3.3)$$

where  $R_C$  is the nominal capacity (in displacement or force) of the element;  $\sum Q_i$  are the total demands (forces or displacement) for cases with different seismic load and  $Q_{EQ}$  is the demand (force or displacement) for seismic design charges.

The  $C/D$  ratios are calculated with the nominal capacity, without any alteration factors by uncertainties in resistance and dimensions. This calculation is thus accomplished to estimate the best possible the failure of the element. Elements with ratios smaller than one indicate possible faults before future earthquakes. The ratios  $C/D$  should be calculated for those elements that cause the greater damage problems.



Parameters	Sub-areas	Values
<i>Structural characteristics</i>		
Superstructure	Discontinuous superstructure	5
	Continuous superstructure	0
Number of expansion joints	There are not expansion joints	3
	2 or 3 expansion joints	4
	4 or more expansion joints	5
Bearing type	Sliding bearing	0
	Elastomeric bearing pad	3
	Roller bearing	4
	Rocker bearing	5
Alignment	Depending of the skew angle	1 – 5
Year of built	Depending of the Seismic Code	1 - 10
	Application of the current Seismic Code	0
Classification	Regular bridges	0
	Irregular bridges	5
Height of the piers	Height of the piers < 5 m	0
	Height of the piers > 5 m	5
Support length	Support length < $Nd$ (equation 3.4)	0
	Support length > $Nd$ (equation 3.4)	5
<i>Importance of the bridge as a vital transportation link</i>		
Average Daily Traffic (ADT)	ADT < 2000 vehicles	0
	2000 vehicles < ADT < 10 000 vehicles	5
	ADT > 10 000 vehicles	10
Detour length (DL)	DL < 4 miles (6.4 km)	0
	2 miles (3.2 km) < DL < 4 miles (6.4 km)	5
	DL > 4 miles (6.4 km)	10
<i>Foundation and site characteristics</i>		
Soil profile	Depending of the studied soil	1 – 10
Liquefaction potential	Null susceptibility to soil liquefaction	0
	Moderate susceptibility to soil liquefaction	5
	Greater susceptibility to soil liquefaction	10
Abutment height	0 m < abutment height < 4.6 m	0
	4.6 m < abutment height < 9.1 m	5
	abutment height > 9.1 m	10

**Table 3.1** Parameters of the Pezeshk et al. model

### 3.2.2. Model of Pezeshk et al.

In general, the seismic retrofitting process can be divided into three mayor steps: preliminary screening, detailed screening and design of retrofit measures. A preliminary screening for bridges retrofitting is proposed by Pezeshk et al. (Chang et al. 1995 and Pezeshk et al. 1993). This preliminary screening methodology requires access to a seismic inventory of all bridges to be screened, followed by the execution of a numerical rating system.

In his research, Pezeshk et al. propose a preliminary vulnerability evaluation by means of a detailed information, considering three principal areas: a) structural characteristics; b) importance of the bridge as a vital transportation link; and, c) foundation and site characteristics. Each of these areas are divided into several sub areas which are given a score, determined on the basis of its relation to the effect of seismic damage due a moderately strong earthquake. The maximum score is of 100 points, 50 distributed in different structural parameters, 20 for its importance and 30 for foundation and site characteristics. In table 3.1, the parameters used by Pezeshk et al. are shown. In this table, are also presented the considered sub areas for each parameter and the fragility values of these.

Variable	Description	Variable	Description
$Y_1$	Peak ground acceleration	$Y_7$	Type of foundation
$Y_2$	Design specifications	$Y_8$	Material of the substructure
$Y_3$	Type of superstructure	$Y_9$	Structural irregularity
$Y_4$	Shape of the superstructure	$Y_{10}$	Soil conditions
$Y_5$	Internal hinges	$Y_{11}$	Liquefaction
$Y_6$	Type of pier	$Y_{12}$	Seat length

**Table 3.2** Parameters of the Kim model

As was commented, the fragility by lost of support is defined comparing the real support length in the bridge with a reference support length. In the model of Pezeshk et al. (1993), the reference support length,  $Nd$ , is obtained by means of equation 3.4.

$$Nd = 12 + 0.03L + 0.12H \quad (3.4)$$

where  $L$  is the length of the bridge deck to the adjacent expansion joint or to the end of the bridge deck,  $L$  is the sum of  $L_1$  and  $L_2$ , the distance to either side of the hinge. For single span bridges,  $L$  is equal the length of the bridge deck (in ft).  $H$  is the average height of piers supporting the bridge deck to the next expansion joint ( $H = 0$  for single span bridges). Otherwise,  $H$  is the average height of the two adjacent piers, in feet.

If the structure to be analysed has been seismically retrofitted, this method subtract 5 points to the 100 outlined. The seismic vulnerability of the studied structure is determined by the simple addition of the assigned values,  $Y_i$ , to the selected parameters. Then, the Pezeshk et al. vulnerability index,  $VI_p$ , is defined as:

$$VI_p = \sum_{i=1}^{13} Y_i \quad (3.5)$$

A bridge with 100 points represents an ideally perfect bridge and that with 0 points one without seismic resistance. Additionally, the authors estimate that all the structures analysed are located within the same seismological region. Therefore, they are submitted to the same seismic hazard category and it is not granted any weight to this aspect.

The methodology outline by Pezeshk et al. was applied as a preliminary screening in Memphis, USA (Chang et al. 1995 and Pezeshk et al. 1993) and in Istanbul, Turkey (Can and Yüzügüllü 1995). The obtained results helped to separate structures with a more reduced capacity.

### 3.2.3. Seong Kim model

The model proposed by Kim (Ren and Gaus 1996) was developed starting from the idea to use only the information on inventory and inspection data to construct the model. Kim identifies 12 statistical parameters that represent the seismic behaviour of bridges. These parameters are described in table 3.2.

To difference of the model of Pezeskh et al., Kim includes as analysis parameter the seismicity of the zone (parameter  $Y_1$ ) and considers for each selected parameter four categories of valuation. In table 3.3 parameters, categories and the its associated values of vulnerability of the model of Kim are indicated. To a greater fragility of a parameter, a greater value is assigned to it.

Variables	Classification	$\beta$	Rate contribution (%)
$Y_1$	1; $a_{max} < 0.1g$ , 2; $0.1g < a_{max} < 0.2g$ , 3; $0.2g < a_{max} < 0.3g$ , 4; $0.3g < a_{max}$	0.141	31.4
$Y_2$	1; after 1981 2; 1972 - 1980 3; 1940 - 1971 4; before 1940	0.456	10.4
$Y_3$	1; cable-stayed, suspension or single span bridges 2; arch or monolithic girders and piers or trusses 3; continuous girders and trusses 4; simply-supported girders and trusses – multi spans or 2 level or more elevated structures	0.114	5.5
$Y_4$	1; straight 2; 20-45° skewed or 45-90° curved 3; 45-60° skewed or 90-180° curved 4; more than 60° skewed or 180° curved	0.437	7.3
$Y_5$	1; none 2; yes with cable restrainers or seat length > 12" 3; yes with 6" (0.15 m) < seat length < 12" (0.30 m) 4; yes with seat length < 6" (0.15 m)	0.089	5.6
$Y_6$	1; monolithic multi-pier bent or solid 2; pinned multi-pier bent 3; monolithic single pier 4; pinned single pier	0.029	0.4
$Y_7$	1; single pier shaft 2; spread footing 3; piled footing 4; pile bent	-0.024	2.2
$Y_8$	1; steel 2; ductile concrete 3; non-ductile concrete 4; timber, masonry or other old materials	0.034	0.2
$Y_9$	1; none 2; any 2-pier heights differ by more than 1.25 times 3; any adjacent pier heights differ by more than 1.25 times 4; any adjacent pier heights differ by more than 1.5 times	0.278	3.4
$Y_{10}$	1,2,3, or 4 for different soil types in the USA Code	0.188	4.4
$Y_{11}$	1; $LSI < 5$ , 2; $5 < LSI < 25$ , 3; $25 < LSI < 100$ , 4; $100 < LSI$	0.932	20.5
$Y_{12}$	1; good, 2; fair, 3; poor, 4; extremely poor	0.511	8.7
		C=-3.84	

g = gravity acceleration,  $a_{max}$  = peak ground acceleration and LSI = Youd and Perkins factor that characterise the effect of liquefaction

**Table 3.3** Parameters, values and rate conditions for Kim model

The calculus of parameter  $Y_5$  requires the numbers of hinges and the seat lengths of the spans in the bridge. The number of hinges ( $N_{joint}$ ) can be indirectly obtained by subtracting from the span number ( $N_{span}$ ) the total pier number ( $n_p$ ), in accordance with the following expression:

$$N_{joint} = N_{span} - n_p - 1 \quad (3.6)$$

The parameter  $Y_4$  is expressed as a shape factor, which is calculated by the following relationships:

$$\begin{aligned}\alpha_{skew} &= \alpha_i - \alpha_f \\ Y_{cur} &= \frac{L}{R_c}\end{aligned}\quad (3.7)$$

where  $\alpha_{skew}$  is the skew angle;  $\alpha_i$  and  $\alpha_f$  are the skew angle to the beginning and final of the structure;  $Y_{cur}$  is the curvature angle;  $L$  is the length of the bridge and  $R_c$  is the curvature radio.

On the other hand, the parameter  $Y_{12}$  takes into account the appropriateness of seat length (continuous minimum bearing support length) in the performance of the system. When no information is provided, Kim proposed the calculation of the minimal support length by means of the following expressions:

$$\begin{aligned}N_d &= 8 + 0.02L + 0.08H & a_{max} \leq 0.19g \\ N_d &= 12 + 0.03L + 0.12H & a_{max} > 0.19g \\ S &= N_d \sqrt{a_{max} / 0.19}\end{aligned}\quad (3.8)$$

where  $N_d$  is the minimum bearing support length;  $L$  is the length of the bridge deck to the adjacent expansion joint;  $H$  is the pier height;  $a_{max}$  is the ground acceleration as percentage of gravity and  $S$  is the continuous minimum bearing support length.

Starting from the values of the selected parameters (tables 3.2 and 3.3), Kim proposes two vulnerability indices, one lineal and the other non-linear. The lineal index, equation 3.9, is the addition of the product of the values of the parameter and its weight factor  $\beta_i$ . In the report describing this model (Ren and Gaus, 1996), no reference is made to the selection procedure for the constant values of each parameter, though it is supposed that these values are related to statistical adjustments between the results of the model and the actual damages in the referenced bridges.

$$VI_{KI} = \sum_{i=1}^{12} (\beta_i Y_i) + C \quad (3.9)$$

The rank of the lineal seismic index was classified into five categories, used to define qualitatively the extent of damage in the bridge. These five categories are:

- **No damage**,  $VI_{KI} = 0$ .
- **Minor damage**,  $VI_{KI} = 1$ . Damage which does not directly deteriorate bearing capacity such as: deformation of secondary member of steel structures, small cracks in reinforced concrete member or settlement and cracks of retaining walls.
- **Moderate damage**,  $VI_{KI} = 2$ . Damage which directly deteriorates bearing capacity such as: buckling of primary members of steel structures, major cracks of reinforced concrete members larger than 1 mm, failure of bearing supports or moderate movements of substructure. Permanent and/or temporary repair is possible.

Variable	Description	Variable	Description
Y <sub>1</sub>	Seismic code	Y <sub>11</sub>	Soil type
Y <sub>2</sub>	Superstructure type	Y <sub>12</sub>	Abutment type
Y <sub>3</sub>	Superstructure form	Y <sub>13</sub>	Support length of abutments
Y <sub>4</sub>	Internal joints	Y <sub>14</sub>	Bearings type
Y <sub>5</sub>	Superstructure material	Y <sub>15</sub>	Conservation state
Y <sub>6</sub>	Pier type	Y <sub>16</sub>	Constructive procedure of girders
Y <sub>7</sub>	Foundation type	Y <sub>17</sub>	Constructive procedure of piers
Y <sub>8</sub>	Pier material	Y <sub>18</sub>	Liquefaction potential
Y <sub>9</sub>	Longitudinal irregularity	Y <sub>19</sub>	Non structural elements
Y <sub>10</sub>	Support length	-	-

**Table 3.4** Parameters of the Maldonado et al. model

- **Severe damage**,  $VI_{K1} = 3$ . Severe damage which is likely to produce the collapse of the superstructure starting from the substructure such as: extensive spalling-off of concrete and rupture of reinforcements of reinforced concrete members, extensive failure of concrete supporting bearings or extensive movement of substructure including settlement and lateral movement. Permanent and/or temporary repair impossible.
- **Collapse**,  $VI_{K1} = 4$ . Collapse of bridge.

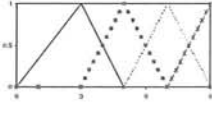
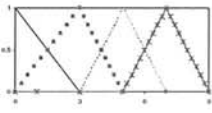
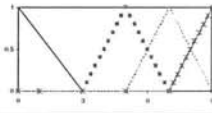
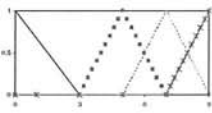
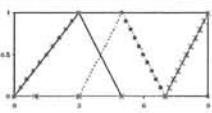
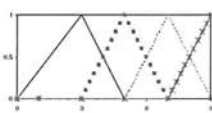
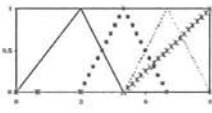
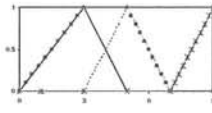
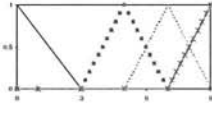
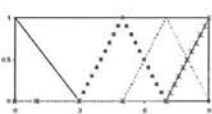
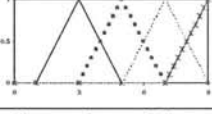
For non-linear statistical models, the index designed by Kim as a damage index, but which rigorously speaking represents a risk index (because it consider the seismic hazard,  $Y_1$ ), is obtained as:

$$VI_{K2} = Y_1 \times \left( \sum_{i=1}^{12} (\beta_i Y_i) \right) \quad (3.10)$$

where  $VI_{K2}$  is the vulnerability index;  $Y_i$  are the parameters that affect the vulnerability of the bridges;  $Y_1$  is the value of the first parameter and  $\beta_i$  are constants. It can be observed in expression 3.10 that the first factor is considered of primary importance in this index. For non-linear model, there are only three estimated risk ranges:

- **Minor damage**,  $VI_{K2} < 1.5$ .
- **Moderate damage**,  $1.5 < VI_{K2} < 2.5$ .
- **Mayor damage**,  $VI_{K2} > 2.5$ .

According to the table 3.3, some of the factors are more dominant than others are. The most significant factors in this model (by descending order) are: the intensity of peak ground acceleration, the effect of liquefaction, the design specifications and the seat length of support. The sum of these factors is 71%, which is almost 3/4 of the total contribution.

Variables	Classification	Functions
$Y_1$	1; after 1995 2; between 1975 and 1994 3; between 1968 and 1974 4; before 1968	
$Y_2$	1; cable-stayed, suspension or single span 2; arch, frames or with two or more spans 3; simply-supported girders with two or more spans	
$Y_3$	1; straight 2; skew angle < 20° 3; skew angle between 20° and 45° 4; curved bridges or skew angle > 45°	
$Y_4$	1; without internal hinges 2; with internal hinges and real support length > $N_d$ (equation 3.11) 3; with internal hinges and $0.5N_d \leq$ real support length $\leq N_d$ 4; with internal hinges and real support length < $N_d$ in any case	
$Y_5$	1; steel 2; reinforced or prestressed concrete 3; wood 4; masonry or others	
$Y_6$	1; without piers, solid wall piers or frame piers 2; pile bent piers 3; multiple span piers 4; single column piers, hammerhead piers or piers with deficient design	
$Y_7$	1; pile-piers 2; piles 3; superficial with multiple span piles 4; superficial with single span piles	
$Y_8$	1; steel 2; reinforced or prestressed concrete 3; wood 4; masonry or others	
$Y_9$	1; without piers 2; height of 2 piers $\neq$ more than 1.25 times 3; height of 2 adjacent piers $\neq$ more than 1.25 times 4; height of 2 adjacent piers $\neq$ more than 1.5 times	
$Y_{10}$	1; real support length > $1.5N_d$ (equation 3.11) 2; $N_d <$ real support length < $1.5N_d$ 3; $0.5N_d <$ real support length < $1.0N_d$ 4; real support length < $0.5N_d$	
$Y_{11}$	1; rock 2; granular and dense soil or consolidated clay 3; medium sands 4; soft to medium clays	

**Table 3.5** Parameters, classification and functions of the Maldonado et al. model

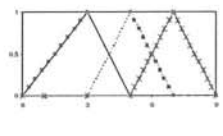
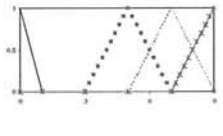
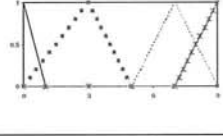
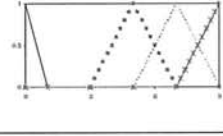
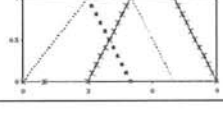

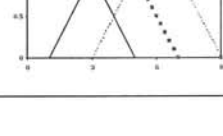
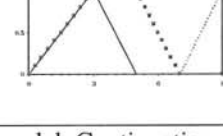
$Y_{12}$	1; closed, with frontal wall and/or counterfort 2; opened 3; reinforced earth 4; spill-trough	
$Y_{13}$	1; without internal hinges 2; bridges with internal hinges and support length $> N_d$ (equation 3.11) 3; with internal hinges and $0.5 N_d \leq \text{real support length} \leq N_d$ 4; with internal hinges and support length $< N_d$ in any case	
$Y_{14}$	1; with seismic isolation or dissipation elements 2; elastomeric bearings 3; sliding bearings 4; metallic bearings	
$Y_{15}$	1; good conservation state 2; apparently good conservation state 3; reasonable doubt of the conservation state 4; bad conservation state	
$Y_{16}$	1; cast in place concrete 2; prefabricated beams 3; prefabricated sections with epoxy joint 4; prefabricated sections with dry joint	
$Y_{17}$	1; cast in place concrete 2; prefabricated in a simple piece 3; prefabricated sections	
$Y_{18}$	1; without liquefaction potential 2; unknown liquefaction potential 3; with liquefaction potential 4; with liquefaction potential and single, hammerhead or bad designed piers	
$Y_{19}$	1; there are not non-structural elements or not affect bridge behaviour 2; there are non-structural elements but unknown influence in the bridge behaviour 3; there are non-structural elements that affect bridge behaviour	

Table 3.5 Parameters, classification and functions of the Maldonado et al. model. Continuation

### 3.2.4. Maldonado et al. model

A recent model which permits to obtain the vulnerability index of bridges was proposed by Maldonado et al. (Maldonado et al. 2000a, Maldonado et al. 2000b). Similar to the Kim model, Maldonado et al. define a series of parameters of analysis classified in four categories, being the last one the most vulnerable. After various studies, the parameters selected were the 19 that are shown in table 3.4. In table 3.5 are indicated the four categories used in the evaluation of the vulnerability of each one of the parameters of table 3.4.

For this model, the minimum length of reference of the bearing, used to evaluate parameters  $Y_4$ ,  $Y_{10}$  and  $Y_{13}$ , is determined by means of the simplified expression proposed by the ATC (ATC-6 1981), that is:

$$N_d = 305 + 2.5 L + 10 H \quad (3.11)$$

where  $N_d$  is the minimum length of reference of the bearing,  $L$  is the bridge length, and  $H$  is the height of the adjacent piers.

Starting from the values of the selected parameters (tables 3.4 and 3.5), Maldonado et al. (2000a y 200b) propose the following weight factor as a vulnerability index:

$$VI_M = \frac{\sum_{i=1}^{19} \beta_i Y_i}{\sum_{i=1}^{19} \beta_i} \quad (3.12)$$

where  $VI_M$  is the vulnerability index,  $\beta_i$  are weight factors, and  $Y_i$  are the model parameters.

The evaluation of the parameters and of their respective weight is based on the arithmetic of the Fuzzy Sets, which is applied in cases of subjective or imprecise information. As a rule, the methodology of the Fuzzy Sets considers that each parameter of the model is qualified through a membership function. In addition, the methodology of the Fuzzy Sets requires the utilization of linguistic variables to qualify each parameter of the model.

In the case proposed by Maldonado et al. (2000a) the degree of vulnerability is assigned through the linguistic variables: not vulnerable, little, moderate, high and very high, with associated values of 0, 3, 5, 7 and 9, respectively. The membership functions were calculated by means of interpolation of the results generated through expert's opinion. The membership functions obtained for the 19 parameters of this model are shown in the figures of the third column of table 3.5. These figures have fragility values (in ordinate) between 0 and 9 and membership functions (in abscissa) normalised to one. In all these figures are distinguished three or four types of graphics related to the vulnerability categories 1, 2, 3, and 4. For the definition of the weight factors,  $\beta_i$ , a similar procedure was followed, which allowed concluding that the parameters  $Y_{17}$  and  $Y_{18}$  are those with less influence and  $Y_3$ ,  $Y_4$ ,  $Y_9$ ,  $Y_{10}$ ,  $Y_{11}$ ,  $Y_{13}$  and  $Y_{15}$  are the most important of the method.



## Chapter 4

### Seismic models of bridges

As it is known, there are a whole variety of structural models to evaluate the behaviour of structures. For bridges, the structural models go from the simplest of a single-degree-of-freedom to the most complex than require important computational efforts in time and space. In this chapter, some individual evaluation models of the seismic vulnerability of bridges through structural analysis will be commented. In general, the procedures selected in each case depend on the data and tools available, the accessible economic expenses and the quality of the results to be obtained.

#### 4.1. Single-degree-of-freedom equivalent model (SDOF)

A way to estimate the behaviour of existing structures is by modelling them as single-degree-of-freedom systems (SDOF). Several methods for developing an equivalent SDOF system from a MDOF (multi-degree-of-freedom) system have been proposed in the literature, one of them is given by Miranda (1993 and 1996). The technique of Miranda can be adapted for bridge structures, if the structural behaviour really follows the fundamental mode of vibration.

In his research, Miranda proposes to estimate the fragility of the structure by comparing the maximum lateral displacement and ductility demands (due to seismic action) with their corresponding capacities. This comparison of demands and capacities is made both at the global level and at local level. The use of this simplified method provides a vulnerability function through the relationship that exists between the damage index and the maximum displacement. Summarising, the simplified evaluation of the existing structure consists of the following steps:

- Construction and calibration of linear and non-linear models of the structure.
- Non-linear pushover static analysis.
- With the results of the previous steps, ductility demands and drift indices are obtained. Their values are defined by means of the following expressions:

$$\begin{aligned}\mu_G &= \frac{\delta_{r,max}}{\delta_{r,y}} \\ \gamma_G &= \frac{\delta_{r,max}}{H}\end{aligned}\tag{4.1}$$

where:  $\delta_{r,max}$  is the maximum top displacement,  $\delta_{r,y}$  is the yield top displacement,  $H$  is the total height,  $\mu_G$  is the global ductility and  $\gamma_G$  is the global drift index.

- Development of an equivalent SDOF model of the structure.
- Non-linear time history analyses, using the equivalent model to estimate the global displacement and global ductility demands. Alternatively, one can use inelastic strength demand spectra and inelastic displacement demand spectral (deterministic or probabilistic).
- Evaluation of the fragility of the structure, using the vulnerability function defined by expression 4.2.

$$DI = 1.0 - \exp \left( \ln(0.5) \left( \frac{\gamma_{Gmax}}{\beta_{DI}} \right) \right) \quad (4.2)$$

In this expression  $DI$  is the damage index that varies from 0 (no damage) to a maximum value of 8,  $\alpha_{DI}$  and  $\beta_{DI}$  are parameters and  $\gamma_{Gmax}$  is the maximum drift. The parameters depend on the drift index associated with the onset of damage and the maximum drift index that can resist the specific structural typology. The parameters can be derived from correlation studies from exhaustive data or quantities provided by codes.

#### 4.2. Model of Hristovski and Ristic

In their researches, Hristovski and Ristic (1996) propose an evaluation methodology, as well as a monitoring and maintenance procedure of bridge structures. Their primary objective is the elaboration of a priorities list for the rehabilitation of these structures and the analysis and localisation of possible inadequate structural behaviour before earthquakes. To achieve this purpose, three types of indices are suggested: critical, seismic vulnerability and usefulness. The critical index evaluates the importance of the structure as emergency system and as lifeline link during an event of collapse. The vulnerability index characterises the structural fragility before failure by earthquakes, while the stress-deformation state and the rupture state under service charges are reflected by the usefulness index. The two last indices are obtained by means of non-linear dynamic and static analysis.

The vulnerability index is governed by the diagnosis of the current state of structures, which is obtained by means of evaluations of the characteristic parameters. Among the many diagnosis parameters the following can be cited: rheological characteristics of concrete and steel, soil-structure effect, geotechnical profiles, strength characteristics of the materials, stress state, dynamic characteristics of the system, etc.

The effectiveness of the parameters selected is assessed through field inspections, experimental tests and dynamical analyses. During the field inspections, all the irregularities and general states of the elements are established. Destructive and non-destructive experimental tests permit to obtain the properties of materials. In some of the bridges, Hristovski and Ristic used standard refraction and seismic dispersion methods to obtain different properties as elasticity modulus, Poisson coefficient and shear modulus of the soil. The dynamic characteristics (period, damping and modes of vibration) are estimated by using the environmental vibration method.

All the parameters compiled in field studies and laboratory tests are used to define mathematical models for analysis and, then, iteratively, are obtained the remaining parameters. An additional proposal of Hristovski and Ristic (1996) includes the evolution of the variation of the selected parameters, through functions and gradients of deterioration measured in fixed time intervals. If there is a permanent follow-up of the incremental values of the parameters, positive or negative, it is possible to define continuous functions for each of them. For example, if the damping parameter is related to the variable  $Q$ , as function as the time  $Q = Q(t)$ , its gradient of deterioration is defined as:

$$GD(t) = \frac{dQ}{dt} \quad (4.3)$$

where:  $GD(t)$  is the gradient of deterioration in a given time instant and  $d/dt$  is the differential operator of the function  $Q(t)$ .

The functions of the parameters and of its gradients of deterioration help to procure an adequate monitoring of the structure, whose immediate consequence is the detection of the degradations and the increase of the vulnerability. Thus, this method would be a line opened in the prevention and damage mitigation.

### 4.3. Seismic capacity assessment for bridge piers

To evaluate the efficiency of different techniques for retrofitting of old structures in Italy, Ciampoli (1994) analyses the behaviour of multi-span RC bridges piers. In his research, Ciampoli considers that the piers are the critical elements of the structure and he assumes that the failure of only one pier determines the failure of the whole system. Ciampoli has estimated the effectiveness of the alternative upgrading techniques by means of the fragility curves of original and upgraded design states.

This research examined simply-supported or continuous reinforced concrete bridge decks (with four spans of five meters), resting on three vertical piers (of hollow circular section) with the height varying between 10 to 40 meters. The summary of the hypotheses made during the study is:

- The variation of the height of the piers along the bridge (three cases).
- The way in which the deck is supported (simply supported or continuous).
- Applying the Monte Carlo method to assesses the seismic fragility of the bridge. The random variables of analysis, are: (1) the rotational and translational stiffness of the soil springs; (2) the elastic flexural rigidity of the piers; (3) the length of the plastic hinge zone; (4) the yielding moment and the ultimate curvature of the plastic hinge; (5) the empirical parameter of the damage index (equation 4.4); and, (6) the elastic stiffness and the yield displacement of the isolation devices. All random variables were log-normally distributed, starting from the mean and the values of the coefficients of variation.
- The seismic input is characterised by the peak ground acceleration in the range 0.10 to 0.45 g and by a total duration of 27 seconds. Three artificial accelerograms were calculated.

- Two different retrofit techniques were compared: the first determines an increase of the flexural capacity and shear strength of the piers and the second modifies the structural response by means of isolation devices in place of the existing bearings. The first intervention consists in the jacketing of the pier with a shotcrete cover and the addition of steel reinforcement (two cases).

The damage in the critical sections is obtained by using the damage index of Park and Ang (Park et al 1985), which is a weighted sum of the ratios between the maximum ductility of the plastic hinges and the energy dissipated. This index is expressed as:

$$DI = \frac{\theta_{max}}{\theta_u} + \lambda \frac{\int_0^L M_s d\theta}{M_{s,y} \theta_u} \quad (4.4)$$

where:  $L$  is the length of the element,  $\theta_{max}$  is the maximum curvature,  $\theta_u$  is the ultimate curvature,  $M_s$  is the section moment,  $M_{s,y}$  is the yielding moment and  $\lambda$  is an empirical parameter, whose mean value can be calibrated as function of the degree of confinement of the concrete core. When  $DI = 1.0$  (the maximum value), the bridge pier suffers the total collapse (and so does the entire bridge). If  $DI = 0.4$ , the bridge shows a high level of damage, which compromises its use and requires extensive repair work.

The failure probability of each bridge had been evaluated as:

$$P_f = 1 - \prod_{i=1, n_p} (1 - P_{fi}) \quad (4.5)$$

where:  $P_f$  is the failure probability of the structure,  $P_{fi}$  is the failure probability of the pier  $i$  of the system and  $n_p$  is the number of piers.

The failure probabilities corresponding to the original and the reinforced bridges are represented in fragility curves as those of the figure 4.1. In this figure are represented, as an example, the fragility curves for one of the proposed models: simply supported deck with the height of the piers of 10, 20 and 30 meters. The letters O, I, a, b, c, d and f represent the original structure, the structure retrofitted with steel jacketing and the several types of interventions with the incorporation of isolation devices, respectively. As it can be observed in the figure 4.1, the incorporation of steel jacketing modified not much the failure probabilities of the structure while; the use of isolation mechanisms can arrive to decrease substantially such failure probabilities.

#### 4.4. Quantification of behaviour coefficients for curved RC bridges

Vaz and Bairrao (Vaz and Bairrao 1996 and Vaz 1994) propose a methodology for the assessment of behaviour coefficients to be adopted in the design of RC bridges. These behaviour coefficients are usually used to correct the effects of non-linear behaviours that elastic designs do not consider. This research uses the concept of vulnerability function as a fundamental tool for the computation of the probability of failure of the whole structure.

The procedure of Vaz and Bairrao is based on the theory of the reliability of structures, where is estimated the forces  $F$  that acted in the structures and the resistance  $R_e$  that they have. The intensity of the forces is measured by a real variable,  $x$ . Failure occurs when this variable reaches the resistance  $R_e$ . Assuming that  $F$  and  $R_e$  are independent random variables, it is possible computed the probability of failure as:

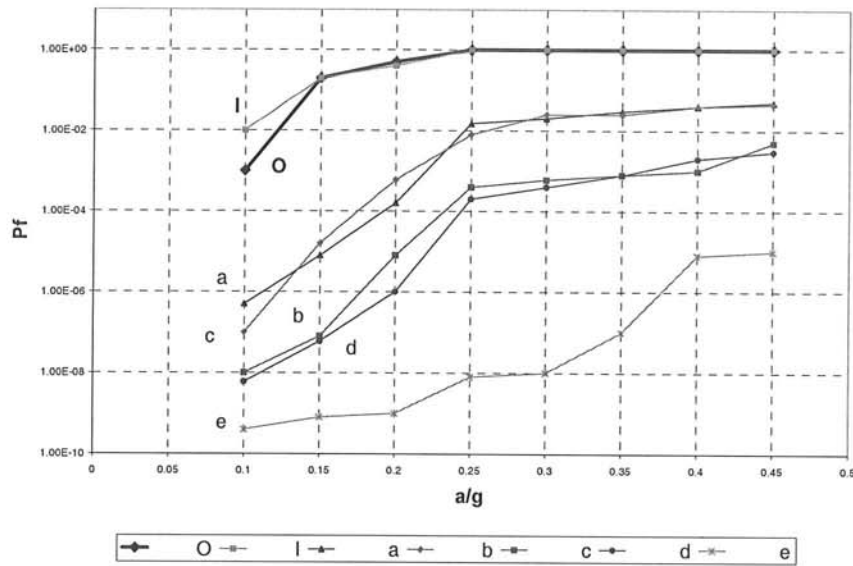


Figure 4.1 Failure probability. Simply supported deck and piers of 10, 20 and 30 meters

$$P_f = \iint_{\Omega} f_F(x) f_{R_e}(x) dF dR_e = \int_0^{\infty} F_{R_e}(x) f_F(x) dx \quad (4.6)$$

or, equivalently,

$$P_f = \int_0^{\infty} (1 - F_F(x)) f_{R_e}(x) dx \quad (4.7)$$

where:  $f_F(x)$  and  $f_{R_e}(x)$  are the density of probability functions of the forces and resistance, respectively, and  $F_F(x)$  and  $F_{R_e}(x)$  are the cumulative probability functions of  $F$  and  $R_e$  respectively.

In this context, the probability characterisation of the variables  $F$  and  $R_e$  is unknown. However, the definition of failure of a structure can be based on the failure of its elements or on values of parameters that define its overall behaviour.

#### 4.4.1. Estimation of the vulnerability function

For the estimation of the vulnerability function for bridges, Vaz and Bairrao assumed that the structure failure depends of its element failure and essentially incorporate the following steps:

1. Definition of the control variables, as the variables that describe the earthquake action effects on the structure. The selection of the type and number of control variables is a consequence of the conditions defined for the failure of the elements.
2. Computation of the control variables by linear analysis, considering the characteristic value of the earthquake actions.

3. Design the structure using the results of the linear analysis corrected with the behaviour coefficients to be assessed.
4. Evaluation of the vulnerability function, defined as a non-linear function relating the values of the parameters describing the loading ( $h$ ) with the values of the control variables ( $c$ ), i.e. the relation between ground motion size and damage. This step is most difficult in the process due to it requires a huge computational effort for the non-linear analyses.

The method described for the above steps requires non-linear analyses for each level of the peak ground acceleration considered. The value of the vulnerability function is estimated, for each ground motion level, as the mean value of the maximum values of the control variables obtained for several input seismic records. To translate the numerical results of the non-linear analyses to a single function representing the overall structural resistance is a very difficult process. To achieve this function, Vaz y Bairrao evaluate the above four step in the next separated points:

- Assignment of a probability distribution of the control variables at the critical sections. Usually, it is acceptable the adoption of a lognormal distribution.
- For a given value of the earthquake size (parameter  $h$ ), it is compute, for each critical section, the local probability of failure  $P_{ih}$ . This failure is evaluate taking the ordinate of the cumulative function corresponding to the density function in equation 4.8. The global probability of failure, the bridge failure, is evaluate as:

$$P_{f(h)} = 1 - \prod_{i=1}^{n_c} (1 - P_{i(h)}) \quad (4.8)$$

where:  $P_{f(h)}$  represents the global probability of failure for the actual value of the parameter  $h$  and  $n_c$  is the number of critical sections. The equation (4.8) assumes that the bridge failure is accomplished by the failure of all independent critical sections.

- The procedure can be extended if the structure has more than one material. In that case, the probability  $P_{f(h)}$  shall be estimate for all the materials and a generalised probability of failure  $P_{g(h)}$  can be calculated. The probability  $P_{g(h)}$  takes into account the behaviour of several critical sections and several materials. The general probability is given by:

$$P_{g(h)} = 1 - \prod_{m=1}^{nm} (1 - P_{f(h)})_m \quad (4.9)$$

where:  $nm$  is the number of materials considered.

- Repeating the procedure for all the values of the parameter  $h$ , so a generalised vulnerability function is obtained and the corresponding cumulative function  $F_c$  as well, whose meaning is similar to  $F_{Re}(x)$  in equation 4.6. The probability of failure is then computed by:

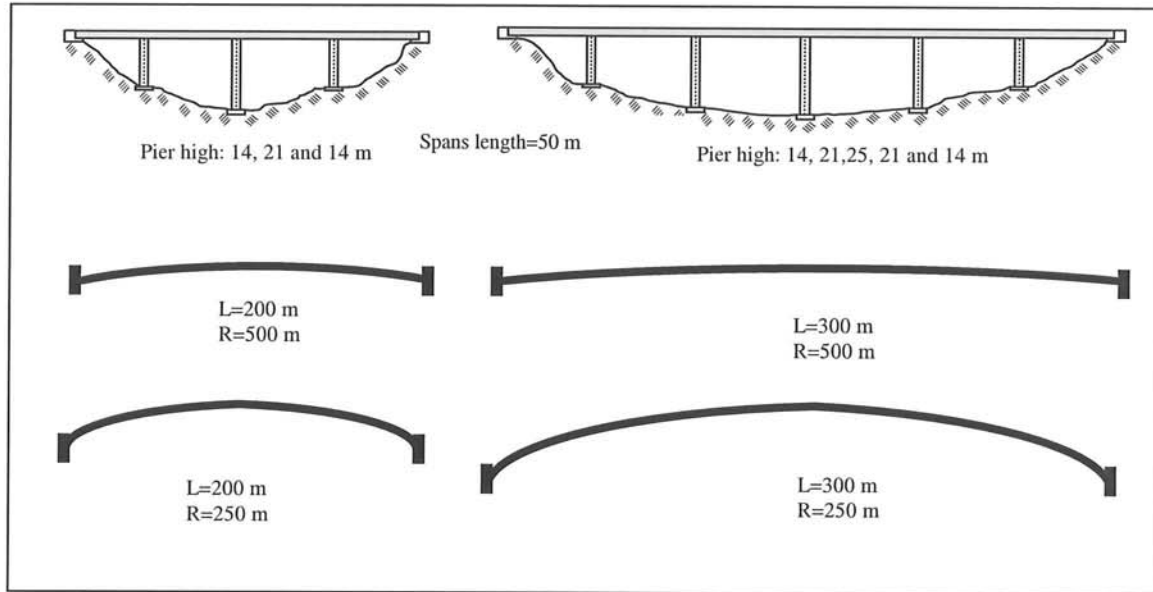


Figure 4.2 Bridge models used by Vaz and Bairrao.

$$P_f = \int_0^{\infty} f_h(h) F_c(V(h)) dh \quad (4.10)$$

where  $f_h(h)$  is the density of probability function of the ground motion (hazard) and  $F_c(V(h))$  is the cumulative probability of the resistance of the structure.

#### 4.4.2. Example of application

To apply the procedure of the vulnerability function of bridges, Vaz and Bairrao propose as structural models regular bridges, with three and five piers of hollow circular sections and pier heights between 14 m to 28 m. In addition, these models consider variations of the curvature radii with values of 250 m, 500 m and an infinite value (straight bridge). The general layout of the bridges used is schematically shown in figure 4.2. Considering the above conditions and the behaviour coefficients, a total of 36 different structures were designed and analysed

After the evaluation of the dynamic characteristics of bridges, the structures were idealised by spatial models with beam elements, considering six degree of freedom per node. Additionally, the deck of the spatial models was assumed as an elastic element with distributed weight.

Normally, any quantity describing the response of the structures can be used as control variables. In the particular case of Vaz and Bairrao, the maximum values of strains in each critical section of the bridge were selected as control variables, principally due to the intuitive characteristics of these quantities and the used of a fibre model. Therefore, the only results retained from the non-linear analyses were the maximum compressive strains at the concrete and the maximum tensile strains at the steel reinforcement in each critical section, taking into account that these two materials defined the local failure conditions.

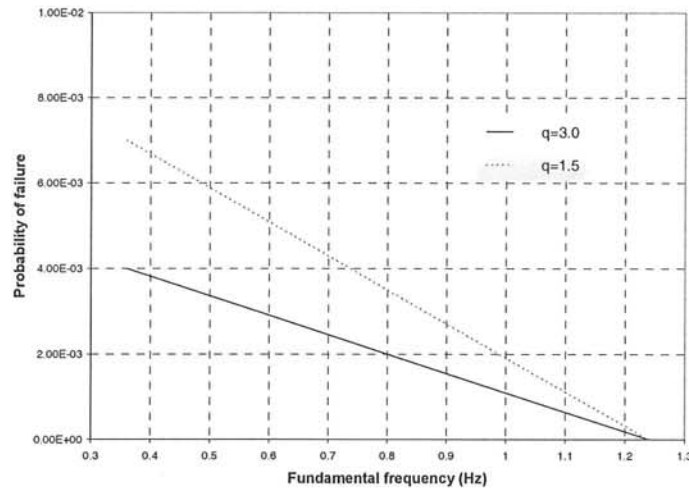


Figure 4.3 Fragility curves of straight bridges

The earthquakes were represented by probability functions of the peak ground acceleration. The extreme type I distribution (considering a 50 years reference period and peak ground acceleration  $a_g$ ) were assumed by Vaz and Bairrao. As an example, the probability of failure obtained for the straight longitudinal axis bridges have been plotted against the fundamental transverse frequency in figure 4.3, as a fragility curve. In this figure can be observed that the structural vulnerability increases when the natural frequencies in the transverse direction decrease.

Vaz and Bairrao concludes that further research is need, considering more complex structural types, the real behaviour of decks and bearings by vertical accelerations, higher values of the peak ground acceleration, improvement in the numerical models (although this conduce to increase the computational costs) and the study of the structures with the simultaneous action of all the earthquake components.

#### 4.5. Seismic fragility curves of bridges using a finite element model

The approach to fragility curves adopted by Mullen and Cakmak (1997) is one in which the relationship between damage and seismic intensity is obtained trough numerical experiments, with artificial events and damage responses of bridges. The damage responses were obtained using non-linear dynamic time history analysis of structural models with a new 3D-pile damage element. The random nature of the above relationship is considered by creating a finite number of realisations first of the system and then of the input motions.

In next sections will be described the steps followed by Mullen and Cakmak in their analytical procedure to obtain fragility curves for bridges. For a more detailed information about the formulation of the 3D-damage pier model, it should be consulted the report of Mullen and Cakmak (1997).

##### 4.5.1. Hypothesis of the analysis

In its analysis, Mullen y Cakmak considered the following hypothesis:

- *3D damage element.* One of the most important aspects inherent to the evaluation of the vulnerability of bridges is the prediction of damage response to seismic events, principally for pier elements. Common design and analytical procedures for highway bridges have tended to ignore the 3D nature of response and its effect on damage



estimation, primarily due to the complexity this introduce to the problem. Unfortunately, in most cases, the 2D approximation not always reproduces the real behaviour and more detailed analyses have required. Attendant to this aspect, Mullen and Cakmak developed a 3D approach to take the damage response of RC highway bridge piers, submit to a flexure state. The formulation proposes by Mullen and Cakmak is consistent with basic principles of continuum mechanics and offers a unique approach to fiber modelling of reinforced concrete piers.

The formulation of Mullen and Cakmak is based on the formulation of a new element. This new element considers behaviours such as concrete tensile cracking, concrete softening and spalling and plasticity of longitudinal reinforcement up to fracture strains. Additionally, confinement effects of transverse reinforcement on concrete strength and ductility are considered. The proposed model incorporate the constitutive law, the kinematics and continuity by means of a fiber approach, where the coupling between normal and shear stress and strains components is neglected.

The formulated element considers the damage through the variation of the secant stiffness of an element of two nodes. This element adopted a lumped mass formulation and it is based on the no-warping Bernoulli-Euler assumption for kinematics of a cross-section during combined axial and biaxial flexure deformation. The stiffness of this element, base on a local element reference system, is integrated by means of a fiber approach; considering discrete section areas with material characteristics constant in each section. Over each of these areas is evaluated the time-dependent variation of the principal axes (translation and rotation) of the cross-section for the integration process of the element stiffness.

- *Constitutive laws.* The tangent stiffness of the element is derived considering the implementation constitutive laws of the materials at every point of the element. Mullen and Cakmak selected two stress-strain relations for concrete material (confined and unconfined) and one for steel fibers.

#### 4.5.2. Fragility curves

Mullen and Cakmak (1997) considered the maximum (inter)story drift ratio as a damage index for use in fragility analyses of 3D bridge systems. This index was used because it shown to be one of the most reliable-damage indices for building columns. The maximum (inter)story drift ratio is defined as the maximum relative displacement of the column ends normalised with respect to the building height. In bridges case there is only one "story". If  $\delta_{r,max}$  is the maximum relative pier end displacement, the drift damage index used is defined as:

$$DI = \frac{\delta_{r,max}}{H} \quad (4.11)$$

where:  $DI$  is the damage index and  $H$  is the height of the taller pier.

The variables selected as random variables for the analysis were:

- $E_c$  = elastic modulus of the concrete.
- $E_a$  = elastic modulus of the trilinear curve of steel elements.
- $\sigma_0^c$  = undamaged compression stress of the unconfined concrete.

No.	$\delta_{r,max}$ (%)	Classification	Material damage behaviour
1	0.4	Light	Moderate unconfined concrete degradation
2	0.8	Minor	Moderate confined concrete degradation
3	1.2	Moderate	Severe confined concrete degradation
4	$\geq 1.6$	Severe	Confined concrete crushing; bar fracture

Table 4.1 Damage limit state classification

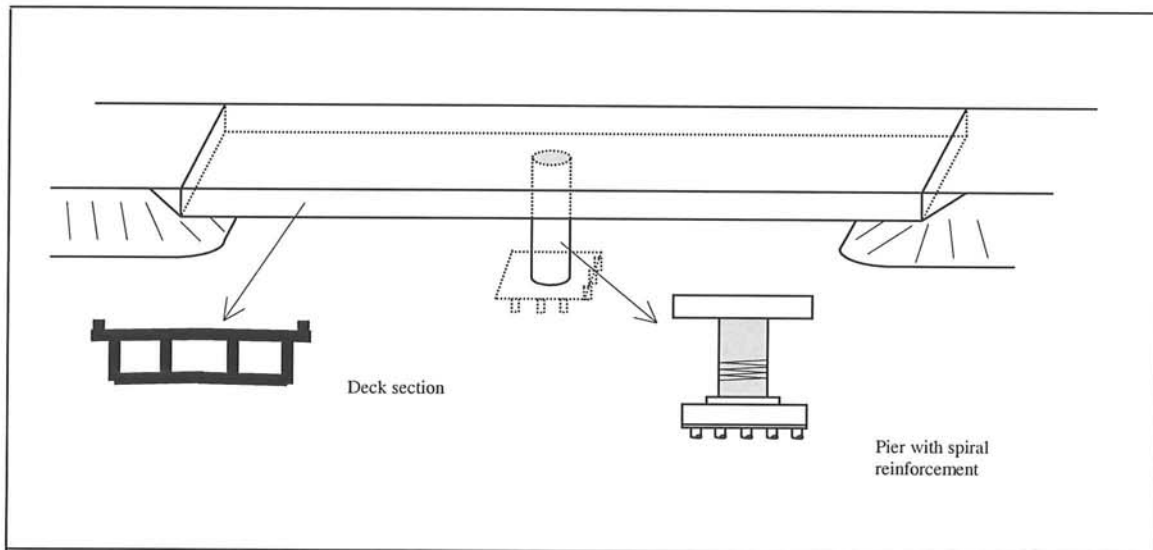


Figure 4.4 MRO bridge scheme

- $k_1, k_2$  = free parameters of the constitutive concrete law.
- $\varepsilon^{cc}(0.2\sigma_0)$  = undamaged compression strain of the unconfined concrete.

These variables were chosen because they were considered representative of the non-linear response of the structural model. For convenience, all the variables were considered uncorrelated. The random variables  $E_c, E_a, \sigma_0^c$  were assumed to be normally distributed with mean given by the calibration values of the pier model and coefficient of variation of 0.1. The remaining variables,  $k_1, k_2$ , and  $\varepsilon^{cc}(0.2\sigma_0)$ , were assumed to be uniformly distributed within a prescribed range value.

For each damage limit state,  $i$ , the value of fragility,  $P_f$ , is defined as the conditional probability of exceeding the damage state,  $DI^i$ , given and excitation of intensity,  $I_e^j$  (with PGA values as measure of intensity), as expression 4.12.

$$P_f = P\left[DI > DI^i / I_e = I_e^j\right] = 1 - F^j(DI^i) \quad (4.12)$$

where:  $F^j$  is the cumulative probability distribution for  $DI^i$  at intensity  $j$ .

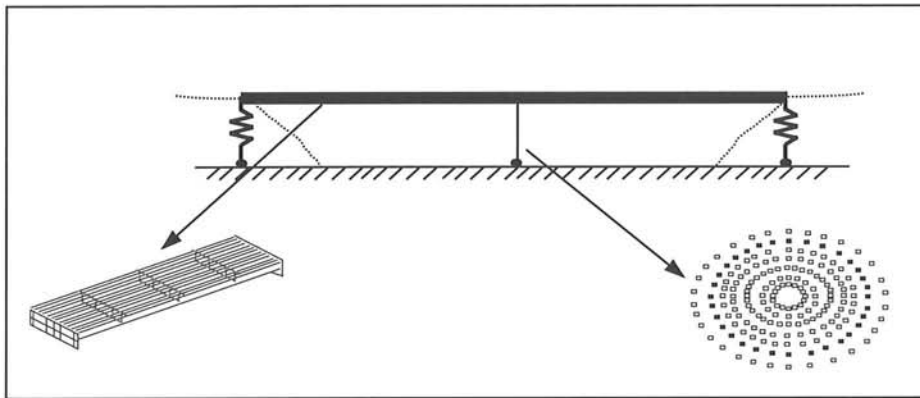


Figure 4.5 Model of the selected structure

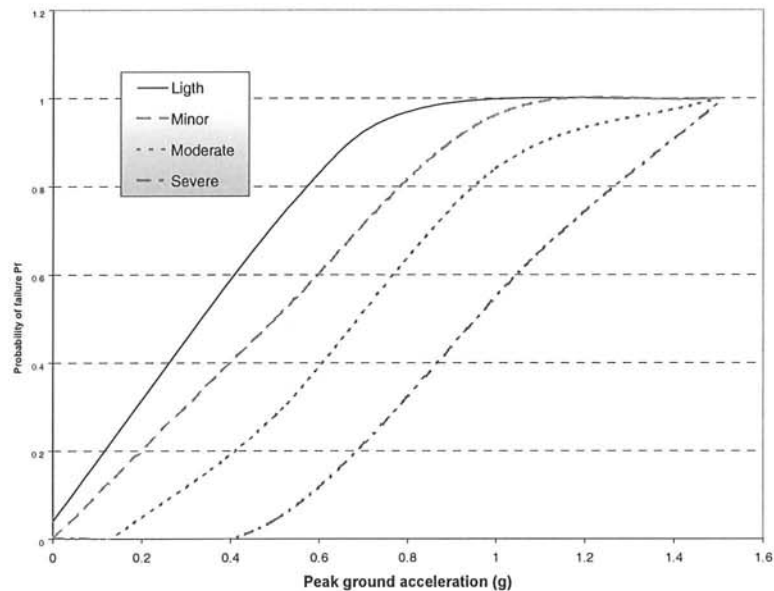


Figure 4.6 Fragility curve for the bridge

The classification of the damage limit states, using the displacement damage index, that was proposed by Mullen and Cakmak is indicated in table 4.1. This classification is principally based on material damage behaviour. The value for severe damage of 0.0016 is close to the value of interstory drift of 0.02, which is considered a severe damage limit state for buildings.

#### 4.5.3. - Example

The formulation of Mullen and Cakmak is used to model the piers of a bridge, for which is obtained the global damage. The modelled bridge is the one represented in figure 4.4, located in El Centro, California.

This bridge is a RC two-span continuous overpass with a single-pier bent at the deck midlength. The deck is a three-cell box-girder, which is integral with the solid pier cap located at the centre and integral with the RC abutment walls at the ends. The bridge was modelled using a finite element with formulations of pier damage (as are shown in figure 4.5). The FE

---

model includes a linear, homogeneous and isotropic deck-element and a fiber pier model with spiral reinforcement detailing and consideration of the confinement effect. The consequence of the surrounding soil at abutments and pier foundation is considered by means of stiffness and mass elements. The artificial records are obtained starting from real records registered during the Imperial Valley earthquake. With the above procedure a set of 30 realisations were generated.

For the modelled structure and for the random variables, the responses to the defined seismic action were obtained. Through these responses the damage index were calculated. Mullen and Cakmak accomplished a minimum least square linear regression analysis of the random input motion results to obtain fragility curves. An example of these continuous curves between drift damage and earthquake size is shown in figure 4.6. Thus, if  $P_f = 0.5$ , is seen that values of PGA of 0.4, 0.55, 0.7, and 1.0g are required to achieve light, minor, moderate, and severe damage limit state, respectively.

## **Chapter 5**

### **Models based on expert's judgement**

In this chapter will be discussed the methodology used by the Applied Technology Council (ATC-13 1985 and ATC-25 1991) to determine the seismic vulnerability, at national level, of the common bridge typologies existing in the United States of America. The evaluation proposal by the ATC to obtain damage probability matrices (DPM) and fragility curves is based on rigorous statistic analysis of expert's opinions about the general behaviour of the structures. As opposed to the methods commented in chapter three, the methodology of the ATC does not assign a global value of fragility to each bridge, in its place provides qualitative classifications of damage states and works with those values. Additionally, the ATC methodology is different of the methodology followed by the examples that are explained in the next chapter six, in that the statistic analyses are accomplished based on the experts opinions and not on real damage data.

In the ATC-25, the principal objective is the estimation of the indirect and direct probable costs of the systems submitted to different seismic action. To obtain these costs, it was: (1) digitised the more complete data inventories; (2) estimated the damage probability matrices; (3) calculated the fragility curves; and, (4) characterised the continuous functions of residual capacity. In the following paragraphs, the methodology followed in the ACT-25 for the calculation of the costs produced by seismic action will be discussed, making special emphasis on the bridge structures.

#### **5.1. Data inventory**

As it was commented previously, an adequate and exhaustive summary of the data can leads to correct results; however, sometimes this is not possible due to economical, political or technical conditions. In ATC-25, a comprehensive national digitised data set on the highway system was obtained. The system includes state and federal highways, but excludes county and local roads. The data include the location of the different facilities and some information of them as, for example, the number of spans or the number of bents. The studied structures are, as a rule, systems adequately designed against lateral loads and earthquakes. They are structures mainly built after the seventies and include systems composed of steel, RC (principally), masonry and wood. The database used in this research includes 144 785 bridges.

#### **5.2. Damage probability matrices (DPM) of the ATC-13**

In the ATC-25 were not estimated the damage probability matrices (DPM) of the structures, since these were taken from the ATC-13 (1985). Such DPM are obtained for all the structural typologies in the American State of California. In ATC-13, a number of classification was assigned to all the structures, starting with its seismic behaviour and

function. For bridges, in ATC-13, the assigned classification and the reference numbers associated to each class are:

Bridges:	Number
• Conventional (spans less than 150 m)	
Multiple/single spans	24
Continuous/monolithic	25
• Greater (spans with more than 150 m)	30

The DPM proposals in the ATC-13 are in accordance with the format shown in table 5.1. This table is the result of the application of Delphis method, which uses questionnaire formulation. The information is obtained from individual expert's answers, repetition of the questionnaires (for information feedback) and, finally, statistical of the answers. In these questionnaires, the experts assign a damage factor and a weight to each structural typology with various degrees of deterioration. Therefore, the values provided by each expert are based on the experience and the quality of their answers. The results obtained from the questionnaires are the average and standard deviation of the random variable "damage factor", for which a function of probability distribution is fitted. For this case, the probability distribution selected to this variable is the Beta function.

Finally, the probabilities (as shown in table 5.1) for each considerate damage state and earthquake size, are obtained through the following expression:

$$P(\bar{X}_j) = \int_{x_j}^{x_{j+1}} f_{\bar{X}}(x) dx \quad j = 0, 1, \dots, N_{ds} \quad (5.1)$$

in which:  $P(\bar{X}_j)$  is the probability of a damage factor between  $x_j$  and  $x_{j+1}$ ;  $\bar{X}_j = \mu [F_{\bar{X}}(x_{j+1}) - F_{\bar{X}}(x_j)]$  is the mean damage state;  $F_{\bar{X}}(x)$  is the cumulative Beta probability distribution, and  $N_{ds}$  is the total number of damage states.

Table 5.1 is a format example used in the ATC-13, but also shows the DPM obtained for the classification number 25 (monolithic bridges with span length smaller than 150 m.). Thus, if in California occurs an earthquake of intensity IX on the Modified Mercalli Intensity scale (MMI), it can be concluded that this type of bridges has a probability of 56.5% to suffer light damage.

### 5.3. Loss of function and restoration times

These functions are obtained by means of statistics from restoration time and loss of function of different structural groups. Such functions are also the result of the research developed by the ATC-13 and are estimated through a similar process as for the damage probability matrices, that is, through statistics of expert's judgements.

In the questionnaires proposed at this stage, it is considered: (1) it was not urgent to repair the damaged structure; (2) there are unlimited resources for its repair; and (3) there is a plan for repairing the structures. Thus, the restoration times are obtained starting from the expert's opinion, for percentages of restoration of 30%, 60% and 100%.

Damage State	Damage Factor (%)	Central Damage (%)	Probability of damage (%) MMI intensity and damage state						
			VI	VII	VIII	IX	X	XI	XII
None	0	0	93.6	8.1	0.9	-	-	-	-
Soft	0-1	0.5	6.4	77.8	17.6	-	-	-	-
Light	1-10	5	-	14.1	78.6	56.5	-	-	-
Moderate	10-30	20	-	-	2.9	43.5	1.8	1.2	0.7
High	30-60	45	-	-	-	-	98.2	36.8	5.7
Great	60-100	80	-	-	-	-	-	61.9	39.1
Collapse	100	100	-	-	-	-	-	0.1	54.5

The damage states are described as:  
None = No damage  
Soft = Minor damage of some elements, not required repair  
Light = Mean damage located in some components, generally repair is not required  
Moderate = Mean damage located in many components, some repair is required  
High = Extensive damage that requires greater repair  
Great = Great scattered damage, it has to be decided between repairing or demolishing  
Collapse = Total destruction of the greater part of the system

**Table 5.1** DPM for conventional bridges (class number 25, ATC-13)

DS	NEXP	M30	S30	M60	S60	M100	S100
Soft	4	0.3	0.4	0.3	0.4	1.1	1.3
Light	4	1.1	1.3	2.2	3.0	8.4	6.2
Moderate	4	33.8	33.9	52.7	43.7	84.4	60.7
High	4	84.4	60.7	146.3	87.4	303.6	72.0
Great	4	419.8	112.1	592.0	87.2	686.0	217.6
Destruction	4	-	-	-	-	752.9	180.9

DS = Damage state  
NEXP = Number of consulted experts  
M30 and S30; M60 and S60; and M100 and S100 = Mean and standard deviation of the experts judgements for a percentage of restoration of the 30%, 60% and 100%, respectively.

**Table 5.2** Loss of function and restoration times, in days. Conventional bridges (ATC-13)

The structures were again classified, according their commercial function. The commercial group of the bridges, highway systems (group 25), is constituted by: important bridges, tunnels, conventional bridges, conventional highways, roads without toll, streets of cities and terminal stations. For each category and for each commercial group, factors of importance were determined, also through expert's judgement, to evaluate the global behaviour within each commercial group.

An example of the obtained loss function and restoration times matrices for conventional bridges is shown in table 5.2. From this table can be concluded, for example, that there are necessary, in average, 592 days to obtain a 60% of reparation, when the structure has suffered a greater damage state.

#### 5.4. Fragility curves

Starting from the damage probability matrices, loss of function and restoration times matrices of the ATC-13; the fragility curves for each structural typology and for each seismic scenario have been obtained. The fragility curves are represented by the repair cost, expressed

as a fraction of the total value of the element. On the other hand, the restoration curves indicate the capacity of the structure as a function of the elapsed time since the earthquake occurred. The calculus process of these curves considers:

1. *Determination of continuous relation between seismic damage and earthquake size.* To achieve these relations, statistical regressions of the form were performed:

$$DMG = \exp(c_1)MMI^{c_2} \quad (5.2)$$

where:  $DMG$  is the central damage factor for each damage state;  $MMI$  is the size of the earthquake and  $c_1$  and  $c_2$  are the regression coefficients, starting from data of the ATC-13, for each class of bridges. A damage curve of the form shown in figure 5.1 is thus determined for conventional highway bridges.

2. Data on time-to-restoration for different social function groups are use to perform the following regression, which gives a continuous relation between the damage state and the corresponding restoration time:

$$T_R = \exp(c_3)DMG^{c_4} \quad (5.3)$$

where:  $T_R$  is the restoration time, in days;  $DMG$  is the central damage factor for each damage state; and,  $c_3$  and  $c_4$  are the regression coefficients. Regressions of the above form are performed for each group using the data of ATC-13 on restoration times for 30%, 60% and 100% restoration.

3. The regressions obtained from the previous two steps are used to arrive at the restoration curves. The restoration curve for each bridge group and for each intensity is obtained by fitting a straight line through the three points corresponding to 30%, 60% and 100% restoration time. The regression line has the following equation:

$$R = c_5 + (c_6)(T_R) \quad (5.4)$$

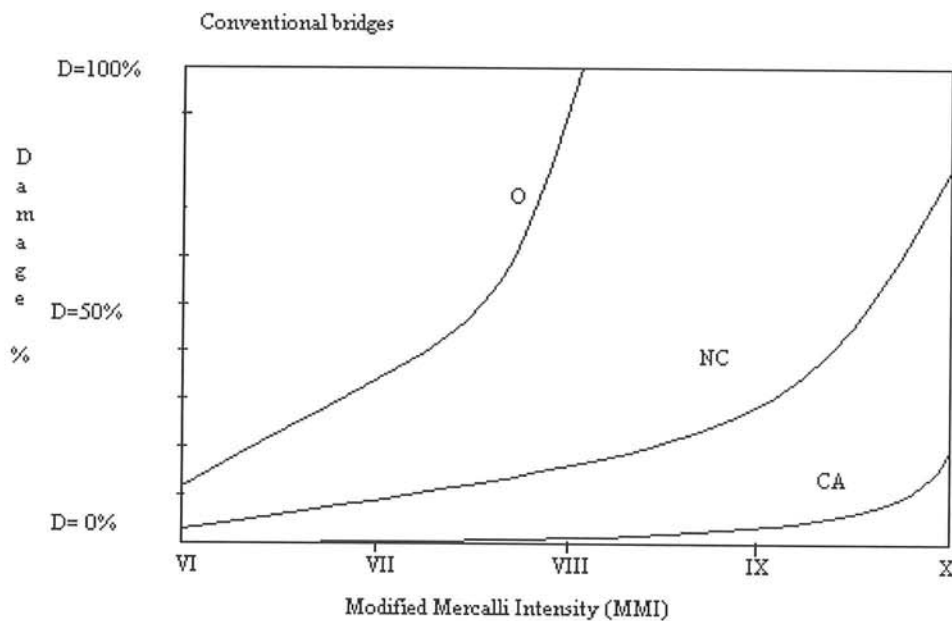
where:  $R$  is the percentage restored,  $T_R$  is the restoration time, in days, and,  $c_5$  and  $c_6$  are the regression coefficients.

Figure 5.2 shows the restoration times relation (in days) versus the residual capacity for conventional bridges in California. This figure also indicates the values of the regression coefficients, calculated for several MMI intensities.

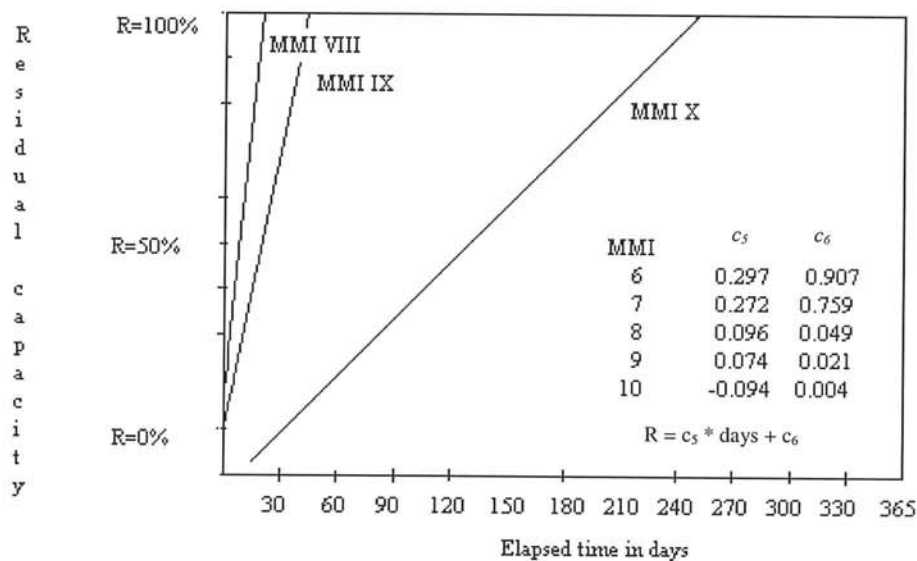
### 5.5. Direct damage

The economic impact of disruption of lifelines is function of the economic losses from damage. These costs were divided into that occasioned by direct and indirect damage. Direct damage is defined as damage resulting directly from ground shaking or other collateral causes, such as liquefaction. For each structural class, it is expressed in terms of cost of repair divided by replacement cost and varies from 0 to 1.0 (0% to 100%).





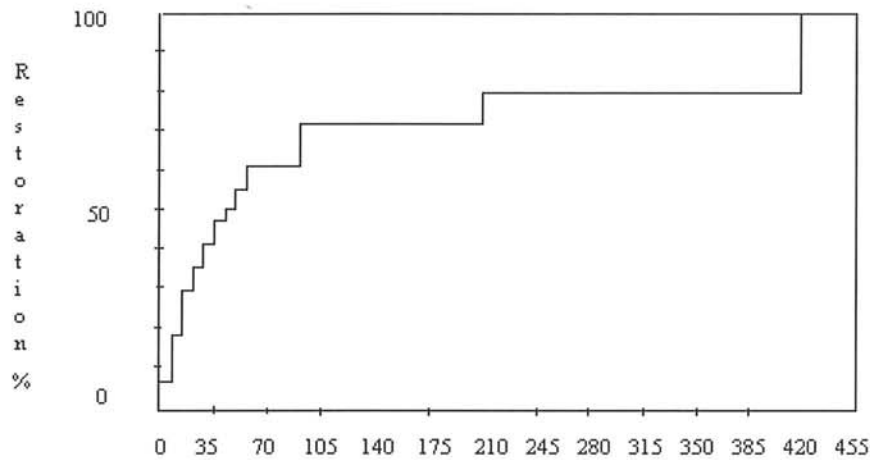
**Figure 5.1** Fragility curves for conventional bridges in USA  
CA= Structures in California, NC= zones of strong intensity outside of California and O = others



**Figure 5.2** Residual capacity for conventional bridges in California.

In the ATC-25 the direct cost is determined using (1) estimations of ground shaking intensity provided by the seismic risk model, (2) inventory data specifying the location and type of structure affected, and (3) fragility curves that relate seismic intensity and site conditions to expected damage.

In ATC-25, the analysis approach to estimate direct damages considers both damage resulting from ground shaking and damage resulting from liquefaction. Damage due to other collateral loss causes, such as landslide and fire following earthquake, are not included because of the unavailability of inventory information and the lack of available models for estimating these losses.



**Figure 5.3** Residual highways capacity in the epicentral region after a given seismic scenario

The analysis approach used for estimating the direct seismic damage assigns, for an earthquake scenario, MMI levels to each 25 km grid cell in the affected region, together with the magnitude and the fault rupture location. Damage states were then estimated for each affected lifeline component in each grid cell, using the fragility curves calculated previously. Damage due to liquefaction was estimated using the probability of ground failure in each grid cell, according to the soil conditions. After the damages due to the seismic ground motion and the liquefaction were established, the total direct damage was calculated. As suggested in ATC-13, the total direct damage being simply the sum of damage due to the earthquake with the damage due to liquefaction, being this sum always equal to or less than 1.0 (100%).

For comparative purposes, four damage states are considered by ATC-25: (1) light damage (1-10% replacement value); (2) moderate damage (10-30% for the replacement value); (3) heavy damage (30-60% of the replacement value); and (4) major damage up to failure (60-100% of the replacement value).

### 5.6. Indirect economic losses

The indirect costs are the economic effects produced by the interruption of the activities after an earthquake. These indirect effects are nowadays very important, however, only a few projects have been directed to their evaluation (Chang et al., 1998).

A simple approximation of the evaluation of these indirect losses is developed in the ATC-25 for the lifeline systems in the United States. The proposed methodology is based on the estimation of the interruption time of the lifeline services by direct damage and the determination of the resulting economic losses of this interruption. The procedure is divided into two parts:

- *Evaluation of the interruption of the service of the system.* The interruption of the service of the structures resulting from direct damage is quantified in residual capacity plots that define the percentage of function restored as a function of time. The curves are estimated for each structure type using: (1) the time-to-restoration curves, (2) estimation of the seismic motion intensity by means of seismic hazard models, and (3) inventory data specifying the location and type of structure affected.

The continuous functions evaluated at point 5.4 (as those of figure 5.2) are applied directly as curves of restoration times if the lifeline components are site-specific systems, such as bridges. For extended regional networks (pipelines or highways), special analysis procedures were used (see ATC-25 1991). The use of the restoration curves origin the residual capacity, defined by means of "structures interruption plots" that show restoration in one-month-interval step function. Initially, these step functions were computed for each structure in a region, and then averaged over all structures of the same type of the region using the following equation:

$$RC_j = \sum_{i=1}^{n_s} (C_i \times R_j) / \sum_{i=1}^{n_s} C_i \quad (5.5)$$

where:  $RC_j$  is the residual capacity at time step  $j$ ,  $C_i$  is the capacity of structure  $i$  (obtained from databases or considerate equal for all the structures, generally the more probable value),  $R_j$  is the restoration of structure  $i$  at time step  $j$ , and  $n_s$  is the number of structures.

An example of such restoration curves for highways group, to which belongs bridges, is showed in figure 5.3. In this figure, one can see that immediately after the earthquake the system losses 95% of its capacity, being its total restoration achieved after 420 days.

- *Indirect economic losses.* Indirect economic losses are estimated for each structural system and seismic scenario using the residual capacity plots and economic tables. The equation used to calculate indirect economic losses is as follows:

$$IEL = \sum_{i=1}^{N_1} \sum_{j=1}^{N_2} \sum_{k=1}^{N_3} (A_{IEL})(B_{IEL})(C_{IEL})(D_{IEL}) \quad (5.6)$$

where  $IEL$  is the Indirect Economic Loss,  $N_1$  is the number of affected regions,  $N_2$  is the number of economic sectors,  $N_3$  is the number of months the structural system has loss in capacity,  $A_{IEL}$  is the percent "Value-Added-Lost" per month,  $B_{IEL}$  is the national percent U.S.A. "Economy Value Added",  $C_{IEL}$  is the percent of population affected, and  $D_{IEL}$  is the monthly "Gross National Product". The economic value is the production cost less the materials cost, for each economic sector. This and the percentage of the economic value of the nation are determined by governmental economic sectors.

### 5.7. Recent researches on loss assessment

After the publication of the ATC-25, the researches that evaluate losses occurred during earthquakes have increased. This increase is mainly due to the huge economic loss produced by recent earthquakes and to the constant development of the computational models. Some of the most recent researches on this topic can be consulted in Alarcón (1997), Bourque (1997), Brookshire et al. (1997), D'Ayala et al. (1997), Eguchi et al. (1997), Hwan et al. (1997), King (1996), King et al. (1997), Kircher et al. (1997a and 1997b), MacCormak (1997), Olshansky (1997), Rojahn et al. (1997), Shinozuka et al. (1997), Werner et al. (1997), Whitman et al. (1997), and Who (1997).

---

Among these, evaluations of losses in the highways system, especially for bridges, are reported in Brookshire et al., Eguchi et al., King et al., Rojahn et al., Werner et al., and Whitman et al. The aspects improved in previous researches included:

1. The acquisition and managing procedures of data (Eguchi, 1997, Rojahn et al. 1997), including the application of Geographical Information Systems and telemetric systems.
2. The estimation of the earthquake size using real and simulated records (Whitman et al. 1997).
3. The improvement of the damage probability matrices. Some researches include the estimation of damage caused by post-earthquake fire and other collateral effects as landslide and fault displacement (Kiremidjian et al 2001).
4. The improvement of the loss of function matrices, considering for its evaluation aspects as: the percentages of deaths and injured, rates of loss in contents, people translation, time delays, etc (Rojahn et al. 1997, Whitman et al. 1997, King et al. 1997).

For the last point, numerous researches are being conducted now, principally to develop reliable models to estimate traffic flows when one or several components of a communication system are collapsed.

## Chapter 6

### Models based on statistics of real damage data

The last type of methodologies to determine the seismic vulnerability of bridges is included in the statistic evaluations of damage data produced by past earthquakes. This type of procedures is used in places where the available information is sufficient to achieve adapted statistics conclusions; therefore, its application is restricted to zones with low or moderate seismicity.

The procedures that will be commented in forward are based on statistic studies of the damages produced in different structural typologies, to assign qualitative values of the damage states, and to build damage probability matrices and fragility curves for each typology.

#### 6.1. DPM for transportation systems after Tangshan earthquake

The 1976 Tangshan earthquake caused important damage to people, building structures and lifeline system. To comprise the earthquakes effects on bridges and to decrease their damage, Xueshen and Shuming (1995) defined some damage probability matrices (DPM) for the transportation system in Tangshan region. The DPM obtained were based on statistics of loss dates of roads and bridges damages by the 1976 earthquake.

To get the DPM for bridges affected by Tangshan earthquake, five levels of damage were selected: scarcely damaging, slightly damaging, damaging, heavily damaging and devastating. Description of each level is as follow:

- **Scarcely damaging.** Bridges that have not been affected by earthquakes damage.
- **Slightly damaging.** There are not damages in the main load structure of the bridge. The structure has some cracks, but these not affected the load force of the structure. The bridge can be used after slight repair.
- **Damaging.** The main bridge structures were damaged or there are local damages. Therefore, additional structure elements are heavily destroyed. The piers and abutments have been lightly dipped and deformed. There are some small cracks in piers and union zones. The seat support is displaced and displacements occurred in main girders. The road approach is dipped. All of these problems have decreased the structural behaviour, so normal use will be possible if the bridge is repaired.
- **Heavily damaging.** The main bridge structures were heavily damaged. Bridge piers and abutments have been dipped. Horizontal displacement and inhomogeneous subsidence are obvious. All of these problems have produced a structure in a dangerous state; thus, it is impossible to use it normally without heavy repair and transforms.

State	Intensity			
	6	7	8	9-11
Devastating	0	0.038	0.052	0.289
Heavily damaging	0	0.019	0.287	0.267
Damaging	0	0.192	0.316	0.177
Slightly damaging	0.167	0.076	0.052	0.067
Scarcely damaging	0.833	0.769	0.289	0.200

Table 6.1 Damage Probability Matrix for Tangshan bridges

State	Intensity			
	7	8	9	10-11
$A_{LF}$	0.020	0.050	0.250	0.285
$B_{LF}$	0.080	0.263	0.125	0.250
$C_{LF}$	0.900	0.680	0.625	0.464

Table 6.2 Loss of function matrix for Tangshan bridges

- **Devastating.** The structure of the bridge is fallen; its piers and abutments are broken to fall. These bridges should not be used, so they will be demolished.

In this investigation, also, three classification of loss of function were used, these are defined as  $A_{LF}$ ,  $B_{LF}$  and  $C_{LF}$ . The classification  $A_{LF}$  is assigned when interruption of the traffic system take place. Bridges not used until important repair are included in  $B_{LF}$  class, and  $C_{LF}$  class is for structures with normal function.

All the bridges located in the affected region were classified conform its typology, damage level and classification of loss of function. Additionally, for each bridge was assigned the intensity level (Chinese scale) suffered during the earthquake.

Based on the statistic methods, only one (because of less of data) DMP matrix of bridges was obtained; this matrix is showed in table 6.1. Thus, conform to table 6.1, a bridge has a probability of 0.287 of suffered a heavily damaging state when an earthquake with a Chinese scale of 8 had occurred. Table 6.2 presents the loss of function matrix of bridges. Conform this last table; a bridge has a probability of 0.250 of sustained interruption of the traffic system ( $A_{LF}$ ) when an earthquake of intensity of 9 acted over it.

## 6.2. Evaluation of bridge damage data from The Loma Prieta and Northridge earthquakes

During the Loma Prieta (1989) and Northridge (1994) earthquakes existing bridges were damaged, principally those designed before the current California seismic code, implemented in 1971. Bridge damage data from these earthquakes were used by Basöz and Kiremidjian (Basöz and Kiremidjian 1995 and 1998, and Kiremidjian and Basöz 1997) to define fragility curves. Reports of bridge damage were analysed by these researches to evaluate its characteristics and correlated them to observed or estimated ground motions levels and repair cost. The research aims were to produce guidance on the seismic assessment, screening, evaluation and retrofitting of transportation systems. Forward, the procedure followed by Basöz and Kiremidjian will be outlined.

### 6.2.1. Database characteristics

The first step for this kind of researches is the compilation of a comprehensive database on bridge damage and repair cost, as was done by Xueshen and Shuming, 1995. This database can be used for comparative studies on bridge damage and for to identify the needs for better data collection and post-earthquake investigation. The collected database by the Californian bridges, compiled for each earthquake, unclosed:

- Structural characteristics, abutment type, number of spans, type of superstructure and substructure, age, etc.
- Damage states for damaged bridges, minor and *major* for bridges damaged during the Loma Prieta earthquake, and *minor*, *moderate*, *major* and *collapse* for those damaged in the Northridge earthquake.
- Repair cost, including total estimated repair cost for a bridge, repair cost ratio, and more detailed information on repair work and cost for each bridge that was repaired. The repair cost ratio was defined as the ratio of repair cost to replacement cost of a bridge.
- Soil type and peak ground acceleration at bridge sites.

Basöz and Kiremidjian consider that the damage states of bridges are a function of the damage state of its components, such as abutments, substructures, connections and bearings. To define a set of preliminary damage states for components of concrete bridges, expert's opinion were consulted by means of a questionnaire. At this questionnaire, Basöz and Kiremidjian ask to several experts if different damage conditions for each bridge components are feasible to group in each damage level. In addition, the questionnaire consults for damage conditions that can be assigned to the damage levels.

### 6.2.2. Classification of bridges. Data sets

Several data sets were used for statistical analyses, considering that similar characteristics are expected to suffer similar damage under a given action. Therefore, aspects such as bridge material, quality of the information, type of structural elements, bridge regularity, or the level of seismic action were used to classify the studied bridges.

### 6.2.3. Correlation studies

The data on bridge damage were compiled in form of damage frequency matrices, which are the number of bridges with each level of observed damage at different PGA levels. Then, the damage probability matrices were obtained for each group of bridges. These were used to define empirical fragility curves, by means of correlation analyses.

For the correlation studies were applied a logistic regression analysis, which are part of the applied statistics. The objective of this kind of analysis is to find the best fitting model to describe the relationship between an outcome and a set of independent variables. A logistic regression model is used as a multivariate technique for estimating the probability that an event occurs (Aldrich and Nelson 1984).

#### 6.2.4. Results

Fragility curves, results of the correlation studies followed by Basöz and Kiremidjian, will be commented in next sections. The description of the results is shown for Loma Prieta and Northridge earthquakes in separate points.

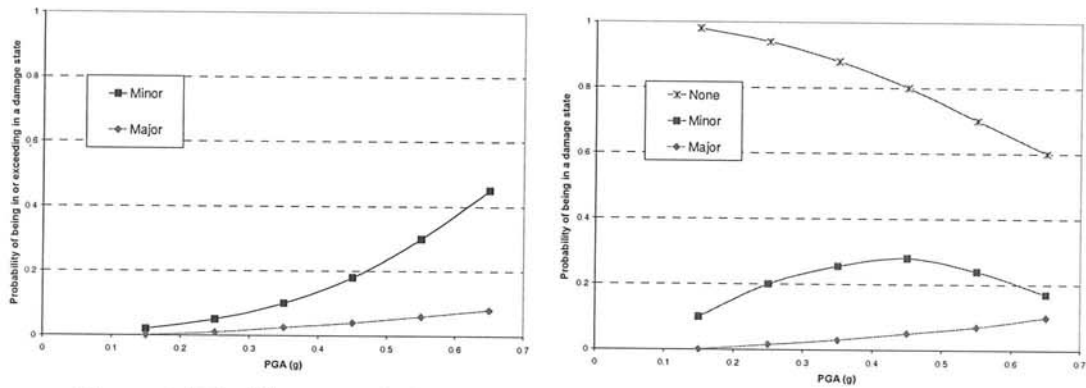
##### 6.2.4.1. Loma Prieta earthquake

In the San Francisco Bay area were located 4785 bridges, 76 of them damaged by the Loma Prieta earthquake. In the analysis were only used 2329 of these structures (state bridges) to conform the next data sets:

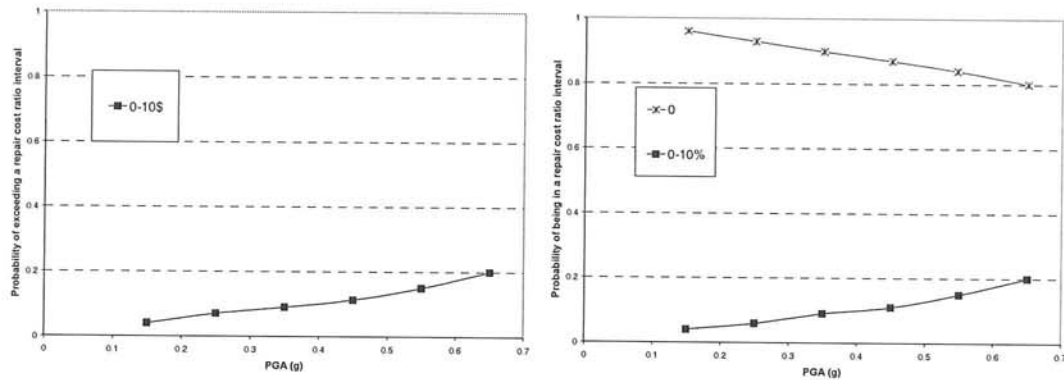
- 2131 structures were gathered in the *highway bridge data set*, classifying by superstructure and substructure. 1883, (80%) bridges are concrete structures and 73% were designed using pre-1971 design standards.
- 869 bridges were included in *concrete highway bridge data set*, considering concrete superstructure and concrete substructure for multiple span bridges and concrete superstructure for single span bridges.
- Bridges with regular structural characteristics were selected from the *concrete highway bridge data set* to form *regular bridge data set*. This set is considered in order to evaluate the effect of structural component types on bridge damage. This data set summarised 1112 bridges. 67% of these bridges were designed according to pre-1971 design standards; almost 50% of the systems had monolithic abutments; 80% of the structures were multiple spans bridges and 2/3 of the multiple span bridges had multiple piers per bent.
- The damage report for bridges include 76 damaged structures, identified with *minor* or *major* damage. *Minor* damage referred to damage of keeper plates and anchor bolts, spalling and cracking of piers, cracking of abutments walls, shear failure, joint shear failure, approach settlement and damage to restrainers. On the other hand, *major* damage includes total or partial collapse, as well as damage to bearings and anchor plates and significant cracking and spalling of the piers.
- 80% of the 76 damage bridges were designed by pre-1971 design standards. Only one bridge designed according to recent design standards sustained *major* damage. In addition, 43 of the 76 damaged bridges were structures with concrete super and substructure subjected to PGA of 0.10g or larger. Due to lack of some information available, only 28 of the 62 concrete bridges, which were reported as damaged, were included in the *correlation data set*. Only six of *correlation data set* elements suffered *major* damage.

Empirical fragility curves were developed from the damage matrices. As an example of the results obtained by Basöz and Kiremidjian (Basöz and Kiremidjian 1995 and 1998, and Kiremidjian and Basöz 1997), figure 6.1 shows the fragility curves obtained for bridges built between 1940-1971. In these figures, the left plot represents the probability of being in or exceeding a damage state versus the earthquake size; while the right represents the probability of being in a damage state for a given earthquake size.





**Figure 6.1** Fragility curves for bridges built between 1940-1971. 639, 27, 4 not damaged bridges, bridges with *minor* damage and bridges with *major* damage, respectively. Loma Prieta earthquake



**Figure 6.2** Empirical fragility curves for bridges built between 1940-1971. 635 not damaged bridges and 35 bridges with *minor* damage. Loma Prieta earthquake

In other context, a database on the estimated repair cost was compiled for 84 bridges, including total estimated repair cost and more detailed information on repair work. \$280 millions were reported as repair cost for these bridges, 90% of it was for the repair of the Cypress Viaduct, one of the collapse bridges. The distribution of all damage bridges by repair cost and damage state shows that pier damage was the costliest for bridges with *minor* damage, and the repair on piers, joints and decks contributed almost equally to rehabilitate bridges with *major* damage.

Similar to ground motion-damage relationships, empirical fragility curves were obtained for seven repair cost ratio levels (0-10%, 10-20%, 20-30%, 30-40%, 40-50% and >50%). Examples of these fragility curves for single span bridges are shown in figure 6.2.

Based on the above analyses, Basöz and Kiremidjian conclude:

- The poor bridge classification in *minor* and *major* damage makes difficult to identify structural characteristics that contribute to damage.
- Bridges with monolithic abutments performed better than those with non-monolithic abutments, while bridges with partial abutments had a better performance at higher PGA levels than bridges with monolithic abutments. Bridges with single pier bents had a worst performance than those with multiple pier bents and pier walls.

- Among the bridges with reported repair cost, about 50% of the repair cost was due to pier damage, and about 21%, 18% and 2% of the damage was due to deck, joint and abutment damage, respectively.

#### 6.2.4.2 Northridge earthquake

A similar procedure to evaluate of fragility curves for bridges in Loma Prieta was followed by Basöz and Kiremidjian for bridges affected by Northridge earthquake. The database compiled includes 3533 state bridges and 2571 local bridges. Of the 3533 state bridges, 3318 were grouped in the *highway bridge data set*. In addition, 76% of the bridges in the *highway bridge data set* were designed according to pre-1971 design standards.

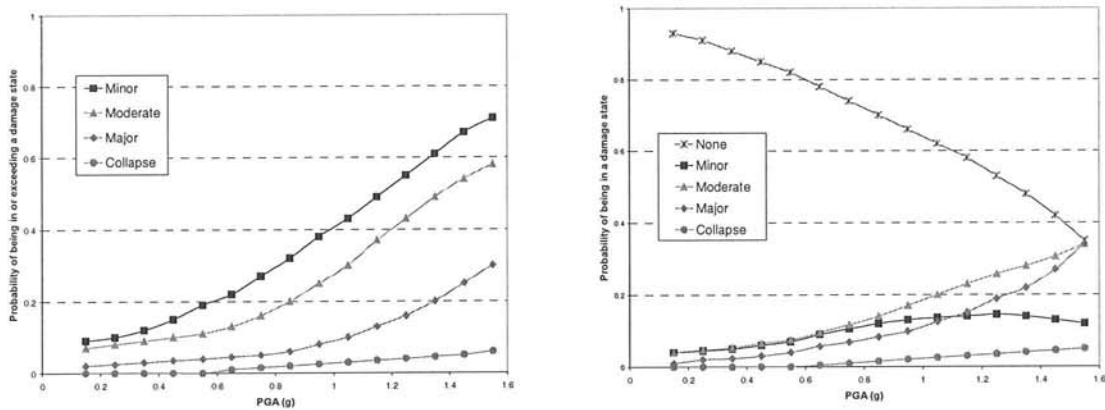
More than 85% of the bridges damaged in Northridge earthquake were concrete structures. Among the concrete bridges, systems with concrete superstructure and concrete substructure for multiple span bridges and concrete superstructure for single span bridges totalised 3102 systems. 72% of the bridges were built between 1940-1971, 21% were built between 1972-1980 and 5% were built before 1980. 64% and 31% of the single span bridges had monolithic and non-monolithic abutments, respectively. Finally, 63%, 22% and 15% of the multiple span bridges have multiple piers/bents, single pier/bent and pier walls, respectively.

The studied bridges were assigned into four damage states: *minor*, *moderate*, *major* and *collapse*. *Major* damage generally referred to bridges where piers spalling and rebar buckling extended over a length of one pier diameter or more, or to cases where severe hinge damage and near unseating occurred. *Moderate* damage was considered in bridges with pier spalling or shear cracking without buckling, or with substantial damage in abutment/pier elements. *Minor* damage was used for bridges with no danger or imminent structural collapse or easily repairable damage.

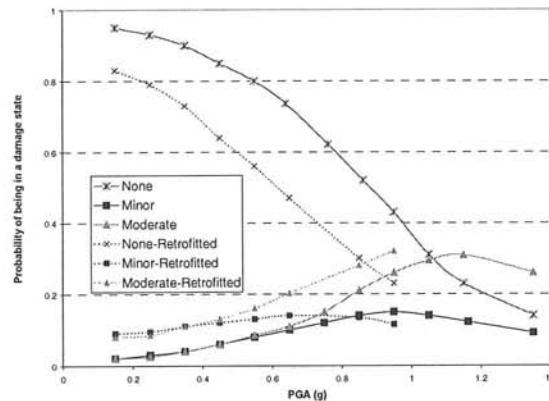
After the earthquake, 233 damaged bridges were reported, 200 of them were concrete highway bridges (28 single span bridges and 172 multiple span bridges). Only 164 of the damaged bridge (27 single span bridges and 137 multiple spans bridge) had regular abutment and/or pier bent types. Additionally, 160 of these 164 bridges were exposed to PGA levels of 0.15g or higher. 68% and 73% of the damaged bridges were designed by pre-1971 and 1972-1980 design standards, respectively. Six bridges collapsed due to the earthquake. 20% of the damaged bridges were single span bridges, 63% of them with monolithic abutments. At last, 61%, 25% and 14% of damaged multiple span bridges had multiple piers/bents, single pier/bent and pier walls, respectively.

Empirical fragility curves were developed for the damage probability matrices using logistic regression analysis, for the probability of exceeding a given damage state and the probability of being in damage state (like to it was done with Loma Prieta damage data). The empirical fragility curves, both unconditional and conditional on damage: that is, considering all the study bridges (unconditional) or only those in which damage has occurred (conditional) were computed when enough number of damaged bridges was available. As an example, figure 6.3 shows the empirical fragility curves for bridges built between 1940-1971, unconditional and conditional on damage, respectively.

The availability of information about retrofitted bridges permit to compute some fragility curves for retrofitted and unretrofitted structures, some of these curves are presented in figure 6.4. The probability of being in a damage state is a little greater for retrofitted structures when *minor* and *major* damage states occurred.



**Figure 6.3** Empirical fragility curves for bridges built between 1940-1971. 887, 49, 59, 28 and 3 none, minor, moderate, major and collapse damaged bridges, respectively.



**Figure 6.4** Comparison of empirical fragility curves for retrofitted and unretrified bridges

A total of \$190 millions were registered as the repair cost in the reports. The total repair cost for the six collapsed bridges correspond to 75% of the reported repair cost of all damaged bridges. The estimated repair cost are of \$152.85, \$30.87, \$5.66 and \$0.54 millions for *collapse*, *major*, *moderate* and *minor* damaged bridges. Most of the repair cost for bridges with *minor* damage was for approach settlement; piers and joints did not suffer damage. The damage to abutments was the most significant type of *moderate* damaged bridges, while the highest repair cost for bridges with *major* damage was due to pier failure. The average repair cost for bridges that suffered *major* damage was about five times that for bridges with *moderate* damage

The repair cost ratio was defined as the ratio of repair cost to replacement cost. Seven repair cost ratio intervals were used: 0-10%, 10-20%, 20-30%, 30-40%, 40-50% and >50%. Similar to ground motion-damage relationships, empirical ground motion-repair cost ratio relationships were developed. Figure 6.5 shows the fragility curves obtained for bridges built between 1940-1971.

Based on the analyses of data presented, Basöz and Kiremidjian emphasise several important observations, these are summarised as follow:

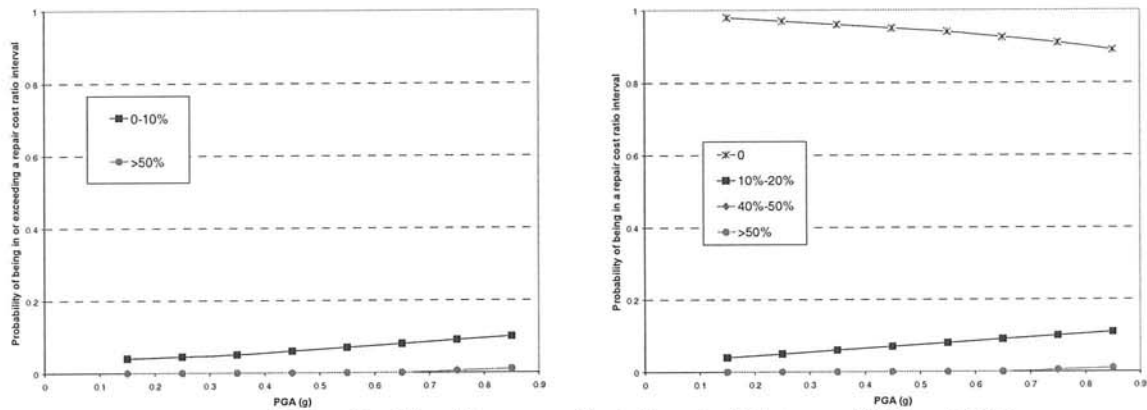


Figure 6.5 Empirical fragility curves for bridges built between 1940 and 1971

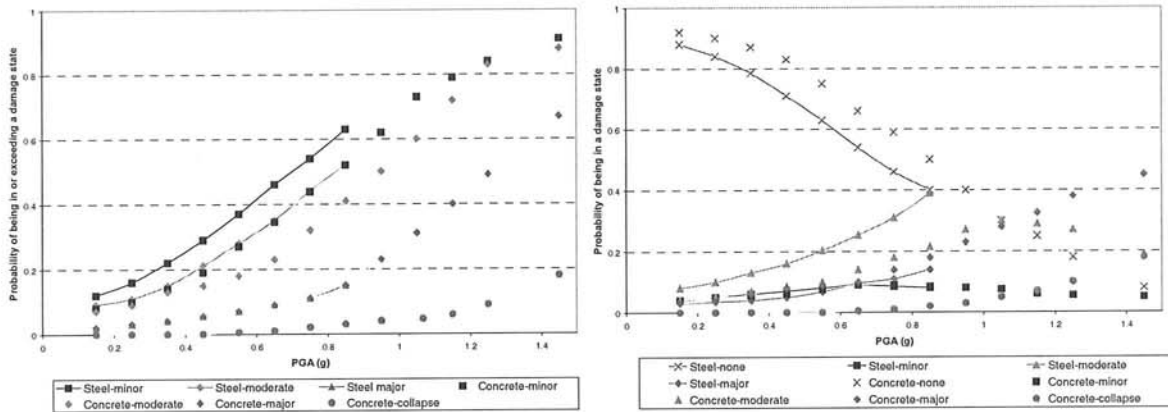


Figure 6.6 Empirical fragility curves for steel and concrete bridges.

- None of the steel bridges in the affected area collapse. Based on the damage data, the probability of *major* damage at a given PGA level below 0.85g was the same for concrete and steel bridges, as can see in figure 6.6. Steel bridges were more likely to experience *moderate* or *minor* damage than concrete.
- Bridges with piers retrofits performed well and bridges retrofitted with hinge restrainers suffered major damage. Additionally, bridges with single pier bent had the worst performance among the pier bent types.

About 75% of the repair cost was due to collapsed bridges. Spent cost for pier and joint damages, principally in bridges with major damage, were the majority of the repair cost. The observed repair cost ration for single and multiple span bridges was not more than 10% and as high as 50%, respectively

### 6.3. Fragility curves of bridges based on reported damages after Kobe earthquake

The bridges failure during the Kobe (1995) earthquake produced economical losses, time delays and inadequate emergency activities. The necessity of characterizing the seismic fragility of these structures, with the aim of performing their reinforcement and maintenance to reduce their risk, had as a consequence many researches on this topic. Among these

researches, the analysis of Tanaka (2000) and Yamazaki (2000) define the seismic vulnerability of RC and steel bridges through the study of the reported damages after of the Kobe earthquake.

The seismic vulnerability of the bridges of the affected zone was defined through damage probability matrices and restoration matrices. To obtain such matrices, the studied bridges were classified in five damage states (according to the remaining capacity of the structures), in three states of traffic condition, and in different levels of peak ground acceleration (PGA) or levels of the Japanese intensity. The five damage states were defined as:

- **A<sub>S</sub>** – Collapse,
- **A** - Major damage,
- **B** - Moderate damage,
- **C** - Minor damage,
- **D** - No damage.

while the states of the traffic condition were: (a) impossible traffic of vehicles, (b) difficult traffic of vehicles, and (c) traffic of vehicles without problems. The statistical analyses of the digitised data give as result damage probability matrices for the studied structures. As an example of the obtained results, the damage probability matrix for 216 RC bridges studied by Yamazaki (2000) in four routes is shown in table 6.3. Starting from DPM and considering that the PGA and the Japanese intensity have a lognormal and normal distribution function, respectively, fragility curves were fitted through the minimal square technique. The resulting fragility curves for the 216 bridges are shown in figure 6.7.

#### 6.4. Hypothesis testing and confidence intervals for empirical fragility curves for bridges

As a preliminary bridge screening, Shinozuka developed a methodology mixture among the analytical research (like the one used by Ciampoli, chapter 4) and the empirical way based on the study of damage reports (like the researches of Xueshen and Shuming, and Basöz and Kiremidjian).

The methodology proposes by Shinozuka to obtain the fragility curves of bridges includes the following aspects: (1) professional judgement, (2) quasi-static and design code consistent analysis, (3) utilisation of damage data associated with past earthquakes, and (4) numerical simulation of bridge seismic response based on structural dynamics.

##### 6.4.1. Empirical fragility curves for bridges affected by the Northridge earthquake

The empirical fragility curves obtained by Shinozuka (1998) are based on statistical conclusions of records of the damage resulting from the 1994 Northridge earthquake. While Basöz and Kiremidjian calculated the empirical fragility curves evaluating the statistical data with a logit method, Shinozuka expressed they in the form of two parameters of the lognormal distribution function. The empirical fragility curves of Shinozuka additionally are based on the maximum likelihood method for estimation of the two parameters (median  $c$  and the log-standard deviation  $\zeta$ ) of the lognormal distribution. The likelihood function  $L_f$  is expressed as:

$$L_f = \prod_{i=1}^{n_s} [P(a_i)]^{q_i} [1 - P(a_i)]^{1-q_i} \quad (6.1)$$

Route	Bridge damage					Total
	A <sub>s</sub>	A	B	C	D	
Chugoku Expressway	4	0	7	5	55	71
Kinki Expressway	0	0	0	0	30	30
Meishin Expressway	3	4	5	1	74	87
Daini Road	0	0	1	2	25	28
Total	7	4	13	8	184	216

Table 6.3 Damage probability matrix for Kobe bridges

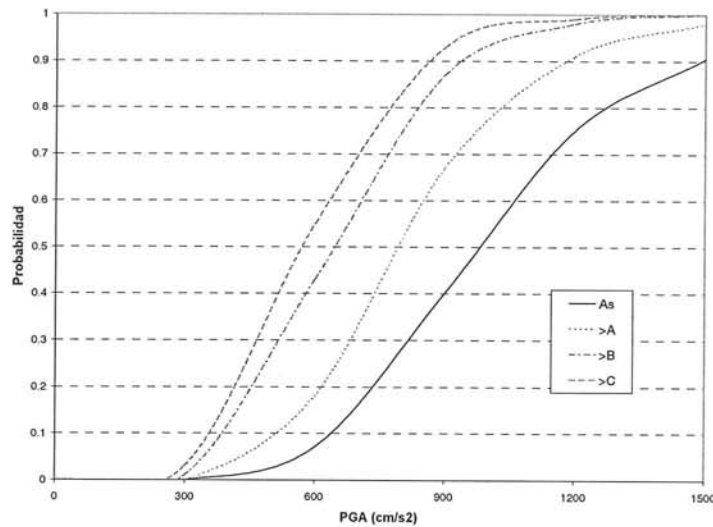


Figure 6.7 Fragility curves for the Kobe bridges

where:  $P(\bullet)$  represents the fragility curve for a specific state of damage,  $a_i$  is the PGA value to which bridge  $i$  is subjected,  $q_i$  is equal to 1 or 0 depending on whether or not the bridge sustains the state of damage under PGA ( $a_i$ ), and  $n_s$  is the total number of bridges within the region affected by the earthquake of interest.

The parameters of the lognormal distribution are estimated as  $c_0$  and  $\zeta_0$  satisfying the following equations and maximising  $L$ :

$$\frac{\partial \ln L}{\partial c} = \frac{\partial \ln L}{\partial \zeta} = 0 \quad (6.2)$$

The above describe method was applied to statistical data reported after Northridge earthquake, using a PGA reported values at bridge sites and reported damage state at each bridge. The fragility curves obtained for the studied bridges, associated with four damage states, are plotted in figure 6.8 In this figure are shown, also, the median and standard deviation of the lognormal distribution functions for each damage state.

The analysis of Shinozuka, to difference of the research of Basöz and Kiremidjian, do not classified the study bridges in terms of such attributes as age, design code, structural type, materials, etc. The decision of not to classified bridges was made because it requires a significant effort, a detailed database and an enough population size to permit a classification with sufficient statistic information for each group.

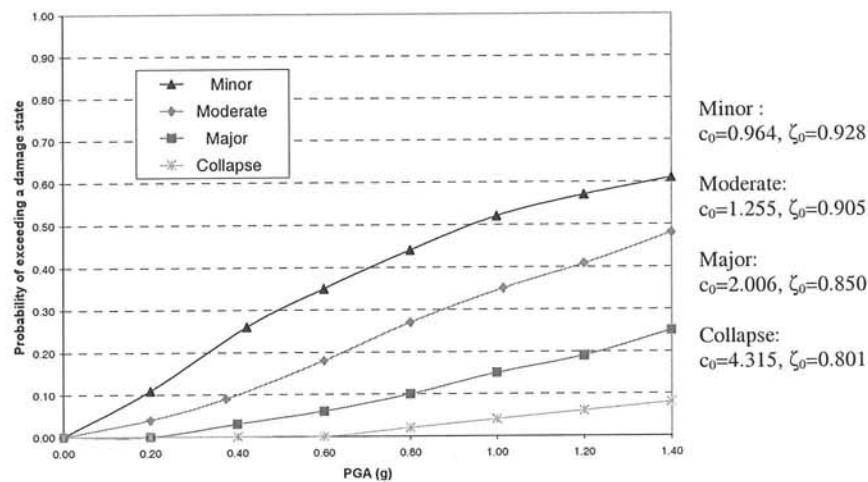


Figure 6.8 Fragility curves obtained by Shinozuka

#### 6.4.2. Hypothesis testing and confidence intervals

To complete his statistical analysis, rather than making a fitting exercise, Shinozuka accomplishes hypothesis testing and confidence intervals for the fragility curves in figure 6.8. The steps followed to complete these analyses are:

1. **Test of goodness to fit.** The probabilistic interpretation of the fragility curve  $P(a)$  as a function of  $a$ , suggest that a structure will sustain a damage state with a probability  $P(a)$  and will not sustain the damage state with the probability of  $1-P(a)$ , under an earthquake size  $a$ . This means that, under each earthquake size, the phenomena can be described by a random variable  $X_i$  following the Bernoulli distribution such that  $x_i=1$  when the state of damage is reached under  $a_i$  and  $x_i=0$  otherwise. The variable  $Y_i=(X_i-p_i)$ ,  $p_i=P(a_i)$ , has the next probability distribution function:

$$f(Y) = \begin{cases} (x_i - p_i)^2 & \text{for } x = 0,1 \\ 0 & \text{otherwise} \end{cases} \quad (6.3)$$

Considering statistical independence of  $N$  random variables with Bernoulli distribution, the sum of  $Y_i$  variables, approaches asymptotically to a Normal distribution as  $n_s$ , the total number of structures considered, is large enough ( $\gg 1$ ). The mean and variance of this new variable are obtained by means of the expressions on equation 6.4.

$$Y = \sum_{i=1}^N (X_i - p_i)^2 \quad (6.4)$$

Since  $p_i$  depends on the values of  $c_0$  and  $\zeta_0$  the standard procedure of hypothesis testing suggests that for a significance level  $\alpha_{SL}$  and a probability

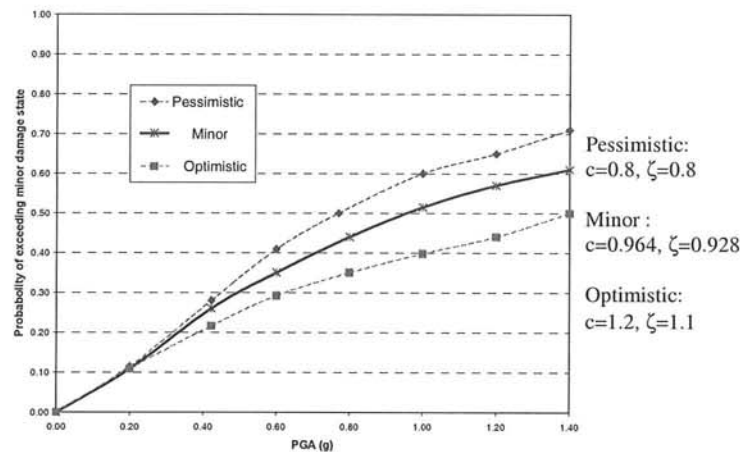


Figure 6.9. Confidence intervals for the minor damage state defined in figure 6.7

$$P_Y = \Phi\left(\frac{y - \mu_y}{\sigma_y}\right) \geq 1 - \alpha \quad (6.5)$$

the hypothesis that  $c_0$  and  $\zeta_0$  are indeed the true value of  $c$  and  $\zeta$  will be accepted with the significance level usually set equal to 0.05 or 0.10. The application of equations 6.3 to 6.5 to the fragility curve of figure 6.8 produced the next values of  $P_Y$ , which passing the test of goodness of fit at the significance level of 10%.

$P_Y$	For
0.638	Minor damage
0.668	Moderate damage
0.548	Major damage
0.497	Collapse

2. **Confidence intervals.** The confidence intervals are used to estimate the statistical variability between estimators and parameters, that is, the uncertainty associated with  $c_0$  and  $\zeta_0$ . To obtain the confidence intervals, Monte Carlo simulation techniques were used to generate realisations of the estimators  $\hat{c}$  and  $\hat{\zeta}$ . As an example, the confidence intervals for the minor damage state fragility curve (figure 6.8) is shown in figure 6.9.

The difference between the curves of figure 6.9 indicates a confidence band in an engineering sense. The confidence analysis described would have a significant impact on the way in which the results of the socio-economic analysis are interpreted.



## Chapter 7

### Simplified elastic model

A first step in the analysis of damage caused in structures by dynamic loads is the definition of the elastic properties of these systems. The characterization of structures in its elastic range requires the definition of the dynamic properties, that is, mode shapes and frequencies of vibration. To reach this objective, this work opted for the use of simplified models that describe in a reasonable way the complex interaction between the elements of the bridge.

As known, the determination of the modal frequencies or periods, that is, of the dynamic characteristics of a structure can be complicated in the case of multiple degrees of freedom systems, though simplified analysis procedures have been proposed. (Clough y Penzien 1975, Craig 1981, Barbat y Canet 1994, Gómez et al. 2000). Thus, the equation of motion of an  $n$  degrees of freedom system in free vibration and without damping is defined as

$$\mathbf{M} \ddot{\mathbf{v}}(t) + \mathbf{K} \mathbf{v}(t) = \mathbf{0} \quad (7.1)$$

where  $\mathbf{M}$  and  $\mathbf{K}$  are the mass and stiffness matrices and  $\ddot{\mathbf{v}}(t)$  y  $\mathbf{v}(t)$  are the acceleration and displacement vector, respectively. For this system, particular solutions of the following type are considered:

$$\mathbf{v}(t) = \mathbf{D} \sin(\omega t + \varphi) \quad (7.2)$$

where  $\mathbf{D}$  is a vector that contains the amplitudes of the vibration and  $\varphi$  is the phase angle of the motion. Deriving two times equation 7.2 with respect to time and substituting in 7.1, we obtain:

$$\mathbf{M} \omega^2 \mathbf{D} \sin(\omega t + \varphi) + \mathbf{K} \mathbf{D} \sin(\omega t + \varphi) = \mathbf{0} \quad (7.3)$$

which, eliminating the terms of the arbitrary sine function, can be written as

$$(\mathbf{K} - \omega^2 \mathbf{M}) \mathbf{D} = \mathbf{0} \quad (7.4)$$

The system of equations 7.4 has solutions different from the trivial one if the determinant is null

$$\det [\mathbf{K} - \omega^2 \mathbf{M}] = 0 \quad (7.5)$$

Equation 7.5 is the characteristic equation of the system with  $n$  degrees of freedom. Its solution provides on  $n$  degrees polynomial function of  $\omega^2$ , whose roots constitute the

oscillation frequencies of the system in absence of external forces. Each frequency is associated with a mode shape described by the corresponding eigenvector, or natural form of vibration. The eigenvector, generally normalized to its maximum value, does not describe the value of the amplitude of vibration; it only indicates the shape of the system during the vibration for each of the eigenvalues. With the normalized eigenvectors, it is possible to build the modal matrix  $\Phi$ , whose rows contain each one of the mode shapes of the system.

It can be demonstrated that for stable systems with real symmetrical and positive definite matrices of mass and stiffness (the general case in structural analysis), all the roots of equation 7.5 are real and positive.

### 7.1 Simplified elastic formulation of the bridge

As a rule, the proposed simplified model considers continuous elements, with distributed mass in piers and concentrated in girders. It is understood that when a pier is subjected to seismic excitation at its base in transversal direction, the motion of the adjacent girders restricts partially its transversal oscillations. Thus, a pier subjected to dynamic load is displaced and causes the distortion of the bearings over it and the subsequent rotation of the rigid continuous girders. In the proposed model the following general hypotheses were considered:

1. The piers are modelled as continuous elements with distributed mass and infinite axial stiffness.
2. The girder are modelled as a perfect stiff elements with concentrate mass, thus the longitudinal and transversal deformations of the girders are neglected.
3. All the piers have the same longitudinal displacement.
4. The structure has bigger redundancy and strength in its longitudinal direction; therefore greater damage will occur in its piers when subjected to transversal excitation.
5. The bearings of the girders are modelled as equivalent short members. These have circular cross section with real dimensions, and are supposed to work mainly to shear; therefore the equivalence in stiffness will be achieved by modifying the shear modulus.
6. The rotations of the girders, produced by the displacements at the top of the piers by the seismic action, are simulated by using rotational-linear springs.
7. The soil-structure interaction effect in piers and abutments is considered by means of linear springs that represent the rotational stiffness of the soil.
8. In the longitudinal direction, the girders are supported at its extreme by abutments, also included as linear springs of great strength.
9. In the transversal direction, very rigid abutments are supposed. Therefore, the displacements in this direction are neglected.

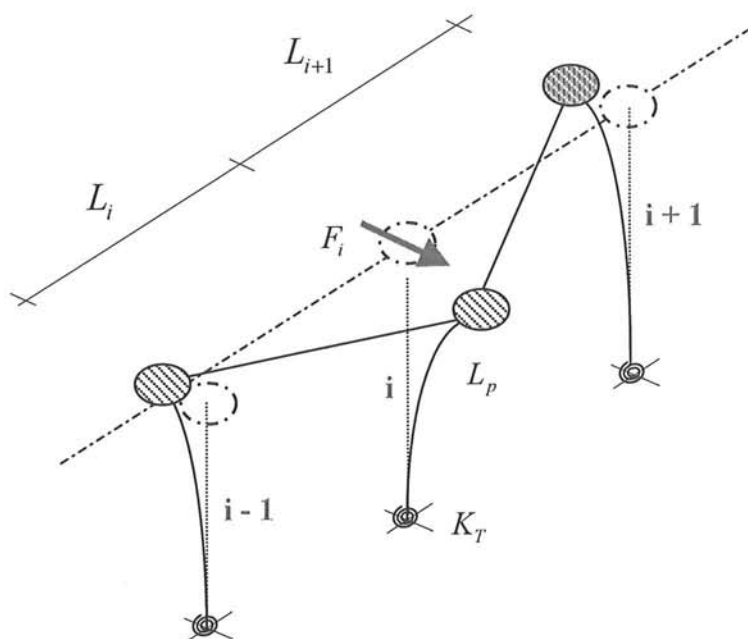


Fig 7.1 Basic scheme for the analysis of the bridge

In a rigorous 3D analysis, six degrees of freedom by node are considered, what can lead to very complicated analyses. Because of this, in certain cases simplifications that guarantee satisfactory results are used. In the case of RC bridges with single pier bent (bridge typology of analysis), the proposed simplifications are based on the previous hypotheses. A structural model with  $n$  degrees of freedom was thus developed, being  $n$  the number of piers plus the number of abutments. The transversal displacement at the top of each pier, assuming that this displacement is governed by the rotational stiffness of the adjacent girders and the transversal stiffness of each pier, were taken into account as the only degrees of freedom of the problem (see figure 7.1). In addition, for this model a different seismic excitation is associated to each pier. Thus, the spatial variability of the external load is considering. It is important to include this aspect when geological or topographic discontinuities exist or in the case of structures with large longitudinal or transversal dimensions, like bridges (E8 1998).

### 7.1.1. Evaluation of transversal stiffness of bridge in a mode $i$

The displacement of pier  $i$  generates a force distribution like the one indicated in figure 7.2. In this figure,  $F_i$  is the inertial force,  $F_i^{i-1}$  and  $F_i^{i+1}$  are the elastic forces produced by the rotation of the girders adjacent to the  $i$ -pier, and  $F_{i-1}^i$  and  $F_{i+1}^i$  are the elastic forces produced in the piers  $i-1$  and  $i+1$  by the rotation of the contiguous girders, respectively. That is, for the study pier, the super-index shows the pier where the forces acted and the sub-index is associated to the pier with it has the same rotated girder, left  $i-1$  and right  $i+1$ . A same logic is followed for the indices of the forces acted in the adjacent piers.

As it can be observed in figures 7.2 and 7.3, the worst condition occur where the two adjacent piers are displaced in opposite sense to that of the displacement of the studied pier.

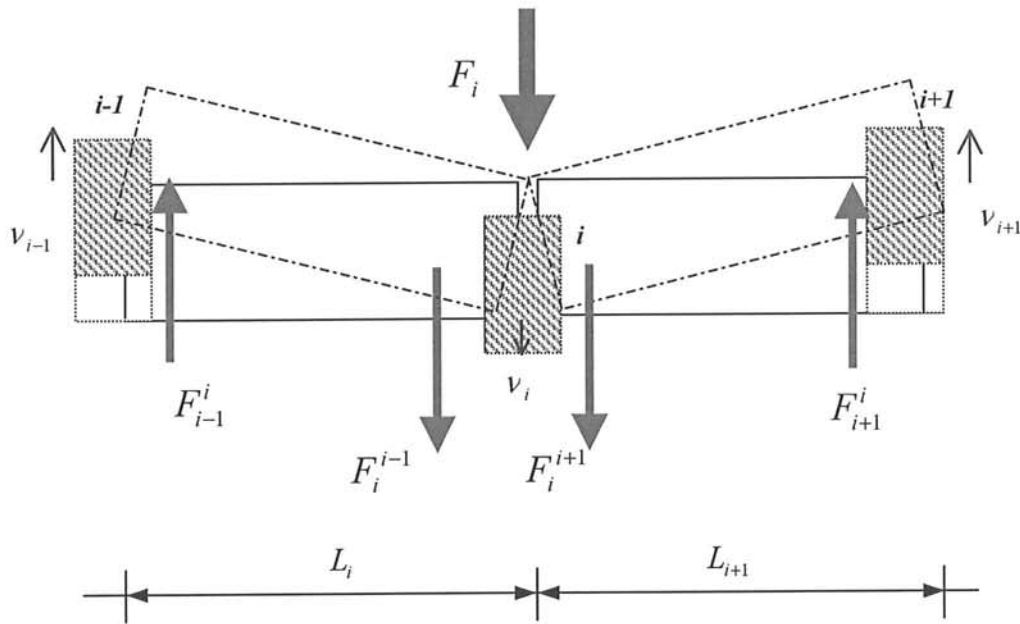


Figure 7.2 Scheme of the rotation of the adjacent girders

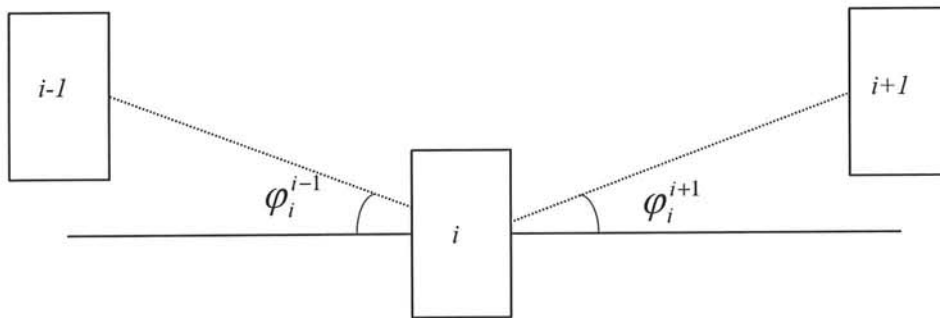


Figure 7.3 Rotation of the girder elements

To determine the elastic forces due to the rotation of the girders, their motion is analysed. It can be seen in figures 7.2 and 7.3 that the rotations produced at left,  $\varphi_i^{i-1}$ , and at right,  $\varphi_i^{i+1}$ , which depend on the relative displacement between the three contiguous piers, are

$$\varphi_i^{i-1} = \left( \frac{v_i - v_{i-1}}{L_i} \right) \quad (7.6)$$

$$\varphi_i^{i+1} = \left( \frac{v_i - v_{i+1}}{L_{i+1}} \right) \quad (7.7)$$

where  $L_i$  and  $L_{i+1}$  are the length of the left and right girders adjacent to pier  $i$ , respectively, and  $v_i$ ,  $v_{i-1}$ , and  $v_{i+1}$  are the maximum displacements of the piers  $i$ ,  $i-1$  and  $i+1$ , respectively.

On the other hand, there are bearings on each pier of the studied bridge (see figures 7.4 and 7.5), simulated as short members with circular cross section whose behavior is mainly governed by shear deformations. The influence of the supports on the behavior of the bridge is associated to their shear modulus,  $G$ , the distance in plant between the geometric centers of the bearings of each girder,  $h_a$ , their height,  $a$ , and the area of their cross section,  $A_p$ .

In figures 7.4 and 7.5, the deformation produced by the loads transmitted from the piers to the bearings can be seen. The displacement of the bearing,  $u_p$ , produces a couple of forces  $F$

$$F = \tau A_p = (G\gamma)A_p \cong \left( G \frac{u_p}{a} \right) A_p = \left( \frac{G}{a} \varphi \frac{h_a}{2} \right) A_p \quad (7.8)$$

having a moment defined by

$$M_T = F \cdot h_a = \frac{GA_p}{a} \left( \varphi \cdot \frac{h_a}{2} \right) \cdot h_a \quad (7.9)$$

where  $F$  is the shear force in the bearings,  $\tau$  is the tangential stress and  $u_p = \varphi (h_a/2)$  is the relative displacement between the upper and lower part of the bearing element. Starting from equation 7.9, the total force produced by the girder rotation is given by the following equation:

$$F = \frac{2M_T}{L} = \frac{GA_p h_a^2}{aL} \varphi \quad (7.10)$$

Applying equation 7.10 to each pier of the bridge, and using equation 7.6, the force produced in girder  $i-1$  is

$$F_i^{i-1} = \left[ \frac{GA_p h_a^2}{aL_i^2} \right] v_i - \left[ \frac{GA_p h_a^2}{aL_i^2} \right] v_{i-1} \quad (7.11)$$

Following a similar process, the force due to the rotation of girder  $i+1$  is

$$F_i^{i+1} = \left[ \frac{GA_p h_a^2}{aL_{i+1}^2} \right] v_i - \left[ \frac{GA_p h_a^2}{aL_{i+1}^2} \right] v_{i+1} \quad (7.12)$$

Adding equations 7.11 and 7.12 and reordering the terms, the total elastic force,  $R_i$ , due to the rotation of girders adjacent to the pier  $i$  is:

$$R_i = F_i^{i-1} + F_i^{i+1} = \left[ \frac{GA_p h_a^2}{aL_i^2} + \frac{GA_p h_a^2}{aL_{i+1}^2} \right] v_i - \left[ \frac{GA_p h_a^2}{aL_i^2} \right] v_{i-1} - \left[ \frac{GA_p h_a^2}{aL_{i+1}^2} \right] v_{i+1} \quad (7.13)$$

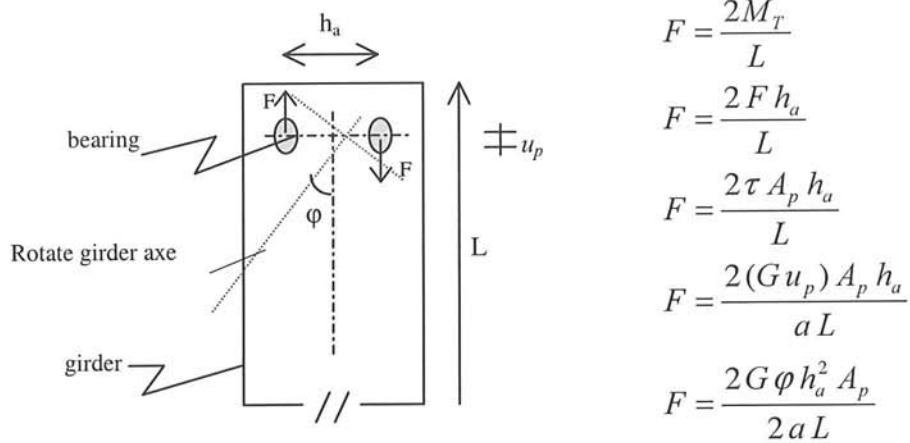


Figure 7.4 Plan view of a girder

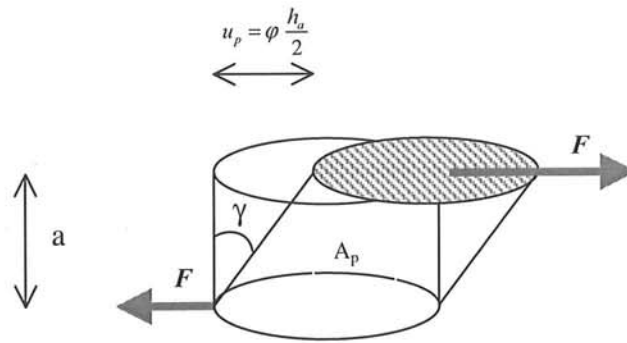


Figure 7.5 Deformation of an equivalent short column

7.1.2. Transversal stiffness of a pier for a mode *i*

Based on the general hypotheses stated previously, the pier is considered as a continuous element with distributed mass. The soil-structure interaction effect is included by means of a spring with rotational stiffness  $K^S$  (see figure 7.6). Thus, the maximum displacement at the top of the pier is

$$v_i = v_\theta^i + v_p^i \tag{7.14}$$

being

$$v_\theta^i = \theta^i L_p^i = \frac{M_p^i}{K_i^S} \tag{7.15}$$

the displacement produced by rotation at the base of the pier, and

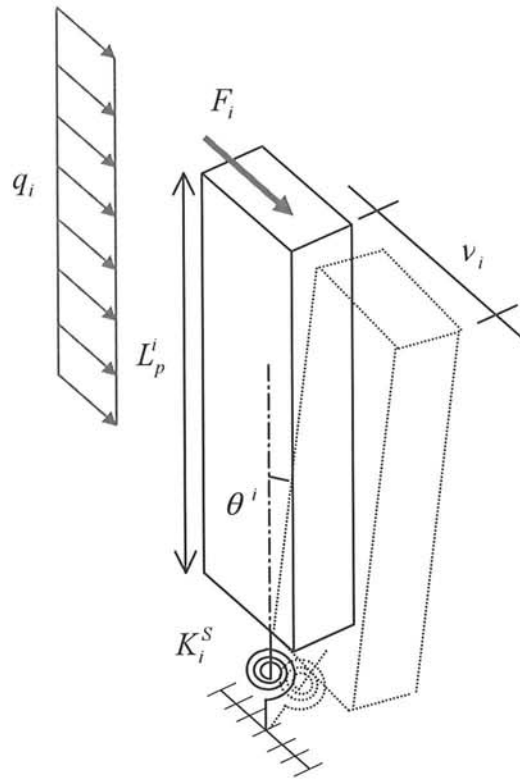


Figure 7.6 Motion of pier i

$$v_p^i = \frac{q_i (L_p^i)^4}{8E_{c_i} I_i} + \frac{F_i (L_p^i)^3}{3E_{c_i} I_i} \quad (7.16)$$

the displacement produced by external actions. In equations 7.15 and 7.16,  $\theta^i$  is the rotation produced by the soil-structure interaction effect;  $M_p$  is the maximum bending moment at the base of the pier;  $K_i^S$  is the equivalent stiffness of the soil;  $q$  is the mass load by unit length;  $L_p^i$ ,  $E_{c_i}$  and  $I_i$  are the length, Young's modulus and the inertia of the cross section, respectively; and  $F_i$  is the total inertial force.

Starting from the applied loads, the equation of moment of the pier is

$$M_i(x) = q_i (x^2 / 2) + F_i x \quad (7.17)$$

For the maximum displacement of the pier, when  $x = L_p$ , the equation of the bending moment becomes

$$M_i(x = L_p) = q_i \cdot \frac{(L_p^i)^2}{2} + F_i \cdot L_p^i \quad (7.18)$$

Substituting equations 7.15, 7.16 and 7.18 in equation 7.14, the maximum displacement of the pier is written as:

$$v_i = \frac{q_i(L_p^i)^3}{2K_T^i} + F_i \left[ \frac{(L_p^i)^2}{K_i^S} + \frac{(L_p^i)^3}{3E_{c_i}I_i} \right] + \frac{q_i(L_p^i)^4}{8E_{c_i}I_i} \quad (7.19)$$

and from here is obtained the inertia force at the top of the pier

$$F_i = \frac{1}{\left[ \frac{(L_p^i)^2}{K_i^S} + \frac{(L_p^i)^3}{3E_{c_i}I_i} \right]} \left[ v_i - \frac{q_i(L_p^i)^3}{2K_i^S} - \frac{q_i(L_p^i)^4}{8E_{c_i}I_i} \right] \quad (7.20)$$

### 7.1.3. Pier-girder equation of equilibrium

At the top of each pier of the bridge, the total effective force is the sum of forces produced by the rotation of girders with the forces due to the displacement of the element, that is, the sum of equations 7.13 and 7.20. Applying now the second law of Newton, the total effective force at the top of pier  $i$  is

$$F_i^T = R_i + F_i = m_i a_i \quad (7.21)$$

where  $m_i$  is the mass associated to the degree of freedom  $i$ , and  $a_i$  is the corresponding acceleration. Substituting the values of  $R_i = F_i^{i-1} + F_i^{i+1}$  (equation 7.13) and  $F_i$  (equation 7.20) in equation 7.21,  $F_i^T$  is expressed as

$$F_i^T = m_i a = \left\{ \left[ \frac{GA_p h_a^2}{aL_i^2} + \frac{GA_p h_a^2}{aL_{i+1}^2} \right] + \frac{1}{\left[ \frac{(L_p^i)^2}{K_i^S} + \frac{(L_p^i)^3}{3E_{c_i}I_i} \right]} \right\} v_i - \left[ \frac{GA_p h_a^2}{aL_i^2} \right] v_{i-1} - \left[ \frac{GA_p h_a^2}{aL_{i+1}^2} \right] v_{i+1} - \left[ \frac{1}{\left[ \frac{(L_p^i)^2}{K_i^S} + \frac{(L_p^i)^3}{3E_{c_i}I_i} \right]} \right] \left[ \frac{q_i(L_p^i)^3}{2K_i^S} + \frac{q_i(L_p^i)^4}{8E_{c_i}I_i} \right] \quad (7.22)$$



Additionally, if the stiffness

$$K_{i,i} = \frac{GA_p h_a^2}{aL_i^2} + \frac{GA_p h_a^2}{aL_{i+1}^2} + \frac{1}{\left[ \frac{(L_p^i)^2}{K_i^S} + \frac{(L_p^i)^3}{3E_{c_i} I_i} \right]} \quad (7.23)$$

$$K_{i,i-1} = \left[ \frac{GA_p h_a^2}{aL_i^2} \right] \quad (7.24)$$

$$K_{i,i+1} = \left[ \frac{GA_p h_a^2}{aL_{i+1}^2} \right] \quad (7.25)$$

and the force

$$F_i^q = \left[ \frac{1}{\left[ \frac{(L_p^i)^2}{K_i^S} + \frac{(L_p^i)^3}{3E_{c_i} I_i} \right]} \right] \left[ \frac{q_i (L_p^i)^3}{2K_i^S} + \frac{q_i (L_p^i)^4}{8E_{c_i} I_i} \right] \quad (7.26)$$

are defined, the final equilibrium equation of each pier can be written as

$$F_i^q + m_i a_i = K_{,ii} v_i - K_{i,i+1} v_{i+1} - K_{i,i-1} v_{i-1} \quad (7.27)$$

Applying the former equation to each degree of freedom of the structure, an elastic system of equations  $\mathbf{F} = \mathbf{K} \mathbf{v}$  is obtained.  $\mathbf{K}$  is the tri-diagonal stiffness matrix of the system ( $K_{i,j}$  is the force corresponding to the coordinate  $i$ , due to a unitary displacement produced according to coordinated  $j$ );  $\mathbf{F}$  is the force vector and  $\mathbf{v}$  is the displacement vector at the top of the piers. Considering that the displacement at the girder-abutments connexion is null in the transversal direction, the final stiffness matrix of the bridge is:

$$\begin{bmatrix} K_{2,2} & K_{2,3} & 0 & \cdot & \cdot & \cdot & 0 & 0 \\ K_{2,3} & K_{3,3} & K_{3,4} & \cdot & \cdot & \cdot & 0 & 0 \\ \cdot & \cdot & \cdot & & & & \cdot & \cdot \\ \cdot & \cdot & \cdot & & & & \cdot & \cdot \\ \cdot & \cdot & \cdot & & & & \cdot & \cdot \\ 0 & 0 & 0 & & & & K_{n-2,n-2} & K_{n-2,n-1} \\ 0 & 0 & 0 & & & & K_{n-1,n-2} & K_{n-1,n-1} \end{bmatrix} \begin{bmatrix} v_2 \\ v_3 \\ \cdot \\ \cdot \\ \cdot \\ v_{n-2} \\ v_{n-1} \end{bmatrix} = \begin{bmatrix} F_2 \\ F_3 \\ \cdot \\ \cdot \\ \cdot \\ F_{n-2} \\ F_{n-1} \end{bmatrix} \quad (7.28)$$

<ul style="list-style-type: none"> <li>• Input data: <ul style="list-style-type: none"> <li>→ Piers: length (<math>L_p</math>); Young's modulus (<math>E_c</math>); area (<math>A_c</math>); mass (<math>\rho_c</math>) and transversal inertia (<math>I</math>)</li> <li>→ Girders: length (<math>L</math>); transversal area (<math>A_v</math>) and mass (<math>\rho_v</math>)</li> <li>→ Bearings: shear modulus (<math>G</math>); area (<math>A_p</math>); height (<math>a</math>) and distance between bearing centres (<math>h_a</math>)</li> </ul> </li> <li>• Initial operations: <ul style="list-style-type: none"> <li>→ Mass associated to each vibration mode: <math>m_i</math> (equation 7.29)</li> <li>→ Mass matrix of the system: <math>\mathbf{M}</math></li> <li>→ Distributed forces: <math>q = A_{c_i} \rho_{c_i}</math></li> <li>→ Elastic forces due to the rotation of girders: <math>F_{i+1}^i</math> and <math>F_{i-1}^i</math> (equations 7.11 and 7.12)</li> </ul> </li> <li>• Stiffness matrix of the system: <math>\mathbf{K}</math> (equations 7.23 to 7.28)</li> <li>• Characteristic equation (equation 7.5) <ul style="list-style-type: none"> <li>→ Estimation of the <math>n</math> natural frequencies of the system</li> <li>→ Determination of the periods: <math>T_i = \frac{2\pi}{\omega_i}</math></li> </ul> </li> </ul>
---

**Table 7.1** Procedure of the dynamic characterization of the bridge

In the case of the proposed simplified analysis procedure, it is assumed that the mass of the bridge is concentrated in the points in which the transversal displacements have to be obtained. Thus, the mass matrix of the bridge is determined as:

$$\mathbf{M} = \begin{bmatrix} m_{22} & 0 & \cdot & \cdot & \cdot & 0 & 0 \\ 0 & m_{33} & \cdot & \cdot & \cdot & 0 & 0 \\ \cdot & \cdot & & & & \cdot & \cdot \\ \cdot & \cdot & & & & \cdot & \cdot \\ \cdot & \cdot & & & & \cdot & \cdot \\ 0 & 0 & \cdot & \cdot & \cdot & m_{n-2,n-2} & 0 \\ 0 & 0 & \cdot & \cdot & \cdot & 0 & m_{n-1,n-1} \end{bmatrix} \quad (7.29)$$

where  $m_{ii}$  is the part of the mass of the girders and piers associated to each degree of freedom.

Substituting equations 7.28 and 7.29 in 7.5, the characteristic equation of the system is obtained. Starting from equation 7.5, modal frequencies or periods and mode shapes can be determined for the  $n$  modes of vibration. A simple scheme describing the complete procedure of dynamic characterization of the bridge is shown in table 7.1.

## 7.2. Application of the proposed model to study the behaviour of the Warth bridge

The Warth bridge, localised to 63 km from Vienna, Austria, was built 30 years ago. It was designed for a horizontal acceleration of 0.04 g, using a quasi-static method. Now, according to the new Austrian seismic code, it is necessary to consider for the bridge site horizontal design acceleration of the order of 0.1g (ÖNORM B4015-2 1998). The variation of the seismic design acceleration aims to take into account the recent seismic activity in the zone and the occurrence of more severe earthquakes than the corresponding to the period of the design of Warth bridge. Therefore, a review of the structural behaviour is necessary to ensure the safety of the structure during future earthquakes.

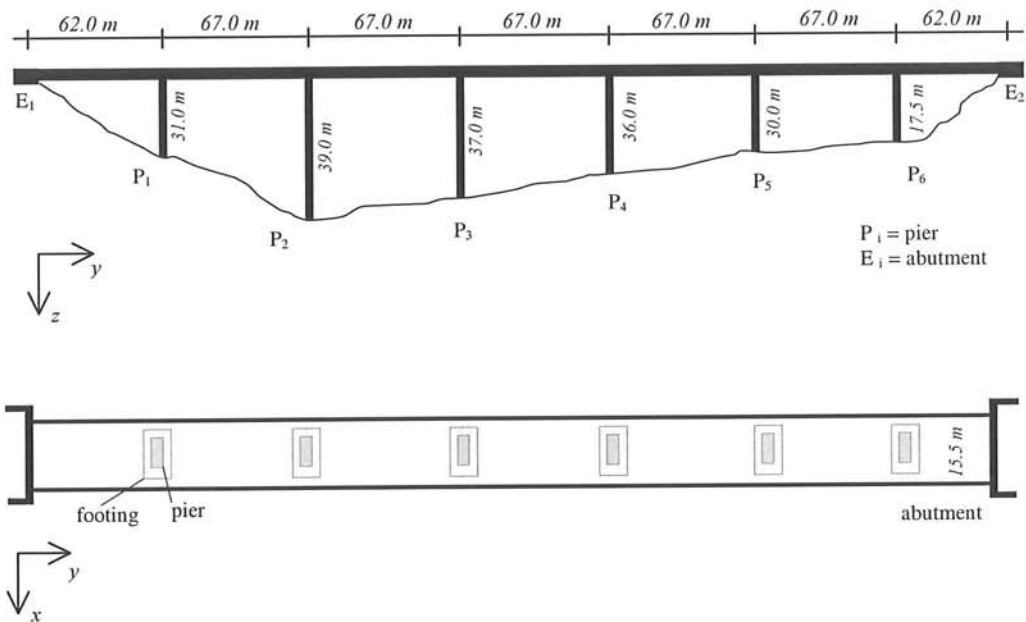
### 7.2.1 Description of the structure

Warth bridge has two spans of 62.0 m and five of 67.0 m, with a total length of 459.0 m. The seven spans of the bridge give rise to six piers with heights of 31.0 m, 39.0 m, 37.0 m, 36.0 m, 30.0 m and 17.6 m, as it can be seen in figure 7.7 (Flesch et al. 2000).

Using the original design drawings of the Warth bridge (Flesch et al. 1999), the geometrical properties of girders, piers and bearings were established. Thus, the following values were considered in the present analysis

$$\begin{aligned}
 \text{piers} & \begin{cases} A_c = 5.98 \text{ m}^2 \\ I_{yy_c} = 103.74 \text{ m}^4 \\ I_{xx_c} = 14.88 \text{ m}^2 \\ J_c = 27.45 \text{ m}^4 \end{cases} \\
 \text{girders} & \begin{cases} A_v = 10.5 \text{ m}^2 \\ I_{zz_v} = 136.65 \text{ m}^4 \\ I_{xx_v} = 129.29 \text{ m}^4 \\ J_v = 73.24 \text{ m}^4 \end{cases} \\
 \text{bearings} & \begin{cases} A = 1.33 \text{ m}^2 \\ a = 0.25 \text{ m} \end{cases}
 \end{aligned}$$

From the drawings it was also determined that the simple compression strength of concrete was  $f'_c = 45.0 \text{ MPa}$  for girders and  $f'_c = 40.0 \text{ MPa}$  for piers. For both elements, the original weight density and the Poisson modulus of concrete were of  $\gamma = 24.0 \text{ kN/m}^3$  and  $\nu = 0.2$ , respectively. In order to consider the weight of the non-structural components (such pavement), the value of the weight density of girders was modified to a value of  $\gamma = 28.0 \text{ kN/m}^3$ . On the other hand, for the reinforcement bars  $\gamma = 78.5 \text{ kN/m}^3$ ,  $\nu = 0.3$  and  $E_a = 2.05 \text{ MPa}$  were considered.



**Figure 7.7** Elevation and plan views of the Warth Bridge

The elastic modulus of the reinforced concrete,  $E_c$ , was obtained using the Mixing Theory (Hull 1987), which determines the properties of the composite elements, composed by more than one material. In particular, the elastic modulus of the reinforced concrete was determined by means of the following expression:

$$E_c = k_h E_h + k_a E_a \quad (7.30)$$

where

$$k_h = \frac{A_h}{A} \quad k_a = \frac{A_a}{A} \quad (7.31)$$

and  $E_h$ ,  $E_a$  and  $E_c$  are the Young's modulus of concrete, longitudinal reinforcement, and composite material, respectively.  $A_h$ ,  $A_a$  and  $A$  are the associated areas to them. A value  $E_h = 2.8E04 \text{ MPa}$  was supposed.

### 7.2.2 Experimental test

For the Warth bridge, the calibration of the proposed model (figure 7.1) was based on the experimental results obtained by the ÖFPZ-ARSENAL Institute (Flesch et al. 1999, Duma and Seven 1998). During the experimental campaigns structural damping, modal shapes and modal frequencies were determined. Among the obtained results, the first modal frequencies and periods of the Warth bridge are shown in table 7.2, in columns two and five, respectively.

Mode Number	Frequency (cycles/s)			Periods (s)		
	Experimental	FE Model	Simplified Model	Experimental	FE Model	Simplified Model
1	0.80 (t)	0.845 (t)	0.858	1.25 (t)	1.18 (t)	1.17
2	1.10 (t)	1.070 (t)	1.064	0.91 (t)	0.93 (t)	0.94
3	1.62 (t)	1.500 (t)	1.282	0.62 (t)	0.67 (t)	0.78
4	2.23 (t)	1.930 (t)	1.400	0.45 (t)	0.52 (t)	0.71
5	2.98 (t)	2.55 (t)	1.68	0.34 (t)	0.39 (t)	0.60
6	3.77 (t)	3.03 (t)	2.982	0.27 (t)	0.33 (t)	0.33

T = transversal

Table 7.2 Frequencies and periods of the experimental and analytical options

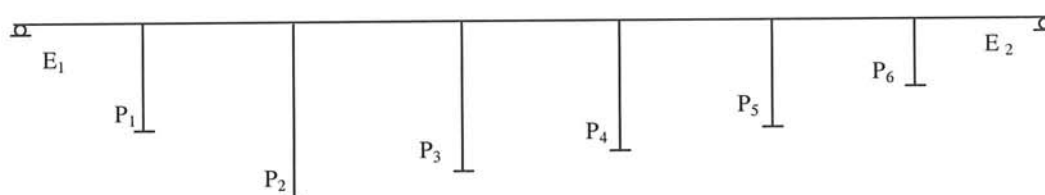


Figure 7.8 Simplified FE model of Warth Bridge

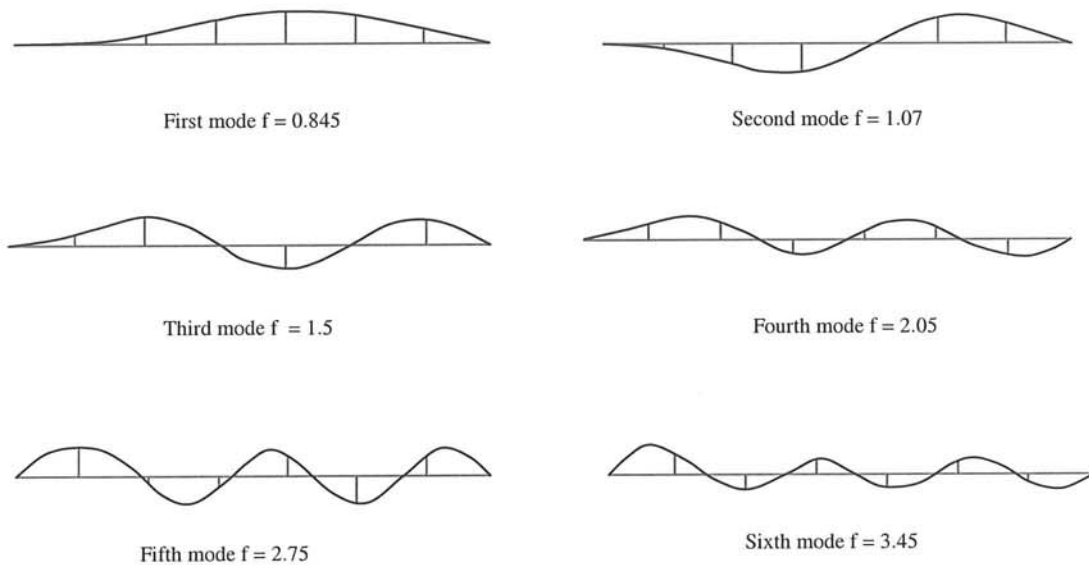
### 7.2.3 Simplified finite element model

As an alternative to calculate the dynamic characteristics of the structure, the bridge was modelled by means of a simplified finite element model (FE model), using beam finite elements. This second calibration model (see figure 7.8) was developed using the commercial code ABAQUS (1999) and was also calibrated based on experimental results.

In this model, eight Timoshenko-beam elements were considered for the girders and piers, and two for the footings (totally 116 elements). Box beams having equivalent elastic properties for girders and pin elements for the pier-girder zone were also used. Furthermore, the following restraints were considered: (1) the three translational degrees of freedom were fixed and the rotations in the connexion zone with the abutments were released; (2) the connections between piers and girders assure the continuity in translation and fix the rotation; and (3) the foundation of the piers was supposed to lean on a rigid base. Thus, the soil-structure interaction effect was not considered. The mode shapes obtained for the simplified FE model are shown in figure 7.9, and in the columns three and six of table 7.2 are given the first six transversal modal frequencies and periods, respectively.

### 7.2.4 Proposed model

Based on the described methodology, the transversal frequencies of Warth bridge were obtained for the first six modes of vibration. The characteristic equation 7.5 is solved using the numerical algorithm of Jacobi (Press et al. 1992). During the analysis, the shear modulus,  $G$ , of the bearings was used as calibration variable. The iterative procedure of calibration was continued until values similar to the experimental ones were obtained.



**Figure 7.9** Mode shape and frequencies for Warth Bridge. FE model

The soil-structure interaction effect was not considered in this model. The main results are the first six modal frequencies (column four of table 7.2) and the corresponding periods (column seven of table 7.2). The mode shapes associated to these periods are shown in figure 7.10

Comparing the values of table 7.2, a good correlation between them is observed. Furthermore, when comparing the mode shapes obtained by means of the simplified FE model and the proposed model (figures 7.9 and 7.10), it can be concluded that the three or four first mode shapes are similar. The last mode shapes are similar, but different in amplitudes. This last aspect is not essential, because it has been observed that in both models the first modes of vibration govern the response of the structure.

### 7.2.5 Elastic analysis

Using the simplified FE model (figure 7.8) and the proposed simplified model, the structural response is obtained by means of an elastic analysis. In this analysis, the following sin function was used as input acceleration

$$a(t) = \begin{cases} 10 \sin(5.0t) & 0 < t < 10 \\ 0 & \text{other case} \end{cases} \quad (7.32)$$

whose frequency is the fundamental frequency of the bridge

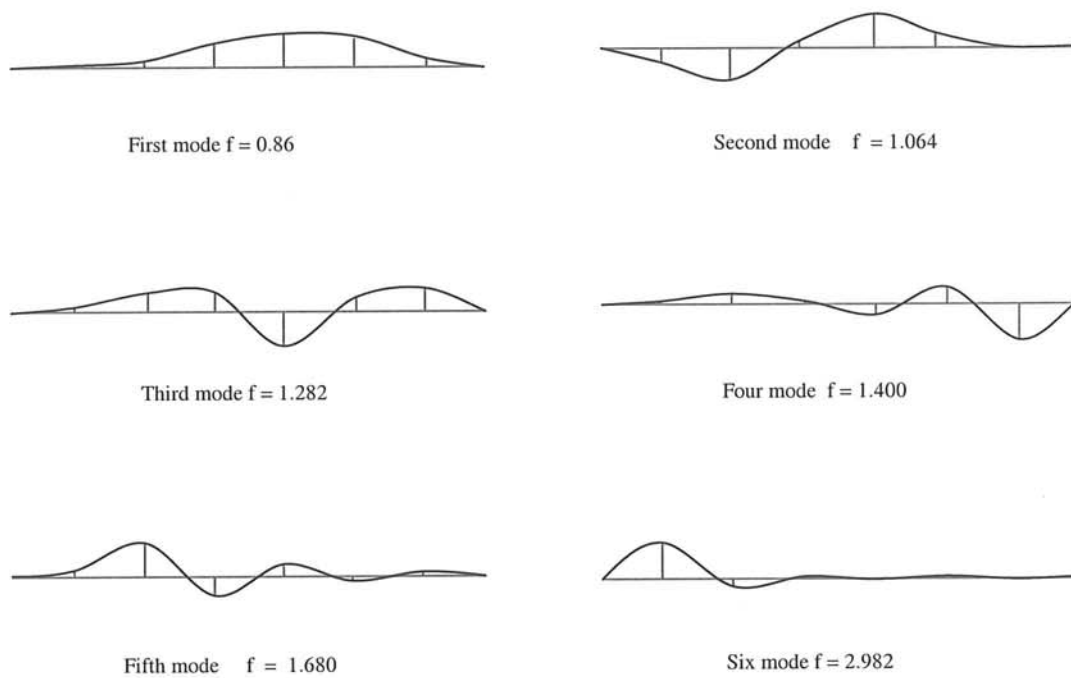


Figure 7.10 Mode shapes and frequencies of Warth Bridge. Proposed model

Number of Pier	Maximums values at the top of the piers		
	Displacement (cm)	Velocity (cm/s)	Acceleration (cm/s <sup>2</sup> )
1	3.52	17.79	95.44
2	7.24	36.64	193.50
3	8.51	42.00	222.70
4	6.22	31.20	166.67
5	2.61	13.11	71.25
6	0.37	1.87	9.02

Table 7.3 Maximum values obtained with the FE model

Number of Pier	Maximums values at the top of the piers		
	Displacement (cm)	Velocity (cm/s)	Acceleration (cm/s <sup>2</sup> )
1	2.16	11.41	61.39
2	6.94	35.85	188.79
3	7.71	39.91	209.11
4	5.62	29.30	154.06
5	1.86	9.42	55.02
6	0.25	1.21	9.93

Table 7.4 Maximum values obtained with the simplified proposed model

Through the elastic analysis the maximum responses, displacement, velocity and acceleration, of the simplified of FE and the proposed model were obtained. In tables 7.3 and 7.4 are shown these results. Comparing the values of these tables, a good agreement is observed for these maximum responses.



## Chapter 8

### Damage characterization using the simplified model

A study of seismic damage requires to understand in which measure different factors are responsible for the damage process and to derive from them some useful information. The structural damage can provide a description of the seismic vulnerability of a structure and is an indicator of various local phenomena.

#### 8.1 Proposed methodology

To evaluate the seismic damage of a bridge, a non-linear analysis procedure is proposed starting from the linear model described in chapter seven and especially from the formulation of the mass matrix (equation 7.29) and of the stiffness matrix (equations 7.23, 7.24, 7.25 and 7.27). According to the general hypotheses of the elastic model, the girders remain in the elastic range when the structure was subjected to the seismic action. Thus, the only members that can be damaged are the piers.

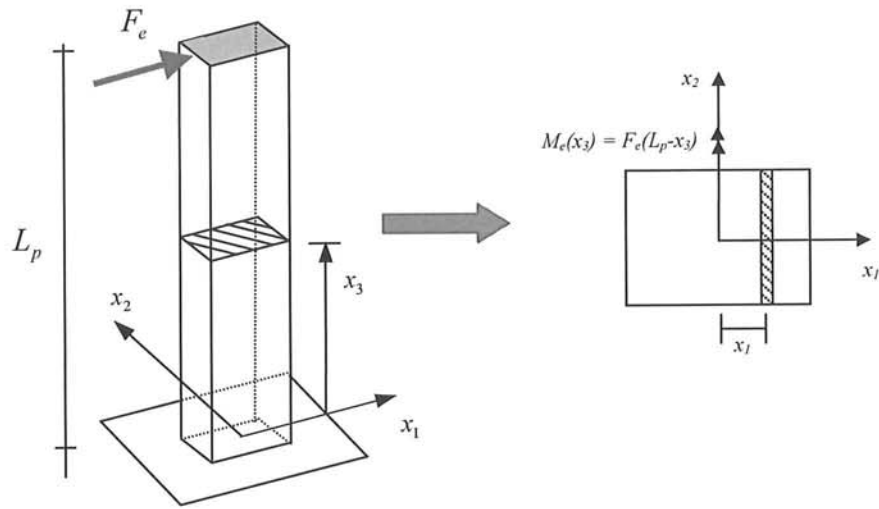
In elastic conditions, the solution of the equation 7.27 assures the equilibrium at each time instant. However, when the non-linear behaviour of the structural materials is taken into account, the equation of motion for each pier is

$$F_i^q + m_i a_i - K_{ii} v_i - K_{i,i+1} v_{i+1} - K_{i,i-1} v_{i-1} - F_a = F_i^R \quad (8.1)$$

where  $F_a$  is the damping force for the pier  $i$  and  $F_i^R$  is the residual force or the out of balance force that must be eliminated through a Newton-Raphson process. This unbalanced force is due to the fact that the stiffnesses  $K_{ii}$ ,  $K_{i,i+1}$  and  $K_{i,i-1}$  are not constant during the analysis process and, consequently, the solution of the equation 8.1 should be obtained from an iterative process.

To obtain the maximum damage for the bridge piers using the model described in figure 7.1, the non-linear equation 8.1 is solved by using Newark's algorithm (Bathe 1996). In this analysis the balance condition is achieved by eliminating  $F_i$  by means of a Newton-Raphson process, what indirectly eliminates the residual bending moment,  $\Delta M$ . Consequently,  $\Delta M = M_e - M_{int}$  is the difference between the moment demand,  $M_e$ , and the resistant moment,  $M_{int}$ . For each step of the non-linear analysis the properties of the system are updated, considering the degradation of the material caused by the seismic action.

The steps followed to define the damage in any of the piers of the bridge are described in following. The maximum global structural damage of the bridge is evaluated by using the proposed simplified model, considering in the analysis only the damage at the base of the piers due to the transversal seismic action.



**Figure 8.1** Simplified model of a pier used in the non-linear analysis

### 8.1.1 Top displacement due to the seismic action

Starting from the current mass, stiffness and damping matrices, the vector of displacement, velocity and acceleration are obtained by means of the non-linear Newmark's method, described in Appendix A. This method obtains in an iterative way the structural response at every time increment. Also, it considers a convergence criterion that assures an out of balance incremental load vector lesser than a predefined tolerance.

### 8.1.2 Maximum external moment

The proposed methodology considers that the piers of the bridge are subjected, predominately, to bending in the direction perpendicular to the bridge axis, as it is observed in figure 8.1. In the following, the evaluation of the damage will be explained for any of the piers of the bridge, without writing a sub-index for the pier.

Knowing the maximum displacement of a pier, the resultant force at the top and the maximum external moment at the base (predictor) are obtained by means of

$$F_e = v \cdot k \quad (8.2)$$

$$M_e = F_e \cdot L_p \quad (8.3)$$

where

$$k = \frac{3E_c I}{L_p^3} \quad (8.4)$$

is the initial bending stiffness of the pier,  $F_e$  is the elastic force produced by an external action at the top of the pier,  $M_e$  is the maximum external moment,  $v$  is the maximum displacement of the pier (obtained by means of Newark's algorithm), and  $E_c$ ,  $I$ , and  $L_p$  are the concrete Young's modulus, the inertia of the cross section and the length of the pier, respectively. Starting from the maximum external moment, it is possible to calculate the maximum damage that a pier can suffer due to the seismic action.

### 8.1.3 Damaged state of the structure

In the case of seismic loads acting in the transversal direction of a bridge ( $x_1$  axis), the elastic state of stress and strains in the longitudinal direction of the pier are

$$\begin{cases} \varepsilon(x_1; x_3) = \chi_1(x_3) \cdot x_1 \\ \sigma(x_1; x_3) = E_c \cdot \varepsilon(x_1; x_3) \end{cases} \quad (8.5)$$

where

$$\chi_1(x_3) = \frac{M_e(x_3)}{E_c I} \quad (8.6)$$

is the curvature of the pier,  $\sigma(\cdot)$  and  $\varepsilon(\cdot)$  are the stress and strain values,  $x_2$  is the distance (in direction of this axis) from the current point to the neutral axis of the cross section of the pier,  $E_c$  is the initial Young's modulus of the pier, and  $M_e$  is the external load function acting on the element.

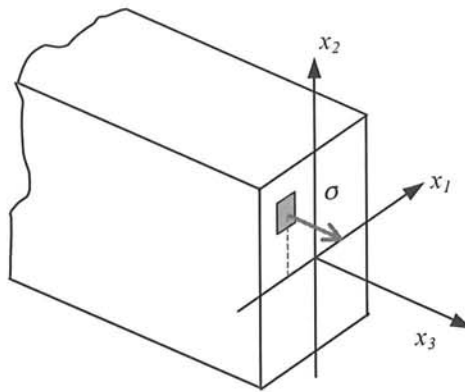
Substituting equation 8.6 in equation 8.5, the cross sectional states of stress and strain in direction  $x_2$  are defined by

$$\begin{cases} \varepsilon(x_1; x_3) = \frac{M_e(x_3)}{E_c I} \cdot x_1 \\ \sigma(x_1; x_3) = \frac{M_e(x_3)}{I} \cdot x_1 \end{cases} \quad (8.7)$$

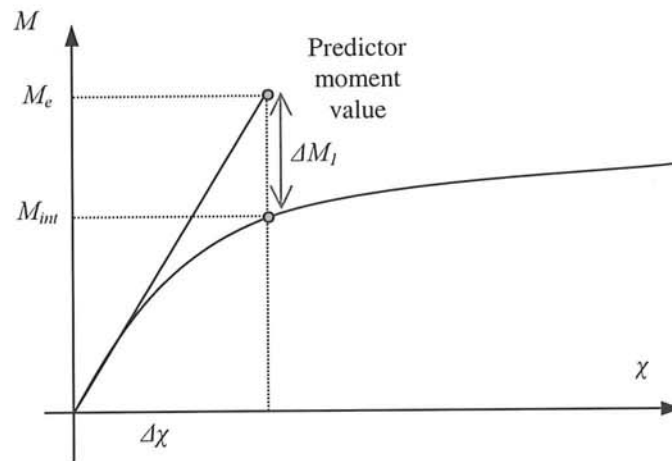
Starting from these equations, the internal moment for the cross section of a pier (see figure 8.2) is given by

$$M_{\text{int}}(x_3) = \int_{A_c} \sigma x_1 dA_c \quad (8.8)$$

where the internal moment in the longitudinal direction  $M_{\text{int}}(x_3)$  is obtained by integrating the moments of the elemental forces  $\sigma dA_c$  on the cross sectional area,  $A_c$ , of the pier.



**Figure 8.2** Evaluation of the internal moment acting on the section of a pier



**Figure 8.3** Moment curvature diagram for a pier

When the studied element remains in the elastic range, the external bending moment and the internal sectional moment of the pier are equal. However, when the elastic limit of the material has been exceeded, the demanded moment,  $M_e$ , is greater than the resistant moment,  $M_{int}$ , and the residual moment (see figure 8.3) is

$$\Delta M(x_3) = M_e(x_3) - M_{int}(x_3) < \text{Tolerance} \quad (8.9)$$

To reach the equilibrium, this residual moment,  $\Delta M(x_3)$ , should be lesser than the imposed tolerance value and has to be reduced by means of an iterative procedure based on Newark's algorithm (shown in Appendix A).

When the pier suffers damage, the state of stress developed in the damaged cross section of the structure (equation 8.7) is evaluated by means of the following equation:

$$\sigma(x_1; x_3) = f(x_1; x_3) E_c^0 \chi_1(x_3) x_1 \quad (8.10)$$

where

$$E_c^d = f(x_1; x_3) E_c^0 \quad (8.11)$$

is the Young's modulus of the damaged material,  $E_c^0$  is the initial Young's modulus (of the undamaged material), and  $f(x_1; x_3)$  is the damage function that will be defined later. Substituting equation 8.10 in 8.8, the internal moment of the cross section of the pier is

$$M_{\text{int}}(x_3) = E_c^0 \chi_1(x_3) I^d(x_3) \quad (8.12)$$

where

$$I^d(x_3) = \int_{A_c} f(x_1; x_3) \cdot x_1^2 dA_c \quad (8.13)$$

is the inertia of the damaged cross section of the studied pier respecting the new neutral axis. For each time increment, a predictor moment is defined by means of the following equation:

$$M^0(x_3) = E_c^0 I(x_3) \chi_1(x_3) \quad (8.14)$$

in which the elastic properties of the material have been used.

Then, for a time increment when the predictor moment produces an unbalanced load increment greater than a tolerance (equation 8.9), the procedure considers an increment in the curvature in order to obtain a moment corrector that could reach the equilibrium state. The iterative process finalises if the out of balance load is lesser than the tolerance.

The convergence criterion used in the proposed methodology states that a stable response can be obtained for the whole structure if

$$C_c = \sqrt{\frac{\sum_i \Delta M_i^2}{\sum_i (M_e^i)^2}} \leq TOL \quad (8.15)$$

where  $TOL$  is the tolerance.

## 8.2. Damage function

Basically, the structural damage can be characterised in two ways. In the first, the damage is described by means of global damage indices, which are scalar functions depending on some variables (or damage parameters) that represent the dynamic response of the system (Aguiar and Barbat 1999, Rahman and Grigoriu 1994, Park et al. 1985, Park and Ang 1985, Powell and Allahabadi 1988). The other possibility is to estimate the structural damage in a point. This is a reliable method to estimate the damage accumulation originated by a micro-structural degradation starting from the Continuous Mechanics (Lemaitre 1992, Oller et al. 1992, Oller et al. 1996, Oller 2001). This former procedure was the methodological path to damage estimation adopted in this research.

In order to define the damaged inertia and the internal moment of a cross section of a pier, the local damage model proposed by Oliver et al. (1990), has been applied. The complete description of this model could be observed in Appendix B of this work.

Then, according to the isotropic damage model of Oliver et al. (see equations B.9 and B.10 of Appendix B), the level of damage of the cross sections of a pier is evaluated by means of the following damage function:

$$f(x_1; x_3) = 1 - d(x_1; x_3) \quad (8.16)$$

where

$$d(x_1; x_3) = 1 - \frac{\tau^*}{\tau(x_1; x_3)} \exp \left[ A - \frac{\tau(x_1; x_3)}{\tau^*} \right] \quad (8.17)$$

being  $\tau^*$  the damage threshold (equations B.7 and B.8),  $\tau$  the effective stress, and  $A$  a parameter depending on the fracture energy (equation B.11).

### 8.3 Determination of the damaged inertia

Due to the difficulties of performing a closed integration of equation 8.13 with the non-linear damage function defined by equation 8.17, the tensor of inertia of the damaged cross section is calculated by means of a numerical algorithm. It is important to note that the selected integration algorithm should consider that one of the points, where the function to be integrated is evaluated, is situated in the extreme of the cross section, being thus possible to capture adequately the beginning of damage. Consequently, the algorithm of Lobato (Press et al. 1992) was considered to perform the numerical integration.

When the cross section of the structure to be analysed is box shape, like the piers of the Warth bridge, the inertia of the damaged cross section is obtained dividing the element in four subsections, as shown in figure 8.4. For each subsection, the damaged inertia (equation 8.13), the damaged area ( $A_c^d$ , equation 8.18) and the distance between its neutral axes and the global neutral axis of the complete cross section are calculated.

$$A_c^d(x_3) = \int_{A_c} f(x_1; x_3) dA_c \quad (8.18)$$

The global inertia of the damaged cross section,  $I_T^d$ , is defined as:

$$I_T^d(x_3) = \sum_{j=1}^4 \left( I_j^d + A_c^{d(j)} l_c^{2(j)} \right) \quad (8.19)$$

where  $I_j^d$  is the damaged inertia of subsection  $j$ , evaluated by means of equation 8.13,  $A_c^{d(j)}$  is the damaged area of the subsection  $j$  and  $l_c^{2(j)}$  is the distance between the neutral axis of subsection and the  $j$  global neutral axis.

In a non-linear problem, when damage occurs due to the seismic load, the particular position of the neutral axis of each subsection is modified according to the portion of the subsection that is damaged.

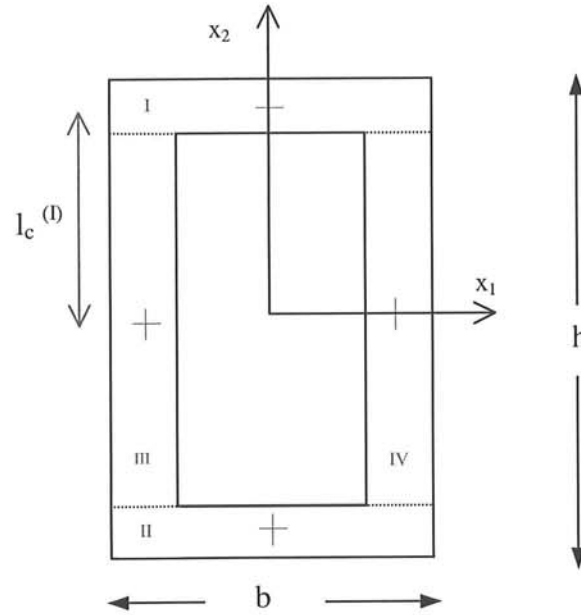


Figure 8.4 Subsections of a box section used to evaluate its global damaged inertia

This modification must be reflected in the calculation of the distances to the global neutral axis of each subsection. Thus, to obtain each  $l_c^{(i)}$ , it is necessary to know for each subsection  $X_1^{CG}$  and  $X_2^{CG}$ , which are evaluated in a general form by means of the following equations:

$$X_1^{CG} = \frac{\int_{A_c} x_1 f(x_1; x_3) dA_c}{\int_{A_c} f(x_1; x_3) dA_c} \quad (8.20)$$

$$X_2^{CG} = \frac{\int_{A_c} x_2 f(x_1; x_3) dA_c}{\int_{A_c} f(x_1; x_3) dA_c} \quad (8.21)$$

#### 8.4 Pier damage and global damage indices

Once the convergence of the process is reached and the damage is calculated at each integration point, the maximum damage at the base cross section of a pier can be obtained. In this work two pier damage indices and three global damage indices are defined. The first pier damage index characterizes the maximum damage at the base of each pier of the bridge

$$D = \frac{M_e(x_3) - M_{int}(x_3)}{M_e(x_3)} \quad \text{for } x_3=0 \quad (8.22)$$

The second pier damage index,  $DP$ , proposed by DiPasquale and Cakmak (Rodríguez and DiPasquale 1990), is based on the dynamic characteristic of the structure to evaluate the seismic damage

$$DP = 1 - \frac{(T_o)^2}{(T_f)^2} \quad (8.23)$$

where  $T_o$  is the period of the structure in the elastic range, and  $T_f$  is the period corresponding to the damaged structure at the end of the analysis.

Starting from the pier damage indices of equations 8.22 and 8.23, the global structural damage caused by seismic action in the studied bridge is described by three indices:

- *Global mean damage index*, which is the simple average of the pier damages indices

$$D_m = \frac{\sum_i D_i}{n_p} \quad i = 1, \dots, n_p \quad (8.24)$$

where  $n_p$  is the number of piers in the studied bridge and  $D_i$  is the damage of piers, defined in equation 8.22.

- *Global functional damage index*,  $D_p$

$$D_p = 1 - [\prod_i (1 - D_i)] \quad i = 1, \dots, n_p \quad (8.25)$$

The functional damage index aims to be an indicator of the capacity of the bridge to give service after an earthquake.

- *Global mean damage index of DiPasquale y Cakmak*, which is defined starting from the pier damage index of equation 8.23

$$D_a = \frac{\sum_i DP_i}{n_p} \quad i = 1, \dots, n_p \quad (8.26)$$

The elastic analysis described in chapter seven is included together with the non-linear procedure in a simplified methodology to evaluate the seismic damage of bridge structures. The complete process of analysis is synthesised in the scheme of figure 8.5, where the elastic predictor and the corrector steps are shown.

### 8.5 Comparison between the results obtained by means of the simplified model and a finite elements model

Using the proposed model and the simplified finite element model of figure 7.8, a non-linear analysis of the Warth bridge (described in chapter 7) is performed. In this analysis the external action at each pier is defined as



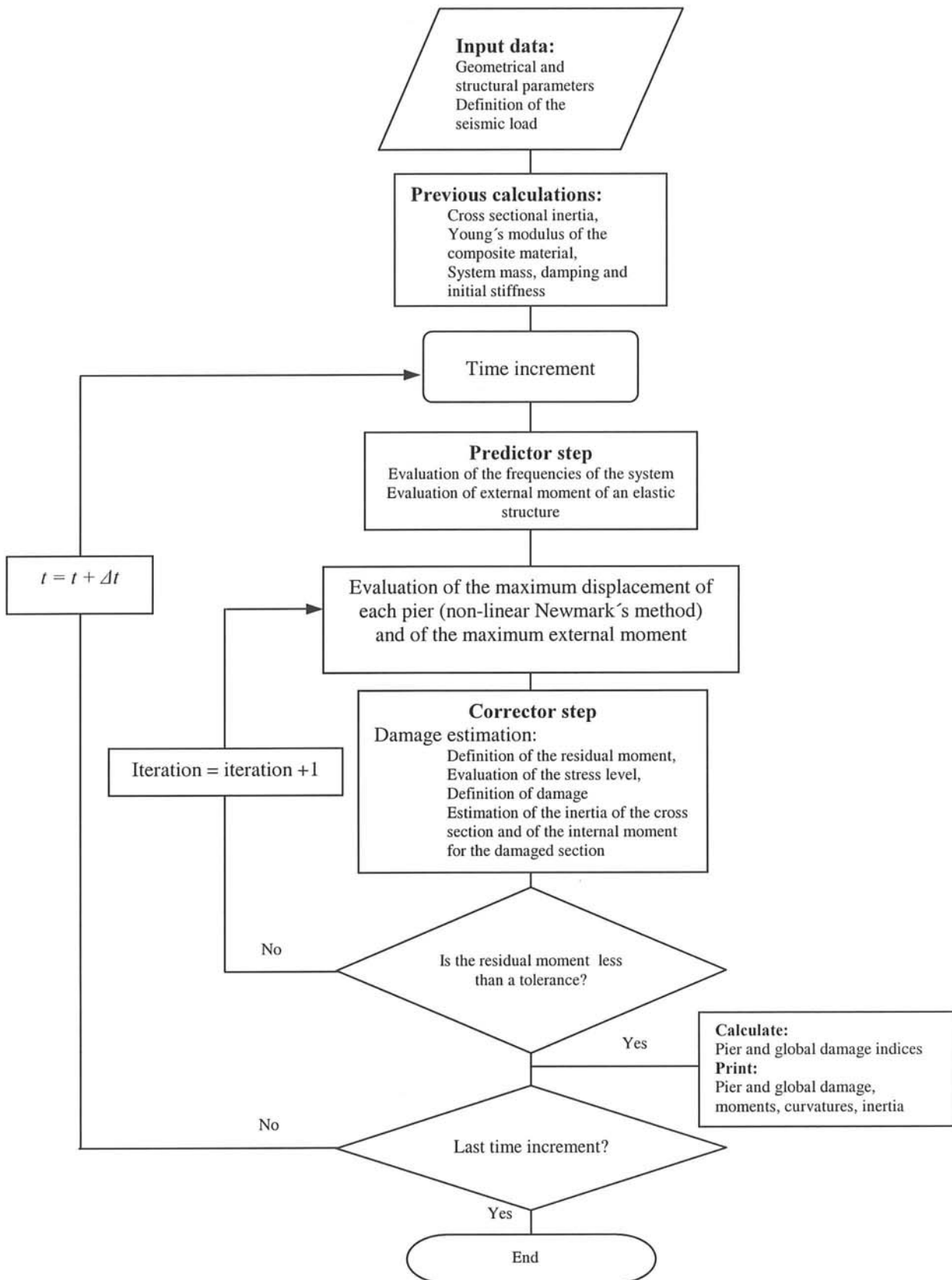


Figure 8.5 Damage evaluation scheme

Pier	Simplified model Maximum damage at a point	ABAQUS model Maximum damage at a point
1	0.9514	1.0000
2	0.9842	0.9831
3	0.9757	0.9820
4	0.9692	0.9844
5	0.9497	0.9834
6	0.8552	0.9950

**Table 8.1** Maximum values of the damage at the integration points of the piers of the Warth bridge. External excitation expressed by equation 8.27

$$a(t) = t \sin(\omega t) \quad 0 < t < 40s \quad (8.27)$$

where  $\omega$  is the oscillation frequency, equal to the fundamental frequency associated to each pier (see table 7.2), and  $t$  is the time.

To define the damage for the finite element model the Oliver et al. (1999) model was implemented in the ABAQUS code (HKS 1999). For this model and for each pier of the bridge, the damages produced at 15 integration points in the cross section were determined. These values are shown in the third column of table 8.1.

On the other hand, using the simplified proposed model, the damages at 36 points of each subsection of the cross section (see figure 8.4) were obtained for each pier of the bridge. From these values, the maximum damages were obtained and are shown in the second column of table 8.1. It is observed from this table that both models provide similar maximum results for damage.

The non-linear analysis performed with the proposed simplified model requires approximately 25 s of CPU in a Silicon Origin 2000 machine. The same analysis with the finite elements model and with the ABAQUS code requires a total time of CPU of 3.27 hours, in the same machine.

## 8.6 Example

Applying the proposed simplified model, the damage estimation of the Warth bridge was performed using as external action six accelerograms defined by Panza et al. (2001) for a seismic scenario with a magnitude of 5.5 and a distance to the source of 8 km. The records were generated using a seismological model that considers the spatial variation of the seismic waves. These records have peak ground accelerations of 90 cm/s<sup>2</sup>, 160 cm/s<sup>2</sup>, 180 cm/s<sup>2</sup>, 100 cm/s<sup>2</sup>, 120 cm/s<sup>2</sup> and 30 cm/s<sup>2</sup>.

Performing the non-linear analysis, the damage indices in piers (equations 8.22 and 8.23) and the global damage indices of the bridge (equations 8.24 to 8.26) were obtained and are shown in the figures 8.6 to 8.8. It is observed in figures 8.6 and 8.7 that piers P<sub>5</sub> and P<sub>6</sub> have an elastic performance, while pier P<sub>3</sub> suffers the greatest damage, with a maximum value close to 6% for both pier damage indices. Furthermore, it is observed in these figures that both pier damage indices are similar, being in all the cases the damage indices  $D_i$  slightly greater than the damage indices  $DP_i$ .

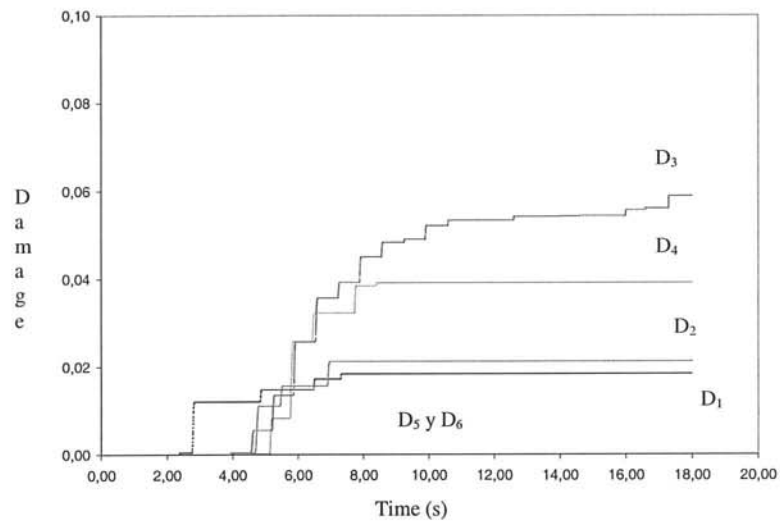


Figure 8.6 Variation of the pier damage indices (equation 8.22)

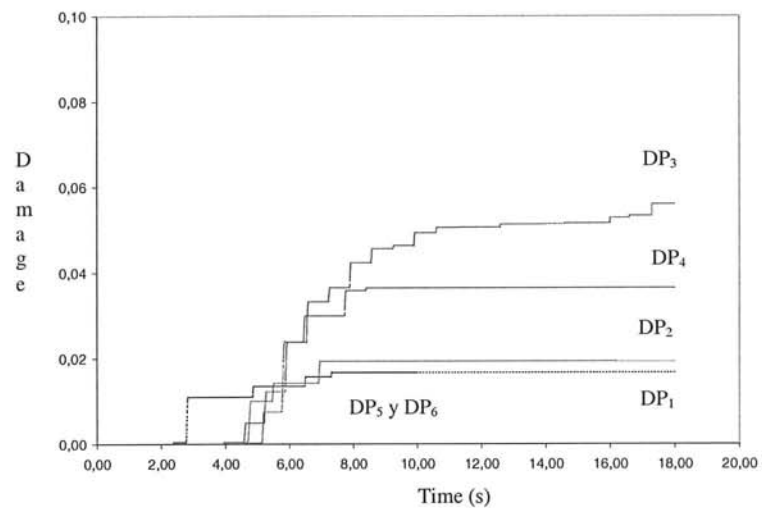


Figure 8.7 Variation of the pier damage indices (equation 8.23)

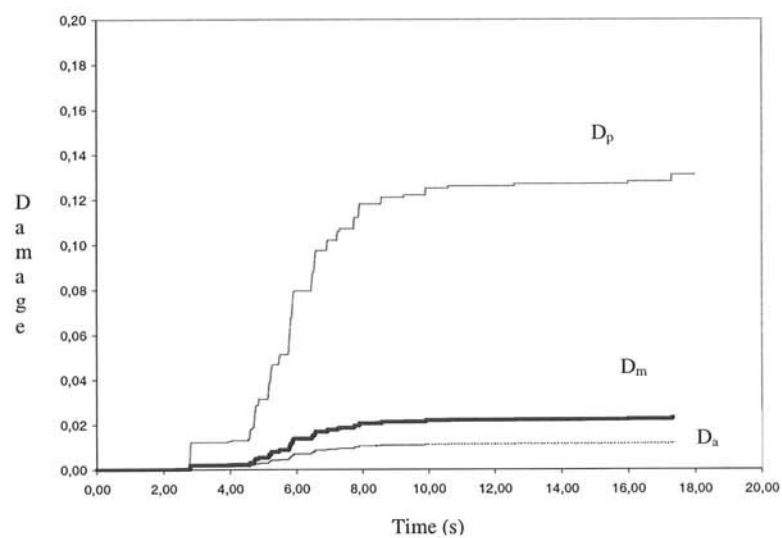
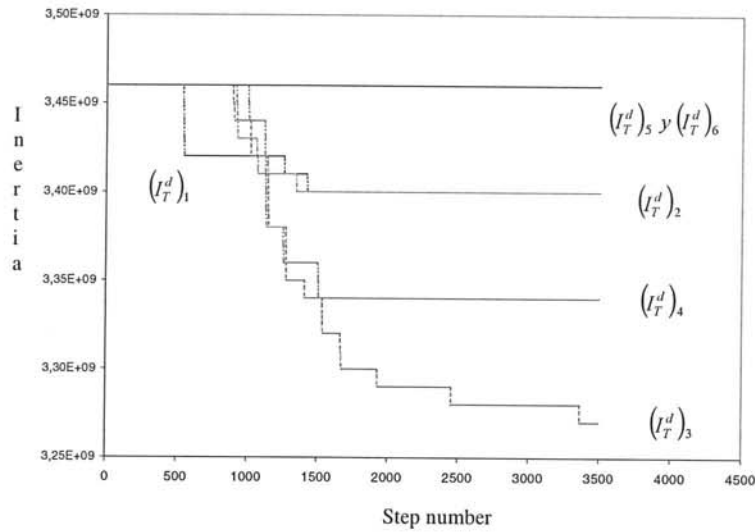


Figure 8.8 Variation of the global damage indices (equations 8.24 to 8.26)



**Figure 8.9** Variation of the cross sectional inertia of the bridge piers

The maximum values of the global damage indices of the bridge obtained in this example are  $D_m = 2.29\%$ ,  $D_p = 13.1\%$  and  $D_a = 1.17\%$ , that is, a minimal damage would occur and a minor repair would be required. As it is observed in figure 8.8 the functional global index  $D_p$  is an extreme value of the damage that would correspond to service states of the structure. The remaining two global damage indices have similar values, being the index  $D_m$  always greater. Finally, figure 8.9 shows the variation of the cross sectional inertia moments of the piers, calculated through the equation 8.19.

Summarizing, the proposed damage evaluation methodology provides a simple way to define pier damage. Its computational cost is low; the computer program runs in a personal computer and the methodology fulfils thus the requirements necessary for its use in a Monte Carlo simulation.

## Chapter 9

### Seismic hazard of the Warth bridge site

To define the seismic vulnerability of the Warth bridge (chapter 10) is necessary the determination of the seismic hazard of the site. This bridge is localised in a moderate seismic zone, where only a few number of real records are available. Thus, to study this structure artificial accelerograms should be generated to obtain reliable responses.

In a previous work, Panza et al. (1999) studied the seismic characteristics of the Warth bridge site. In this research two possible seismic scenarios were defined: (1) earthquake magnitude of 5.5 and distance to the source of 8 km; and (2) earthquake magnitude of 6.5 and distance to the source of 30 km. For each one of these scenarios artificial accelerograms were generated, in three perpendicular directions, at each pier or abutment sites. In the generation process a seismological method that considers the spatial variability of the external load were applied by Panza et al. (1999).

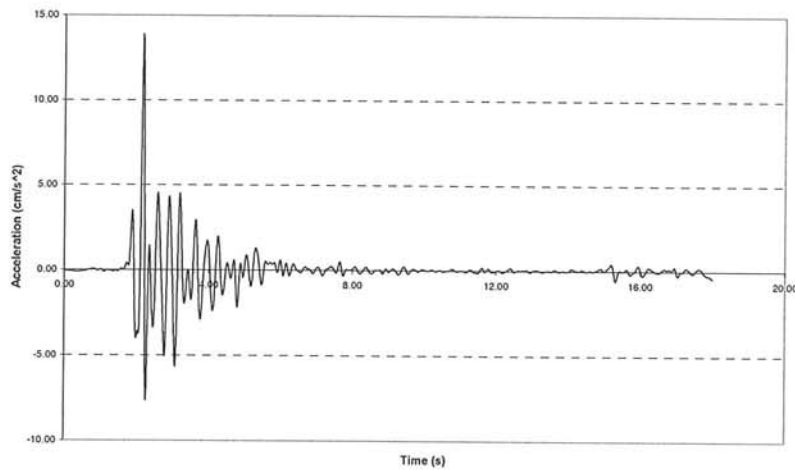
In this work the two seismic scenarios defined by Panza et al. were used to analyse the bridge behaviour. The accelerograms of the second seismic scenario were applied directly, but families of artificial signals were generated starting from the records defined by Panza et al. for the first scenario. This last procedure was performed to consider the inherent uncertainties of the seismic load. In following the procedure to generate these families of artificial accelerograms will be commented.

#### 9.1. First seismic scenario

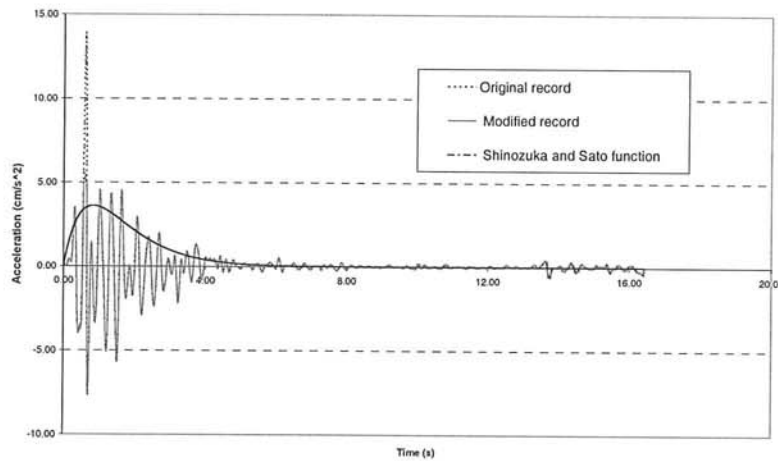
From Panza et al. (1999) we obtained 24 artificial and deterministic accelerograms for the bridge site, 8 for each pier in the longitudinal, transversal and vertical directions. A seismic magnitude of 5.5 and a distance to the source of 8 km were considered for these records.

To consider the uncertainties associated to the future seismic load, families of artificial signals, starting from the 24 original records determined by Panza et al. (1999), were generated. For this process, nonstationary models were used to define artificial records similar in their general aspect but different in details. Accordingly, in this method the seismic action is supposed to be a process with time variations in amplitudes and frequencies (Nigam 1983) considering thus the evolutionary nature of the signal. The nonstationary method defines stationary signals as a finite sum of sin functions with different phase angle. Later, available models of amplitude modulating function and frequency modulating function are used to modify the record in a nonstationary signal.

The procedure is briefly explained in the following, emphasizing as an example some of the results obtained for the third transversal accelerogram (figure 9.1), which corresponds to the original external action for the highest pier of the Warth bridge.



**Figure 9.1** Input earthquake action for pier P<sub>3</sub>. Magnitude of 5.5, distance to the source of 8 km.



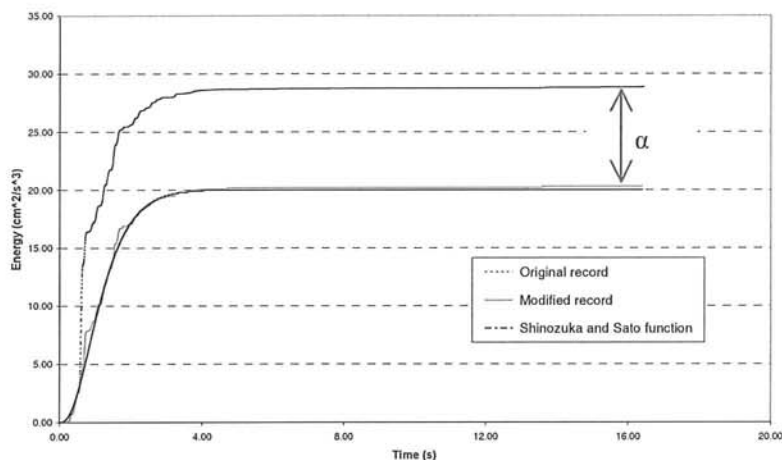
**Figure 9.2** Acceleration functions for the record of figure 9.1

### 9.1.1. Determination of the amplitude modulating function, $\xi(t)$ .

For the original records, some initial tasks are necessary for realizing this step. First, the initial ground accelerations have to be eliminated from the record, up to the actual beginning of the signal (original record, dotted-line in figure 9.2). In addition, the original record has to be again modified, eliminating the upper part of the peak acceleration, as it can be observed in figure 9.2 (continuous line).

This operation is necessary due to the fact that the original records have some peak accelerations with very pronounced values, which are practically impossible to be captured by the modulating functions existing in the literature. The portion of the eliminated peak acceleration is included afterwards in the analysis, expressing the final modulating function of the modified record,  $\xi^{*2}(t)$ , as:

$$\xi^{*2}(t) = \xi^2(t) + \alpha \delta(t - t_1) \quad (9.1)$$



**Figure 9.3** Energy functions of the accelerograms of figure 9.1

where:  $\alpha$  is the mean difference between the energy related to the original record (dotted line, figure 9.3) and the energy of the modified record (continuous line, figure 9.3);  $\delta(t-t_1)$  is the Dirac delta function (obtained from the peak acceleration eliminated from the original record); and  $\xi^*(t)$  and  $\xi(t)$  are the amplitude modulating functions of the original and modified records, respectively.

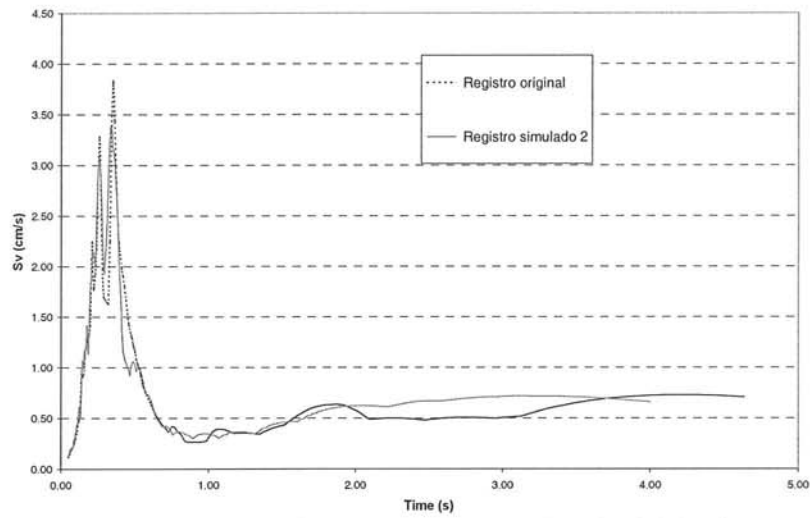
The modulating function of Shinozuka and Sato (1967) was selected as an adequate model. The identification of the parameters of the Shinozuka and Sato function is performed by forcing the equivalence of the energies associated to the function and to modified record, using the Levenberg-Marquart algorithm (Press et al. 1992). Figure 9.3 shows the energy of the Shinozuka and Sato function (discontinuous line) fitted to the modified record (continuous line) of figure 9.2. In figure 9.3, the energy of the original accelerogram (dotted line) and the last value of variable  $\alpha$  are also indicated.

### **9.1.2. Determination of a model for the frequency modulating function,**

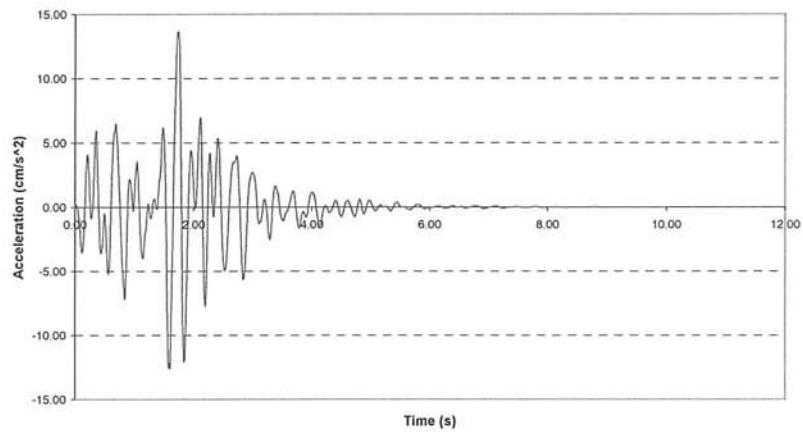
This step considers the variations of frequency content of the original record. A  $M$ -order polynomial function (in this case,  $M=3$ ) is fitted in this step to the empirical function with accumulated zero crossings of the original record (Hurtado 1999, Barbat et al. 1994, Yeh y Wen 1990).

Starting from the original accelerogram, a stationary record is simulated, based on the hypothesis that any stationary process can be approximated by a finite sum of sine functions, modified by a modulating function that defines the shape of the accelerogram. Additionally, the procedure considers that the density spectra of the original accelerogram and of the simulated one are supposed to be compatible, as shown in figure 9.4.

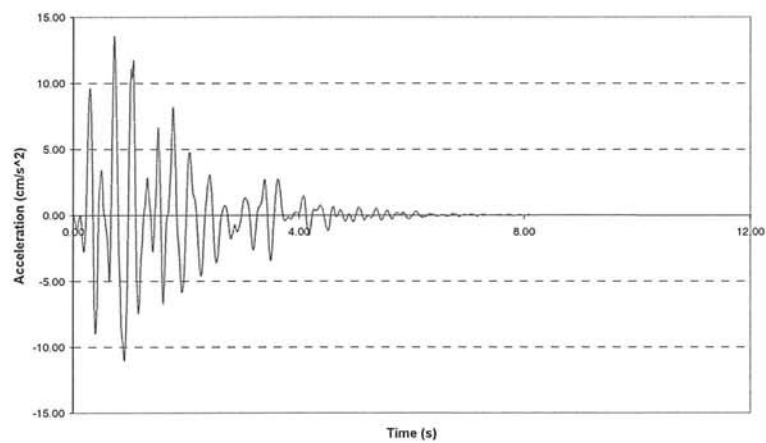
The random nature of the seismic action is introduced by using the random phase angles of the sine functions, considering that they are distributed uniformly between 0 and  $2\pi$ . Then, different artificial records, similar in their general aspect but different in details, are obtained.



**Figure 9.4** Similar response spectrum (in velocity) for the original and generated records

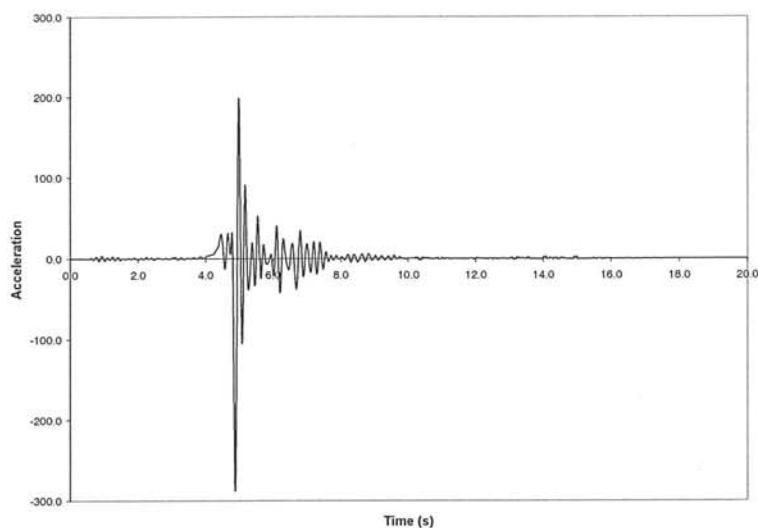


**Figure 9.5** First artificial record generated starting from the accelerogram of figure 9.1



**Figure 9.6** Second artificial record generated starting from the accelerogram of figure 3.1





**Figure 9.7** Input earthquake action for pier P<sub>1</sub>.  
Magnitude of 6.5, distance to the source of 30 km.

### ***9.1.3. Definition of a nonstationary record***

The stationary record defined in the above step is transformed into a nonstationary one, using the modulating functions in amplitudes and frequencies obtained in previous steps of the process.

### ***9.1.4. Improvement of the signal***

The artificial signal, finally, is improved by means of some tasks, as such as: baseline correction (normally considering null velocity at the end of the record), fitting of the maximum acceleration and modification of the spectral response.

Following the above described steps, for each of the 24 accelerograms provided by Panza et al. (1999) a family of 20 artificial records were obtained and used in the stochastic vulnerability assessment of the bridge, which is described in next chapter. An example of two artificial signals corresponding to the original record of figure 9.1 is shown in figures 9.5 and 9.6.

## **9.2. Second seismic scenario**

Panza et al (1999) consider a second seismic scenario with a magnitude of 6.5, a distance of the source of 30 km, and depth of 10 km. For this, 8 accelerograms were simulated using a 2D seismological model. These new earthquakes show a greater damage capacity than the earthquakes used for the other seismic scenario. An example of the used earthquakes for this simulation can be observed in figure 10.29, which represent the external load assigned (see figure 7.8) to pier P<sub>1</sub>.

## Chapter 10

### Probabilistic damage analysis of the Warth bridge

The prediction of the seismic damage that a structure can undergo during its life is a probabilistic problem, due to the uncertainties in the characteristics of the future seismic actions and of the structural model. For instance, it is not possible to predict in advance the precise instant of occurrence of an earthquake and neither can be estimated with precision its amplitude, frequency content or duration. Moreover, the structural response is evaluated by using an idealized model, which leads to results that can vary drastically from the actual ones depending on the characteristics of the model. Finally, a correct characterization of the properties of the structural material, like strength, mass, fracture energy or damping is difficult (Hwang et al. 1999).

Knowing the uncertainties associated to seismic load, to the structural model and to its material properties, it is appropriate to perform a probabilistic simulation to characterise the seismic vulnerability of structures.

#### 10.1. Introduction

When uncertainties are considered in a structural model and in the applied load, a statistical analysis of the response of the structure is necessary. An analysis of this kind allows to know a complete and useful description of the statistical relationship between the input and output variables of the problem.

The most accurate and useful tool to perform this statistical analysis is the Monte Carlo simulation which considers that the responses  $y$  of a system depend on a set of random variables  $x$ , whose marginal probabilistic description is known (Hurtado and Barbat 1998, Sobol 1976). By using statistical algorithms, it is possible to generate large samples (called variates) of the input variables, whose histograms approach the marginal distribution of the population. Therefore, a population of the output variables can be generated making use of a specific deterministic solver.

There are two methods to generate random variables corresponding to marginal distributions: the Inversion and the Rejection methods. In the inversion methods, uniform random numbers (ranged between 0 and 1) are generated and the corresponding values of the input variables are calculated by inversion of its distribution function. The rejection methods are based on a fictitious density function that envelops the real one and whose area can be greater than the real one. This fictitious function is accepted with a specific probability that depends on the ratio of the true to the fictitious density.

The rejection methods are usually named Simple Random Sampling. It does not permit the optimisation of the sample size without sacrificing the quality of the results in the entire input variable space. Therefore, they are costly in the case of large structures. Different techniques have been proposed to reduce the size of the sample used in the analysis. One of them, the Latin Hypercube method (Florian 1992), reduces the relatively high correlation due to the radical decrease of the population with respect to the Simple Random Sampling. In this

study, the Latin Hypercube method to generate samples of random variables was used in the Monte Carlo simulations.

## 10.2. Fragility curves for Warth bridge

Considering the uncertainties associated to the non-linear behaviour of Warth bridge, Monte Carlo simulations have been performed to obtain fragility curves. The analysis was performed by using the STAC (2001) code, which is an advanced computing tool for performing stochastic analysis of generic physical problems.

### 10.2.1 Input random variables

As input data for the Monte Carlo simulation, the random variables and their associated marginal distributions should be defined. According to the input data necessary to obtain the non-linear response of the bridge with the proposed simplified model, the selected structural random variables are shown in table 10.1. As far as it is concerned, the simulation of the seismic action was performed as described in chapter 9.

Using different experimental and analytical tests developed in various researches, the distribution function and the coefficient of variation were defined for every input random variable. Most of the experimental and analytical tests used herein were developed for building columns, however some data for bridge piers are also available. The distribution function, mean and coefficient of variation for each structural random variable are shown in tables 10.2, 10.3 and 10.4. The characteristics of the mechanical random variables are shown in table 10.2, while tables 10.3 and 10.4 present the characteristics of the geometrical random variables and the other random variables used in the Monte Carlo simulations. In these tables the reference from where the random characteristics were taken are also shown in every case.

The nominal value of each variable, obtained from the Warth bridge drawings or supposed, was considered as its mean. Knowing the mean and the coefficient of variation, the standard deviation of each variable was calculated as

$$\sigma = \mu \text{ COV} \quad (10.1)$$

Additionally, the distribution function was limited to more or less three standard deviations, that is

$$x_{\min} = \mu - 3\sigma \quad x_{\max} = \mu + 3\sigma \quad (10.2)$$

where  $\mu$ ,  $\sigma$ ,  $\text{COV}$ ,  $x_{\min}$  and  $x_{\max}$  are the mean, standard deviation, coefficient of variation and minimum and maximum values of the random variable  $x$ , respectively. The equation 10.2 considers, for a normal or lognormal distribution, that 99.7% of the random values lies within this range.

The structural response variables (output variables) corresponding to the non-linear analysis which have been considered are the following:

1. The maximum damage in each pier of the bridge, using equations 8.22 and 8.23.
2. The global damage of the bridge, estimated by means of equations 8.24 to 8.26.

Variable	Description
$f'_c$	Uniaxial compression strength of concrete
$f_t$	Uniaxial tensile strength of concrete
$E_c^0$	Initial Young's modulus for concrete
$E_a$	Young's modulus for reinforced steel
$G_f$	Fracture energy
$b$	Base of the piers box section
$h$	Height of the piers box section
$t_1, t_2, t_3, t_4$	Thickness of the piers box section
$\gamma_c$	Weight of piers
$L_p$	Length of piers
$A_a$	Area of the longitudinal reinforce steel
$A_v$	Area of the cross section in girders
$L$	Length of girders
$\gamma_v$	Weight of girders
$A_p$	Area of the cross section of bearings
$a$	Height of bearings
$h_a$	Length between bearings, in plan
$G$	Shear modulus of bearings

**Table 10.1** Structural random variables used in the Monte Carlo simulations

Variable	Mean	COV	Distribution	Reference
$f'_c$ (MPa)	40.0	0.18	Lognormal	Enrigh et al. 1998, Mirza and MacGregor 1979, Nowak 1980, Trautnet et al. 1991, Bartlett et al. 1996
$f_t$ (MPa)	4.0	0.05	Lognormal	Mirza 1996
$E_c$ (MPa)	2.8E04	0.077	Lognormal	Mirza 1996, Mirza and MacGregor 1979, Shadi et al. 2000
$E_a$ (MPa)	2.1E05	0.08	Lognormal	Diniz et al. 1990, Mirza et al. 1979, Mirza 1996
$G_f$ (KJ/m <sup>2</sup> )	1.0	0.003	Lognormal	Alvaredo and Wittmann 1998, Bazant and Liu 1985
$A_a$ (m <sup>2</sup> )	Different	0.1	Lognormal	Luo et al. 1994, Nowak 1980, Steinberg 1997
$\gamma_c$ (kN/m <sup>3</sup> )	24.5	0.05	Lognormal	O'Connor and Ellingwood 1987
$E_v$ (MPa)	3.18E04	0.077	Lognormal	Mirza 1996, Mirza et al. 1979
$\gamma_v$ (kN/m <sup>3</sup> )	28.2	0.05	Lognormal	O'Connor and Ellingwood 1987
$G$ (MPa)	Different	0.077	Lognormal	Mirza 1996, Mirza et al. 1979

**Table 10.2** Random characteristics of the mechanical random variables

Variable	Mean	COV	Distribution	Reference
$b$ (m)	2.50	0.021	Lognormal	Mirza and MacGregor 1979, Steinberg 1997, Trautner et al. 1991,
$h$ (m)	6.80	0.027	Lognormal	Luo et al. 1994, Mirza and MacGregor 1979, Nowak 1980, Trautner et al. 1991
$t_1$ (m)	0.30	0.06	Lognormal	Steinberg 1997
$t_2$ (m)	0.30	0.06	Lognormal	Steinberg 1997
$t_3$ (m)	0.50	0.06	Lognormal	Steinberg 1997
$t_4$ (m)	0.50	0.06	Lognormal	Steinberg 1997
$L_p$ (m)	Different	0.045	Lognormal	Steinberg 1997, Trautner et al. 1991
$A_y$ (m <sup>2</sup> )	10.141	0.0095	Lognormal	Luo et al. 1994, Nowak 1980, Steinberg 1997, Trautner et al. 1991
$L_y$ (m <sup>2</sup> )	62.0, 67.0	0.045	Lognormal	Steinberg 1997, Trautner et al. 1991
$A_p$ (m <sup>2</sup> )	0.005	0.0095	Lognormal	Luo et al. 1994, Mirza and MacGregor 1979, Nowak 1980, Steinberg 1997, Trautner et al. 1991, Udoyeo 1994
$a$ (m)	0.25	0.027	Lognormal	Luo et al. 1994, Mirza and MacGregor 1979, Nowak 1980, Trautner et al. 1991, Udoyeo 1994
$h_a$ (m)	4.50	0.045	Lognormal	Trautner et al. 1991, Steinberg 1997

Table 10.3 Random characteristics of the geometrical random variables

Variable	Mean	Range	Distribution
Number of the used record	10	1 – 20	Uniform
$K_T$ (MPA)	5.0E10	1.0E08 – 1.0E11	Uniform

Table 10.4 Characteristics of the other random variables

3. The final damaged inertia of every pier.
4. The final period associated to every mode of vibration of the structure.

### 10.2.2 Statistical analysis

For the output variables statistical analyses were developed. These statistical analyses include the determination of the principal statistical moments, histograms and curves of accumulated frequency versus damage. Additionally, for these curves theoretical probability distribution functions were adjusted. The characteristics of this statistical calculus are commented in following.

- **Moments.** These functions define the first statistical moments of a variable in addition to other basic information, such as the 95% confidence intervals. The expressions used to evaluate the first statistical moments are:

Mean:

$$\bar{x} = \frac{1}{N} \sum_{j=1}^N x_j \quad (10.3)$$

Mean confidence interval:

$$(\bar{x}_{low}, \bar{x}_{up})_{95\%} = \bar{x} \pm \frac{1.96\sigma}{\sqrt{N}} \quad (10.4)$$

Variance:

$$Var(x_1, \dots, x_N) = \frac{1}{N-1} \sum_{j=1}^N (x_j - \bar{x})^2 \quad (10.5)$$

Variance confidence interval:

$$(\sigma_{low}, \sigma_{up})_{95\%} = \sigma \pm \frac{1.96\sigma}{\sqrt{2N}} \quad (10.6)$$

Standard deviation:

$$\sigma(x_1, \dots, x_N) = \sqrt{Var(x_1, \dots, x_N)} \quad (10.7)$$

Coefficient of variation:

$$COV = \frac{\sigma}{\bar{x}} \quad (10.8)$$

- **Histogram.** The histogram is a graphic representation of the frequency of occurrence of a variable associated to the intervals in which the range of this variable is subdivided. In this analysis,  $l = \sqrt{N}$  classes were considered for the output variables. The histogram is used here as an approximation of the distribution function of the output variables.
- **Cumulative distribution function.** The cumulative distribution function shows the accumulative frequencies of different values of the output variables. That is, for each output variable this curve represents the relation between the accumulative frequency and the total number of the sample ( $N$ ), given a predefined earthquake size.
- **Adjust of theoretical distribution functions.** Starting from the results of the STAC code, continuous distributions functions were adjusted using statistical hypothesis tests. The assumption that the sample of data comes from a theoretical distribution is considered as a null hypothesis,  $H_0$ , being the alternative hypothesis,  $H_a$ , that the sample of data do not follows a theoretical distribution. To prove the goodness of fit of

the null hypothesis, non-parametric contrast of the chi-square and Kolmogorov-Smirnov tests were used (Canavos et al. 1990).

The chi-square goodness of fit test is based on the comparison between the observed and expected frequencies of a  $l$  class's sample. The chi-square statistic is defined as:

$$\chi^2 = \sum_{i=1}^l \frac{(O_i - E_i)^2}{E_i} \quad (10.9)$$

where  $O_i$  and  $E_i$  are the observed and expected frequencies for class  $i$ , respectively and  $l$  is the number of classes of the sample. The expected frequency is obtained by means of the theoretical distribution function of the variable being tested. The chi-square test is valid for continuous and discrete distributions, but it is sensitive to the choice of the number of classes and it is not valid for size samples lesser than 30.

The Kolmogorov-Smirnov test is used to decide if a sample of data comes from a specific distribution. The Kolmogorov-Smirnov (K-S) test is based on the empirical accumulated distribution function (ECDF), given for  $N$  data points,  $x_1, x_2, \dots, x_N$ , as

$$Fn(x_i) = n(i) / N \quad (10.10)$$

where  $n(i)$  is the number of points less than  $x_i$ . This step function increases by  $1/N$  at the value of each data point. The K-S test is based on the maximum distance between the empirical and the theoretical accumulated curves (see figure 10.1). Then, the statistic of the K-S test is defined as:

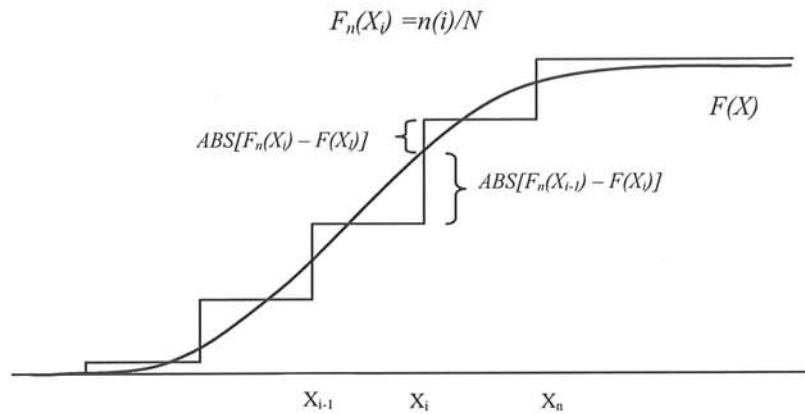
$$D_{K-S} = \max_{1 \leq i \leq N} \left| F(x_i) - \frac{n(i)}{N} \right| \quad (10.11)$$

where  $F(x_i)$  is the theoretical cumulative function of the distribution being tested. An attractive feature of this test is that the distribution of the K-S test statistic itself does not depend on the underlying cumulative distribution function being tested. Another advantage is that it is an exact test, the chi-square goodness of fit depends on an adequate sample size for the approximations to be valid. Despite these advantages, the K-S test has several important limitations: (1) it only applies to continuous distributions, and (2) it tends to be more sensitive near the centre of the distribution than it is at the tails.

For each output variable only was selected one distribution function. The adequate distribution should pass chi-square and K-S goodness of fit tests for significance levels of 0.1, 0.05 or 0.01. When more than one theoretical function is adequate, the one with the greater adjustment was selected.

### 10.2.3 Examples

Different Monte Carlo simulations have been performed for the Warth bridge, considering all or a part of the random variables defined for the structural model and using original or artificial records of the two seismic scenarios defined in chapter 9.



**Figure 10.1** Definition of the Kolmogorov - Smirnov statistic

The principal objective of the incorporation or not of a random variable is to verify its influence on the statistical behaviour of the structure. For all the performed examples of 500 elements were used, value which is considered large enough to obtain statistical conclusions. In following the developed examples will be discussed in detail.

#### 10.2.3.1 Influence of random structural parameters and deterministic seismic action. First seismic scenario

In this case, all the input parameters given in tables 10.2 and 10.3 were considered as random variables. The external action was considered as deterministic, using the six longitudinal accelerograms defined for each bridge pier for the first seismic scenario, magnitude 5.5 and distance to the source of 8 km. Additionally, the soil-structure interaction effect was neglected, what means to consider very large values for the rotation stiffness at the base of the piers.

The statistical moments of the piers damage and the global damages of the bridge are shown in tables 10.5 to 10.7. For the confidence intervals of mean and variance statistical moments, two values are given in these tables, its lower and upper limits. In these tables, when the lower limit of the confidence interval was less than zero, its value was fixed to zero, because a negative value does not has physical meaning.

In table 10.5 is observed that the global mean damage of the structure is 2.6% and the mean damages of the piers lies between 1.5% and 4.0%, except for the shortest pier, for which a null damage can be considered. When the DiPasquale damage index is used, the mean damages of piers are between 1.15% and 3.0%, being its average 1.4%. The functional damage index can be considered as an upper limit of the bridge damage, in this example its mean value is 14.6%. This could represent a minor disruption of the bridge service.

Following this procedure, a theoretical distribution function was adjusted for each one of the empirical fragility curves. As it is observed in the histograms of the output variables, the frequency of the first class is much greater than the remainders. This causes that in some instances the adjustment of the statistical results to a theoretical distribution do not pass the statistical tests. Therefore, in these cases, values assumed as a null damage (1.E-04 or lesser) were eliminated from the sample of the output variables, reducing the size of the sample to less than the original 500 elements. Thus, it could be said that the theoretical curves thus obtained are curves conditioned by the damage occurrence.



Moment	Damage						
	D <sub>m</sub>	D <sub>1</sub>	D <sub>2</sub>	D <sub>3</sub>	D <sub>4</sub>	D <sub>5</sub>	D <sub>6</sub>
$\bar{x}$	2.57E-02	3.16E-02	3.17E-02	4.07E-02	3.61E-02	1.40E-02	1.35E-16
$(\bar{x}_{low}, \bar{x}_{up})_{95\%}$	2.40E-02	2.72E-02	2.69E-02	3.52E-02	3.06E-02	1.03E-02	1.20E-16
	2.74E-02	3.61E-02	3.65E-02	4.62E-02	4.17E-02	1.78E-02	1.49E-16
Var( $x_1, \dots, x_N$ )	2.07E-04	1.39E-03	1.63E-03	2.13E-03	2.14E-03	9.96E-04	1.40E-32
$\sigma(x_1, \dots, x_N)$	1.41E-02	3.72E-02	4.03E-02	4.62E-02	4.63E-02	9.96E-04	1.18E-16
$(\sigma_{low}, \sigma_{up})_{95\%}$	1.32E-02	3.41E-02	3.69E-02	4.23E-02	4.24E-02	2.89E-02	1.08E-16
	1.56E-02	4.04E-01	4.38E-02	5.01E-02	5.02E-01	3.16E-02	1.29E-16
COV	56.0	117.6	127.2	113.5	128.1	224.7	88.1
$x_{max}$	0.08	0.24	0.21	0.22	0.19	0.22	0

Table 10.5 Statistical moments of mean global damage and pier damage. Example 1

Moment	Damage						
	D <sub>a</sub>	DP <sub>1</sub>	DP <sub>2</sub>	DP <sub>3</sub>	DP <sub>4</sub>	DP <sub>5</sub>	DP <sub>6</sub>
$\bar{x}$	1.44E-02	2.98E-02	1.83E-02	1.37E-02	1.30E-02	1.15E-02	7.78E-06
$(\bar{x}_{low}, \bar{x}_{up})_{95\%}$	1.34E-02	2.73E-02	1.65E-02	1.25E-02	1.14E-02	9.87E-03	5.61E-06
	1.54E-02	3.22E-02	2.01E-02	1.50E-02	1.46E-02	1.31E-02	9.94E-06
Var( $x_1, \dots, x_N$ )	7.20E-05	4.05E-04	2.26E-04	1.11E-04	1.82E-04	1.80E-04	3.26E-10
$\sigma(x_1, \dots, x_N)$	8.49E-03	2.01E-02	1.50E-02	1.05E-02	1.35E-02	1.34E-02	1.81E-05
$(\sigma_{low}, \sigma_{up})_{95\%}$	7.77E-03	1.84E-02	1.38E-02	9.63E-03	1.23E-02	1.23E-02	1.65E-05
	9.21E-03	2.18E-02	1.63E-02	1.14E-02	1.46E-01	1.46E-02	1.96E-05
COV	59.0	67.7	82.1	76.6	103.9	117.0	232.2
$x_{max}$	0.047	0.12	0.085	0.0599	0.10	0.16	1.4E-04

Table 10.6 Statistical moments of global and pier damage indices of DiPasquale. Example 1

Damage							
Moment	D <sub>m</sub>	D <sub>p</sub>	D <sub>a</sub>	Moment	D <sub>m</sub>	D <sub>p</sub>	D <sub>a</sub>
$\bar{x}$	2.57E-02	1.46E-01	1.44E-02	$\sigma(x_1, \dots, x_N)$	1.41E-02	7.70E-02	8.49E-03
$(\bar{x}_{low}, \bar{x}_{up})_{95\%}$	2.40E-02	1.36E-01	1.34E-02	$(\sigma_{low}, \sigma_{up})_{95\%}$	1.32E-02	7.05E-02	7.77E-03
	2.74E-02	1.55E-01	1.54E-02		1.56E-02	8.35E-02	9.21E-03
Var( $x_1, \dots, x_N$ )	2.07E-04	5.93E-03	7.20E-05	COV	56.0	52.9	59.0
-	-	-	-	$x_{max}$	0.08	0.41	0.047

Table 10.7 Statistical moments of the global damage indices. Example 1

As an example of this process, the left plot of figure 10.5 shows the histogram and the theoretical distribution (Weibull function in this case) of the mean global damage of the bridge, and the right plot shows the accumulated values of this variable. In this figure a good agreement between theoretical and statistical values are observed.

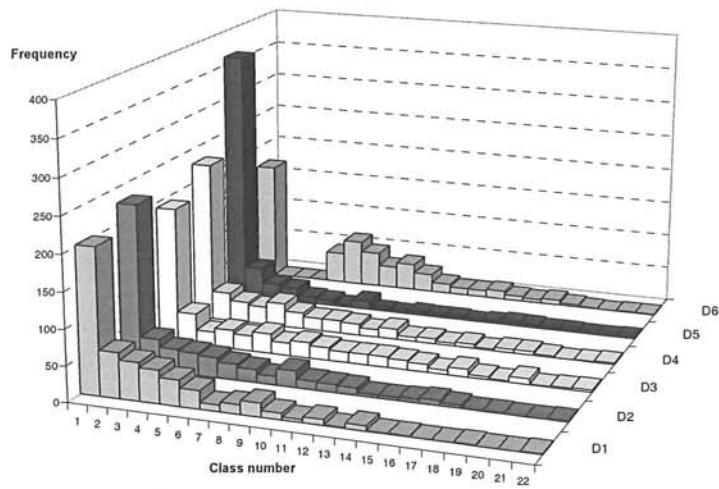


Figure 10.2 Histograms of pier damage and mean global damage indices. Example 1

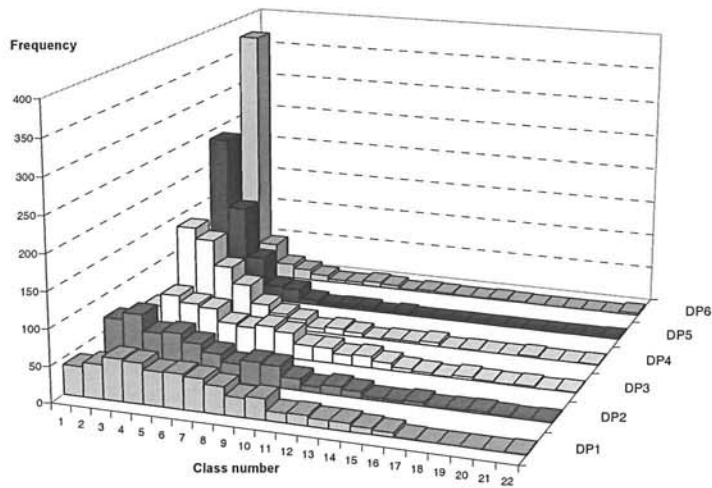


Figure 10.3 Histograms of pier and global DiPasquale and Cakmak damage indices. Example 1

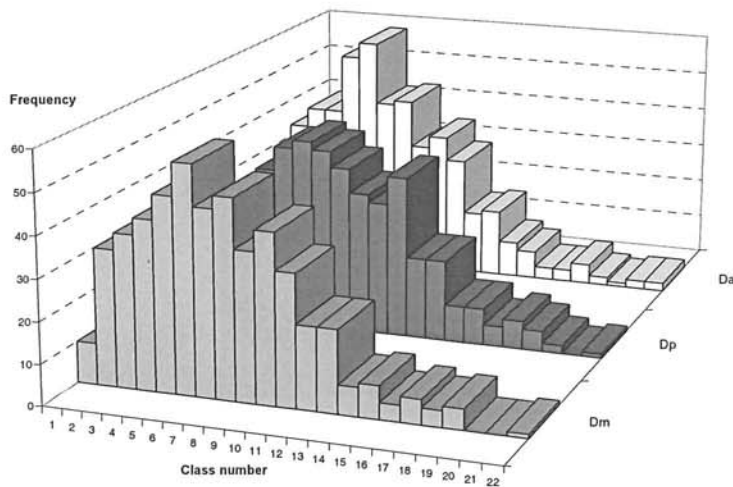


Figure 10.4 Histograms of global damage indices. Example 1

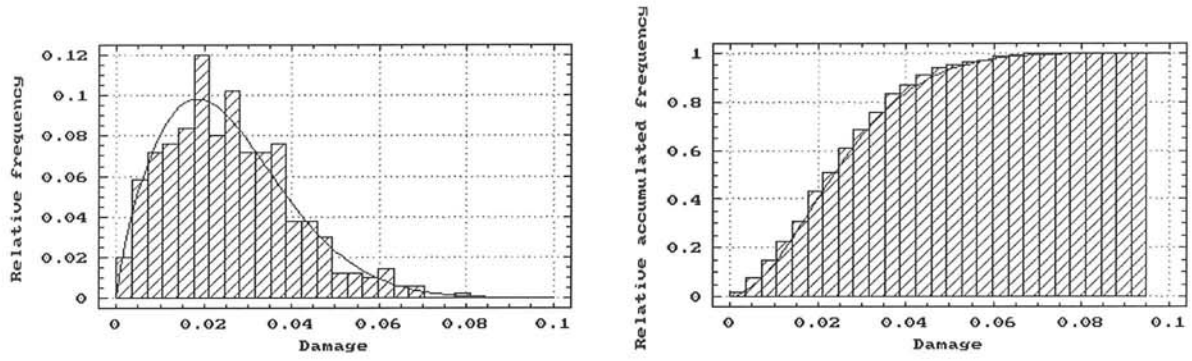


Figure 10.5 Weibull distribution function (left) and accumulated distribution function (right). Mean global damage. Example 1

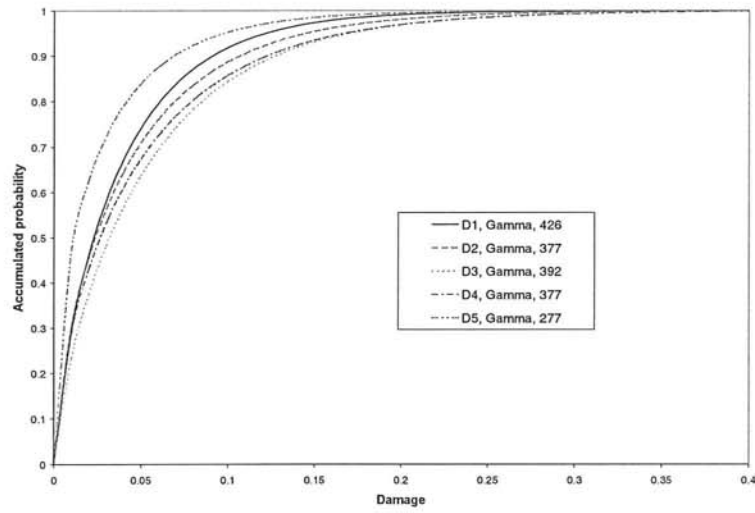


Figure 10.6 Fragility curves of pier damage indices. Example 1

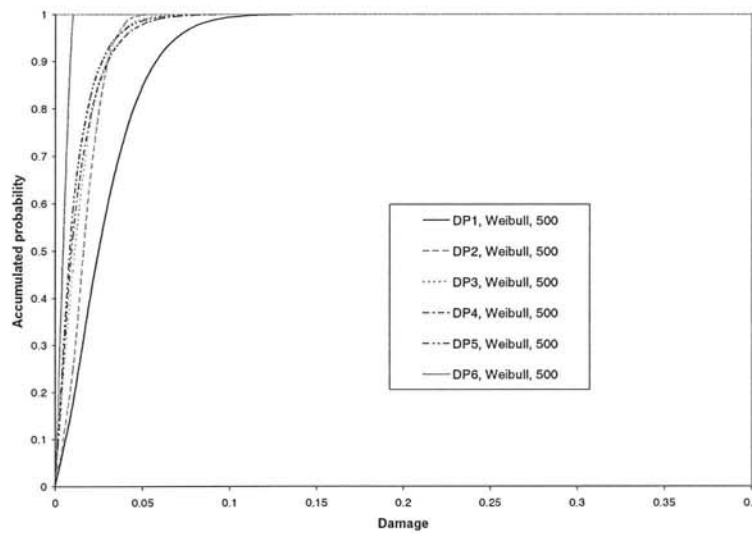
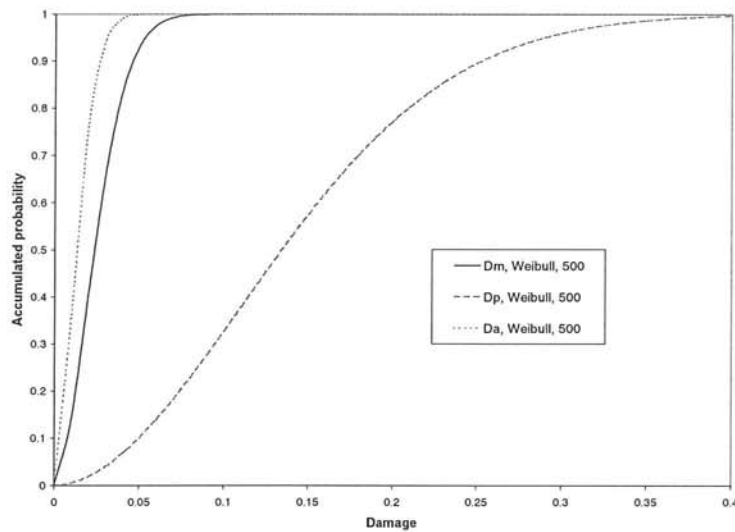


Figure 10.7 Fragility curves of pier DiPasquale and Cakmak damage indices. Example 1



**Figure 10.8** Fragility curves of global damage indices. Example 1

The adjusted probability distribution functions of the output variables of example 1 are shown in figure 10.6 to 10.8. In these figures, the selected theoretical distribution function and the sample number to adjust it are shown in the curve name box of figures 10.6 to 10.8. For example, “ $D_m$ , Weibull, 500” means that for the mean global damage a Weibull distribution of probability was adjusted using a sample of 500 elements.

#### 10.2.3.2 Influence of random structural parameters and simulated accelerograms. First seismic scenario

In this simulation, the same structural random parameters of example 1 were considered (see tables 10.2 and 10.3). In this case, however, the external action for every pier was defined by means of families of 20 accelerograms, using as original signals the records of the first seismic scenario. For the Monte Carlo simulation a different signal element of the family is assigned to each pier considering the associated number of the signal as an entire random variable with uniform distribution between 1 and 20, as was shown in table 10.4.

The statistical moments of the pier damage and the mean global damage indices are shown in table 10.8. Table 10.9 shows these results for all the global damage indices. The results of the DiPasquale damage indices are not shown, because its behaviour is similar to the above simulation. It is observed in tables 10.8 and 10.9 that the global damage indices have means of 3.6% ( $D_m$ ), 19.4% ( $D_p$ ), and 2.1% ( $D_a$ ), which means that to consider the seismic input load as a random process produce increases the global damage of the bridge in about 40%. For this simulation, the mean of the pier damages lie between 0.3% and 7.6%.

The histograms of the pier damage and the global bridge damage are shown in figures 10.9 and 10.10. The maximum values of each one of the output damage variables can be observed in tables 10.8 and 10.9.

Moment	Damage						
	D <sub>m</sub>	D <sub>1</sub>	D <sub>2</sub>	D <sub>3</sub>	D <sub>4</sub>	D <sub>5</sub>	D <sub>6</sub>
$\bar{x}$	3.59E-02	4.52E-02	1.98E-02	2.17E-02	4.97E-02	7.60E-02	2.94E-03
$(\bar{x}_{low}, \bar{x}_{up})_{95\%}$	3.13E-02	3.15E-02	1.45E-02	1.63E-02	3.73E-02	6.32E-02	0.00E+00
	4.05E-02	5.89E-02	2.52E-02	2.72E-02	6.21E-02	8.88E-02	8.30E-03
Var( $x_1, \dots, x_N$ )	1.43E-03	1.28E-03	1.93E-03	2.04E-02	1.05E-02	1.13E-03	1.97E-03
$\sigma(x_1, \dots, x_N)$	3.78E-02	1.13E-01	4.40E-02	4.52E-02	1.03E-01	1.06E-01	4.40E-02
$(\sigma_{low}, \sigma_{up})_{95\%}$	3.46E-02	1.01E-01	4.02E-02	4.13E-02	9.39E-02	9.70E-02	4.06E-02
	4.10E-02	1.23E-01	4.78E-02	4.90E-02	1.11E-01	1.15E-01	4.82E-02
COV	105.3	250.8	221.8	208.4	206.7	139.6	151.2
$x_{min}$	0.36	0.87	0.30	0.31	0.50	0.58	0.14

Table 10.8 Statistical moments of mean global damage and pier damage. Example 2

Damage							
Moment	D <sub>m</sub>	D <sub>p</sub>	D <sub>a</sub>	Moment	D <sub>m</sub>	D <sub>p</sub>	D <sub>a</sub>
$\bar{x}$	3.59E-02	1.94E-01	2.07E-02	$\sigma(x_1, \dots, x_N)$	3.78E-02	1.73E-01	2.49E-02
$(\bar{x}_{low}, \bar{x}_{up})_{95\%}$	3.13E-02	1.73E-01	1.17E-02	$(\sigma_{low}, \sigma_{up})_{95\%}$	2.28E-02	1.58E-01	2.28E-02
	4.05E-02	2.15E-01	2.37E-02		2.71E-02	1.88E-01	2.71E-02
Var( $x_1, \dots, x_N$ )	6.22E-04	2.99E-02	6.22E-04	COV	120.5	89.1	120.5
-	-	-	-	$x_{max}$	0.36	0.99	0.24

Table 10.9 Statistical moments of the global damage indices. Example 2

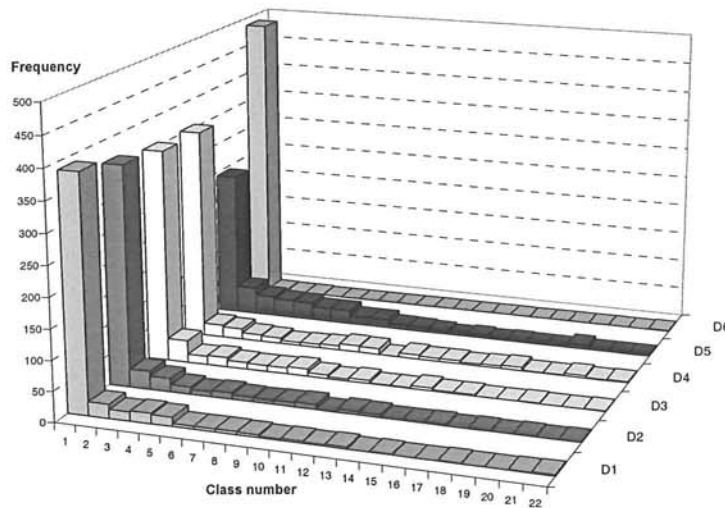


Figure 10.9 Histograms of pier damage and mean global damage indices. Example 2

An example of the selection of an adequate theoretical distribution function can be observed in the plots of figure 10.11 for the mean global damage of the bridge. The distribution functions adjusted to the pier damage indices and global output variables are given in figures 10.12 and 10.13, respectively. In these figures, the selected distributions and the sample size used in the process are also indicated.

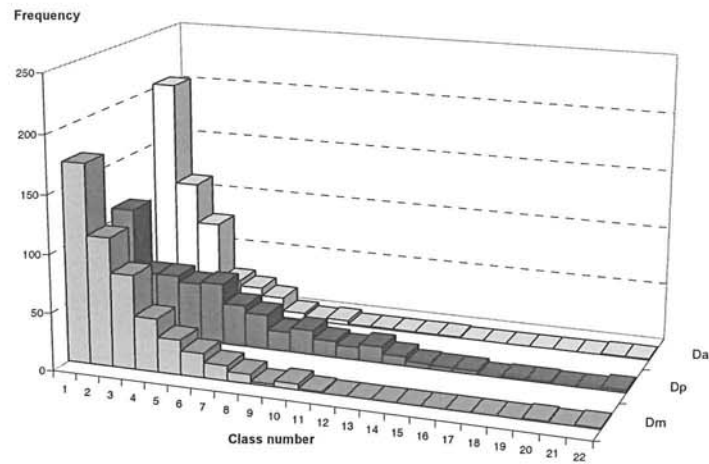


Figure 10.10 Histograms of global damage indices. Example 2

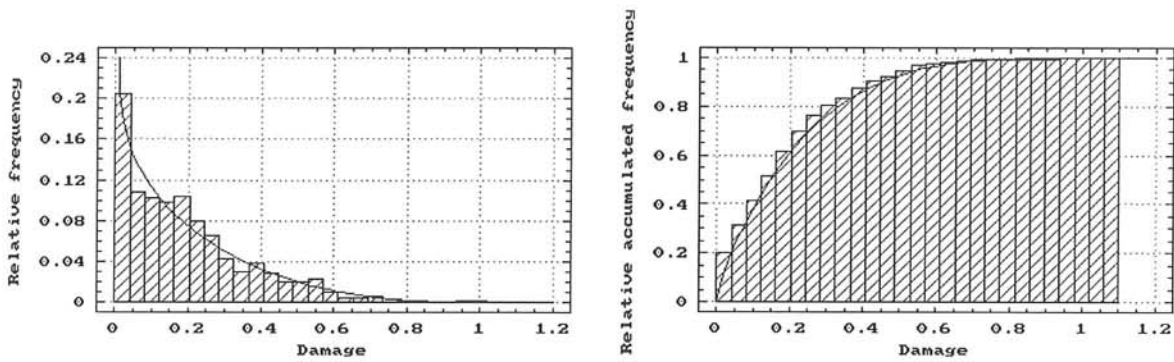


Figure 10.11 Beta distribution function (left) and accumulated distribution (right). Functional global damage. Example 2

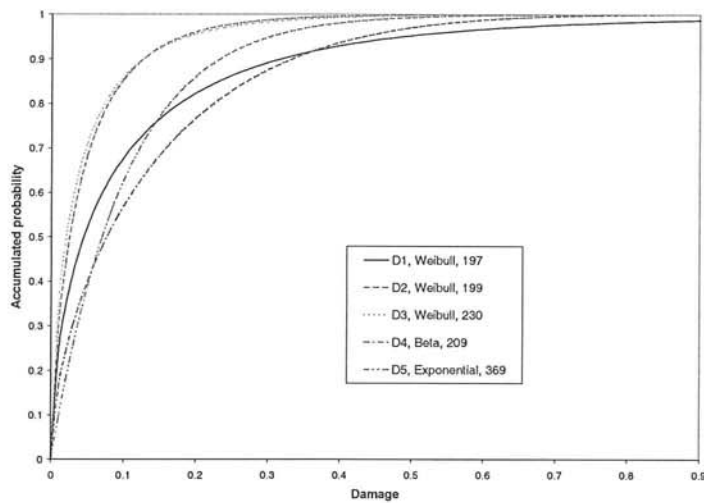


Figure 10.12 Fragility curves of pier damage indices. Example 2

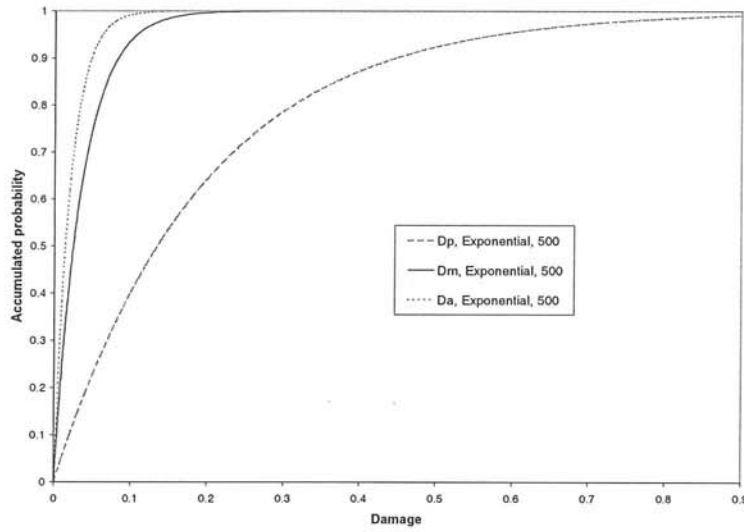


Figure 10.13 Fragility curves of global damage indices. Example 2

Moment	Damage						
	D <sub>m</sub>	D <sub>1</sub>	D <sub>2</sub>	D <sub>3</sub>	D <sub>4</sub>	D <sub>5</sub>	D <sub>6</sub>
$\bar{x}$	3.35E-02	4.14E-02	1.71E-02	2.15E-02	4.20E-02	7.91E-02	2.98E-05
$(\bar{x}_{low}, \bar{x}_{up})_{95\%}$	2.99E-02	3.00E-02	1.27E-02	1.64E-02	3.06E-02	6.69E-02	0.00E+00
	3.71E-02	5.27E-02	2.15E-02	2.66E-02	5.34E-02	9.13E-02	1.10E-03
Var(x <sub>1</sub> ,...,x <sub>N</sub> )	9.26E-04	8.96E-03	1.32E-03	1.79E-03	9.09E-03	1.04E-03	4.43E-07
$\sigma(x_1, \dots, x_N)$	3.04E-02	9.47E-02	3.64E-02	4.23E-02	9.54E-01	1.02E-01	6.66E-04
$(\sigma_{low}, \sigma_{up})_{95\%}$	2.78E-02	8.66E-02	3.31E-02	3.87E-02	8.73E-02	9.32E-02	6.09E-04
	3.30E-02	1.03E-01	3.95E-02	4.59E-02	1.03E-01	1.11E-01	7.22E-04
COV	90.8	228.9	212.8	196.7	227.0	128.8	2233.8
$x_{max}$	0.18	0.83	0.21	0.25	0.49	0.54	0.15

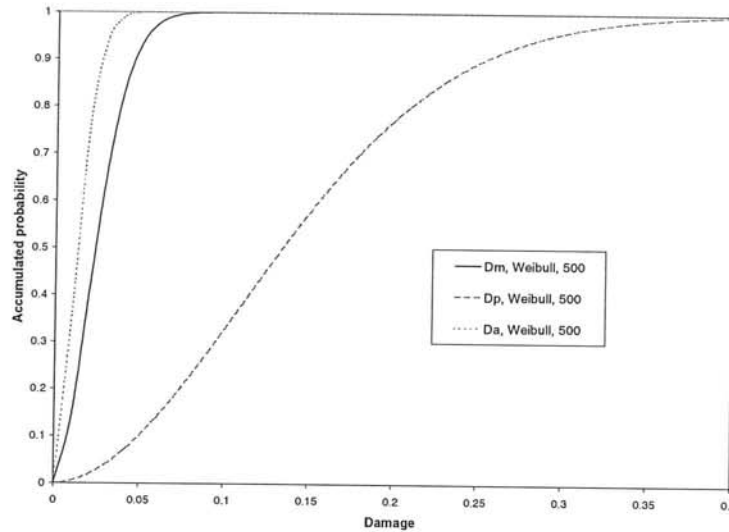
Table 10.10 Statistical moments of mean global damage and pier damage. Example 3

Moment	Damage			Moment	Damage		
	D <sub>m</sub>	D <sub>p</sub>	D <sub>a</sub>		D <sub>m</sub>	D <sub>p</sub>	D <sub>a</sub>
$\bar{x}$	3.35E-02	1.86E-01	1.89E-02	$\sigma(x_1, \dots, x_N)$	3.04E-02	1.56E-01	1.88E-02
$(\bar{x}_{low}, \bar{x}_{up})_{95\%}$	2.99E-02	1.67E-01	1.66E-02	$(\sigma_{low}, \sigma_{up})_{95\%}$	2.78E-02	1.428E-01	1.72E-02
	3.71E-02	2.04E-01	2.11E-02		3.30E-02	1.69E-01	2.04E-02
Var(x <sub>1</sub> ,...,x <sub>N</sub> )	9.26E-04	2.42E-02	3.54E-04	COV	90.8	83.7	99.7
$x_{min}$	0	0	0	$x_{max}$	0.18	0.87	0.15

Table 10.11 Statistical moments of the global damage indices. Example 3

10.2.3.3 Influence of random mechanical parameters and simulated accelerograms. First seismic scenario

For this Monte Carlo simulation, artificial accelerograms were also considered like in example 2, but the only random structural parameters used in the simulation were:  $f'_c, f_b, E_c, E_a, A_a, G_f, G, \gamma_c$  and  $\gamma_v$  (see table 10.2). That is, the variables corresponding to the geometry of the elements were assumed as deterministic parameters (table 10.3), supposing that it is little probable that the element dimensions show important variations in the real case.



**Figure 10.8** Fragility curves of global damage indices. Example 1

The adjusted probability distribution functions of the output variables of example 1 are shown in figure 10.6 to 10.8. In these figures, the selected theoretical distribution function and the sample number to adjust it are shown in the curve name box of figures 10.6 to 10.8. For example, “ $D_m$ , Weibull, 500” means that for the mean global damage a Weibull distribution of probability was adjusted using a sample of 500 elements.

#### 10.2.3.2 Influence of random structural parameters and simulated accelerograms. First seismic scenario

In this simulation, the same structural random parameters of example 1 were considered (see tables 10.2 and 10.3). In this case, however, the external action for every pier was defined by means of families of 20 accelerograms, using as original signals the records of the first seismic scenario. For the Monte Carlo simulation a different signal element of the family is assigned to each pier considering the associated number of the signal as an entire random variable with uniform distribution between 1 and 20, as was shown in table 10.4.

The statistical moments of the pier damage and the mean global damage indices are shown in table 10.8. Table 10.9 shows these results for all the global damage indices. The results of the DiPasquale damage indices are not shown, because its behaviour is similar to the above simulation. It is observed in tables 10.8 and 10.9 that the global damage indices have means of 3.6% ( $D_m$ ), 19.4% ( $D_p$ ), and 2.1% ( $D_a$ ), which means that to consider the seismic input load as a random process produce increases the global damage of the bridge in about 40%. For this simulation, the mean of the pier damages lie between 0.3% and 7.6%.

The histograms of the pier damage and the global bridge damage are shown in figures 10.9 and 10.10. The maximum values of each one of the output damage variables can be observed in tables 10.8 and 10.9.



Moment	Damage						
	D <sub>m</sub>	D <sub>1</sub>	D <sub>2</sub>	D <sub>3</sub>	D <sub>4</sub>	D <sub>5</sub>	D <sub>6</sub>
$\bar{x}$	3.59E-02	4.52E-02	1.98E-02	2.17E-02	4.97E-02	7.60E-02	2.94E-03
$(\bar{x}_{low}, \bar{x}_{up})_{95\%}$	3.13E-02 4.05E-02	3.15E-02 5.89E-02	1.45E-02 2.52E-02	1.63E-02 2.72E-02	3.73E-02 6.21E-02	6.32E-02 8.88E-02	0.00E+00 8.30E-03
Var(x <sub>1</sub> , ..., x <sub>N</sub> )	1.43E-03	1.28E-03	1.93E-03	2.04E-02	1.05E-02	1.13E-03	1.97E-03
$\sigma(x_1, \dots, x_N)$	3.78E-02	1.13E-01	4.40E-02	4.52E-02	1.03E-01	1.06E-01	4.40E-02
$(\sigma_{low}, \sigma_{up})_{95\%}$	3.46E-02 4.10E-02	1.01E-01 1.23E-01	4.02E-02 4.78E-02	4.13E-02 4.90E-02	9.39E-02 1.11E-01	9.70E-02 1.15E-01	4.06E-02 4.82E-02
COV	105.3	250.8	221.8	208.4	206.7	139.6	151.2
x <sub>min</sub>	0.36	0.87	0.30	0.31	0.50	0.58	0.14

Table 10.8 Statistical moments of mean global damage and pier damage. Example 2

Damage							
Moment	D <sub>m</sub>	D <sub>p</sub>	D <sub>a</sub>	Moment	D <sub>m</sub>	D <sub>p</sub>	D <sub>a</sub>
$\bar{x}$	3.59E-02	1.94E-01	2.07E-02	$\sigma(x_1, \dots, x_N)$	3.78E-02	1.73E-01	2.49E-02
$(\bar{x}_{low}, \bar{x}_{up})_{95\%}$	3.13E-02 4.05E-02	1.73E-01 2.15E-01	1.17E-02 2.37E-02	$(\sigma_{low}, \sigma_{up})_{95\%}$	2.28E-02 2.71E-02	1.58E-01 1.88E-01	2.28E-02 2.71E-02
Var(x <sub>1</sub> , ..., x <sub>N</sub> )	6.22E-04	2.99E-02	6.22E-04	COV	120.5	89.1	120.5
-	-	-	-	x <sub>max</sub>	0.36	0.99	0.24

Table 10.9 Statistical moments of the global damage indices. Example 2

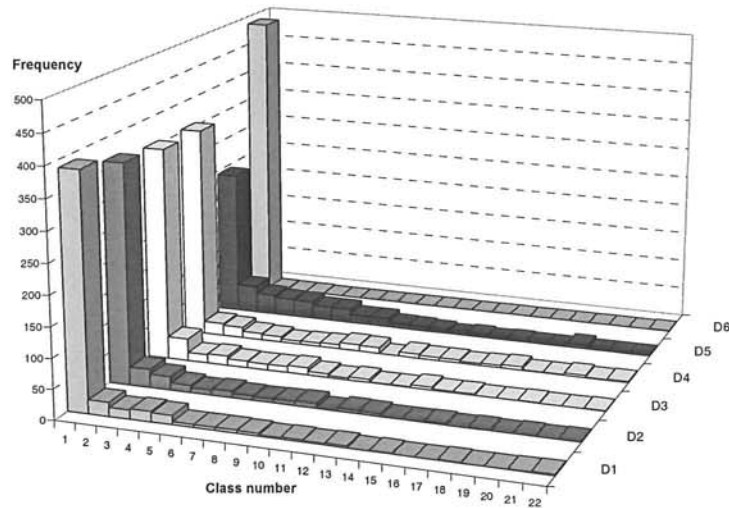


Figure 10.9 Histograms of pier damage and mean global damage indices. Example 2

An example of the selection of an adequate theoretical distribution function can be observed in the plots of figure 10.11 for the mean global damage of the bridge. The distribution functions adjusted to the pier damage indices and global output variables are given in figures 10.12 and 10.13, respectively. In these figures, the selected distributions and the sample size used in the process are also indicated.

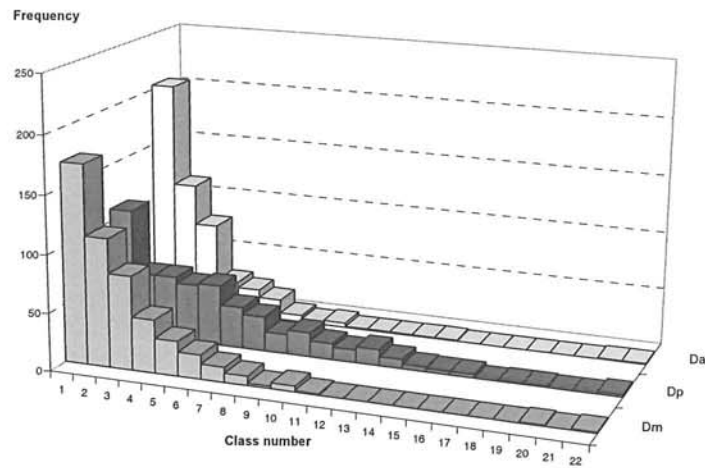


Figure 10.10 Histograms of global damage indices. Example 2

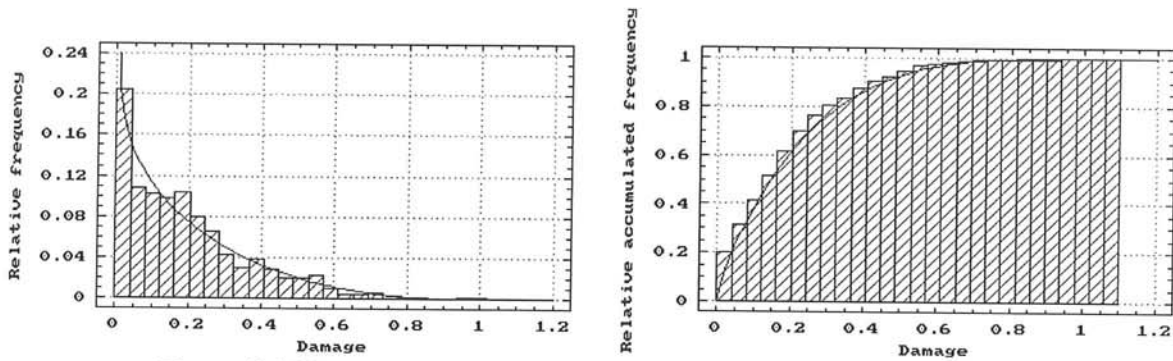


Figure 10.11 Beta distribution function (left) and accumulated distribution (right). Functional global damage. Example 2

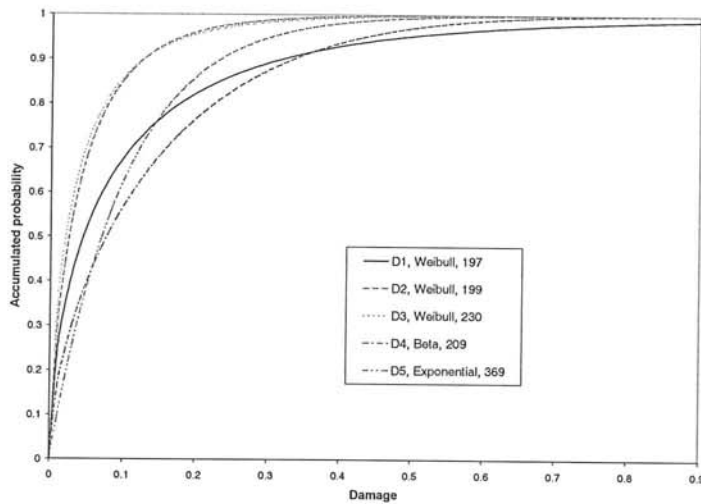


Figure 10.12 Fragility curves of pier damage indices. Example 2

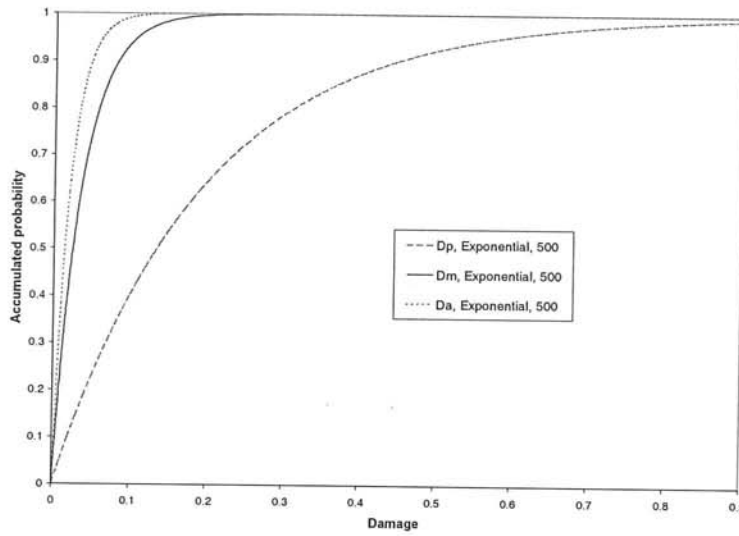


Figure 10.13 Fragility curves of global damage indices. Example 2

Moment	Damage						
	D <sub>m</sub>	D <sub>1</sub>	D <sub>2</sub>	D <sub>3</sub>	D <sub>4</sub>	D <sub>5</sub>	D <sub>6</sub>
$\bar{x}$	3.35E-02	4.14E-02	1.71E-02	2.15E-02	4.20E-02	7.91E-02	2.98E-05
$(\bar{x}_{low}, \bar{x}_{up})_{95\%}$	2.99E-02	3.00E-02	1.27E-02	1.64E-02	3.06E-02	6.69E-02	0.00E+00
	3.71E-02	5.27E-02	2.15E-02	2.66E-02	5.34E-02	9.13E-02	1.10E-03
Var( $x_1, \dots, x_N$ )	9.26E-04	8.96E-03	1.32E-03	1.79E-03	9.09E-03	1.04E-03	4.43E-07
$\sigma(x_1, \dots, x_N)$	3.04E-02	9.47E-02	3.64E-02	4.23E-02	9.54E-01	1.02E-01	6.66E-04
$(\sigma_{low}, \sigma_{up})_{95\%}$	2.78E-02	8.66E-02	3.31E-02	3.87E-02	8.73E-02	9.32E-02	6.09E-04
	3.30E-02	1.03E-01	3.95E-02	4.59E-02	1.03E-01	1.11E-01	7.22E-04
COV	90.8	228.9	212.8	196.7	227.0	128.8	2233.8
$x_{max}$	0.18	0.83	0.21	0.25	0.49	0.54	0.15

Table 10.10 Statistical moments of mean global damage and pier damage. Example 3

Moment	Damage			Moment	D <sub>m</sub>	D <sub>p</sub>	D <sub>a</sub>
	D <sub>m</sub>	D <sub>p</sub>	D <sub>a</sub>				
$\bar{x}$	3.35E-02	1.86E-01	1.89E-02	$\sigma(x_1, \dots, x_N)$	3.04E-02	1.56E-01	1.88E-02
$(\bar{x}_{low}, \bar{x}_{up})_{95\%}$	2.99E-02	1.67E-01	1.66E-02	$(\sigma_{low}, \sigma_{up})_{95\%}$	2.78E-02	1.428E-01	1.72E-02
	3.71E-02	2.04E-01	2.11E-02		3.30E-02	1.69E-01	2.04E-02
Var( $x_1, \dots, x_N$ )	9.26E-04	2.42E-02	3.54E-04	COV	90.8	83.7	99.7
$x_{min}$	0	0	0	$x_{max}$	0.18	0.87	0.15

Table 10.11 Statistical moments of the global damage indices. Example 3

10.2.3.3 Influence of random mechanical parameters and simulated accelerograms. First seismic scenario

For this Monte Carlo simulation, artificial accelerograms were also considered like in example 2, but the only random structural parameters used in the simulation were:  $f'_c$ ,  $f_t$ ,  $E_c$ ,  $E_w$ ,  $A_w$ ,  $G_f$ ,  $G$ ,  $\gamma_c$  and  $\gamma_v$  (see table 10.2). That is, the variables corresponding to the geometry of the elements were assumed as deterministic parameters (table 10.3), supposing that it is little probable that the element dimensions show important variations in the real case.

The most important statistical moments obtained in this simulation are shown in tables 10.10 and 10.11. As it can be observed, the means of the global damage indices of the bridge are of 3.35% ( $D_m$ ), 18.6% ( $D_p$ ), and 1.89% ( $D_a$ ). The comparison of these values with the similar corresponding to example 2 (see table 10.9), makes evident a minor influence of the parameters describing the structural dimensions. For this simulation the mean of the pier's damages are between 3.E-05 and 7.9%.

In figures 10.14 and 10.15 the histograms of the pier damage and global damages are shown, while figure 10.16 shows the adjusted distribution of the mean global damage index. Using the chi-square and the K-S goodness of fit tests, theoretical distributions functions were fixed to the results of the simulation, its accumulated curves for the damage variables are given in figures 10.17 and 10.18.

#### *10.2.3.4 Influence of random mechanical parameters and modified simulated accelerograms. First seismic scenario*

With the aim of studying the influence of a slight modification of the amplitude of the artificial seismic accelerations, example 4 is similar to example 3, except that the ordinates of the ground accelerations are 10% greater. The principal statistical moments of this simulation are shown in tables 10.12 and 10.13, where the mean of the global damages of the bridge of 6.52% ( $D_m$ ), 33.1% ( $D_p$ ), and 3.8% ( $D_a$ ) are observed. Then, an increment of 10% in the seismic load produces increments of almost 80% in the global mean damages of the structure. The mean damage of piers  $P_1$  to  $P_5$  lies between 3.4% and 13.7%. For pier  $P_5$ , the 95% confidence interval of the maximum mean damage lies between 12.1% and 15.3%.

The histograms and the fragility curves of the damage variables are shown in figures 10.19 to 10.23 for the fourth Monte Carlo simulation example. The histograms of the global damages indices show for this example greater frequencies in classes different to the first one, that is, they dominance of a few intervals of damage is smaller. This behaviour is due to the fact that a greater range of the ground accelerations produces a major variation of the damage values.

Greater frequencies in classes different to the first one leads to fragility curves with more soften variations. For example, in this simulation, pier  $P_1$  reaches an accumulated probability of 0.9 for a damage level of 0.45 (see figure 10.22), while this value of damage for the third example is of 0.3, as it can be observed in figure 10.17.

#### *10.2.3.5 Influence of random mechanical parameters, simulated accelerograms and the possibility of pier rotation at its base. First seismic scenario*

Random mechanical parameters and simulated accelerograms are considered in this example, like in example 3, but the rotational stiffness at the pier base is also included as a random variable ( $K_i^S$  in figure 7.5). This variable is assumed to have a uniform distribution between 1.0E08 and 1.0E11, as can be observed in table 10.4

The randomness of the rotational stiffness tries to consider the base rotation of one or various bridge piers. The possible values assumed for this variable have a large range, due to the scarce information existing on this effect.

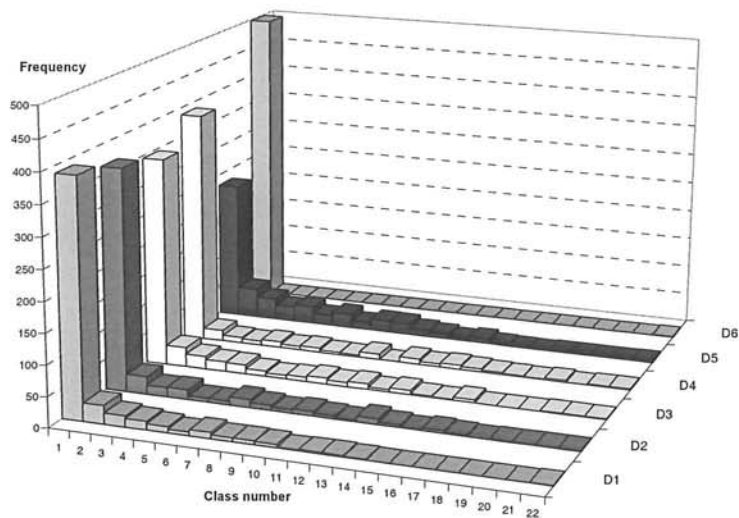


Figure 10.14 Histograms of pier damage and mean global damage indices. Example 3

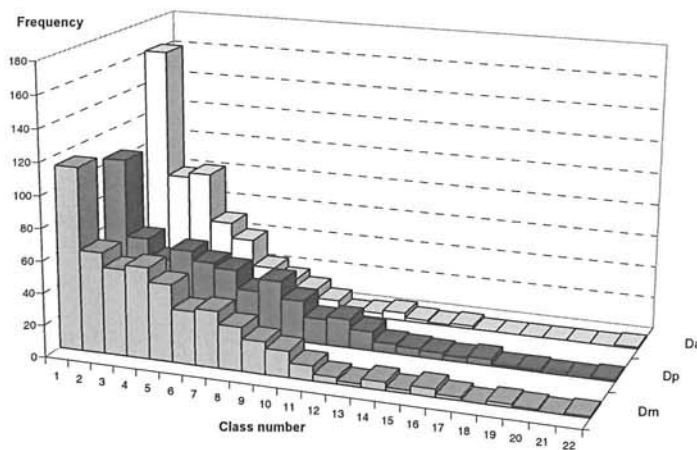


Figure 10.15 Histograms of global damage indices. Example 3

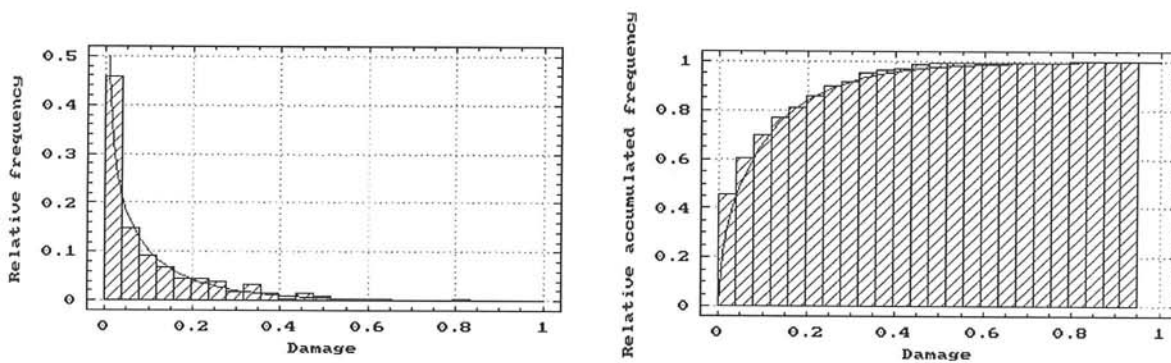


Figure 10.16 Gamma distribution function (left) and accumulated distribution (right). Pier P<sub>1</sub> damages. Example 3

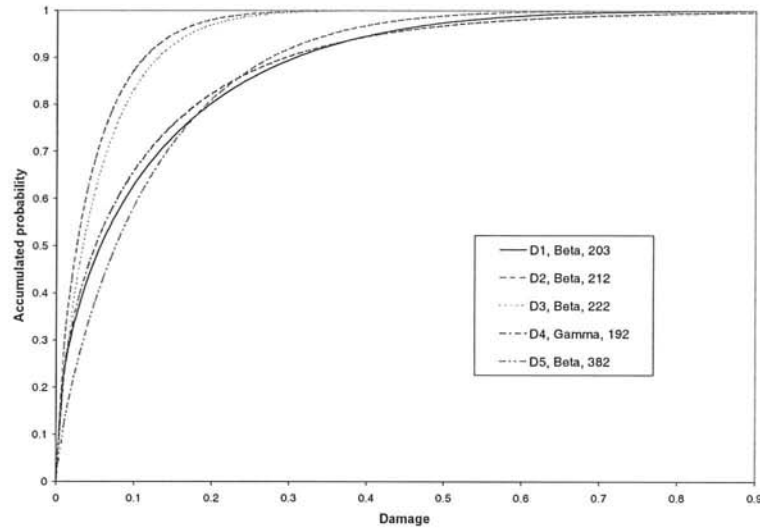


Figure 10.17 Fragility curves of pier damage indices. Example 3

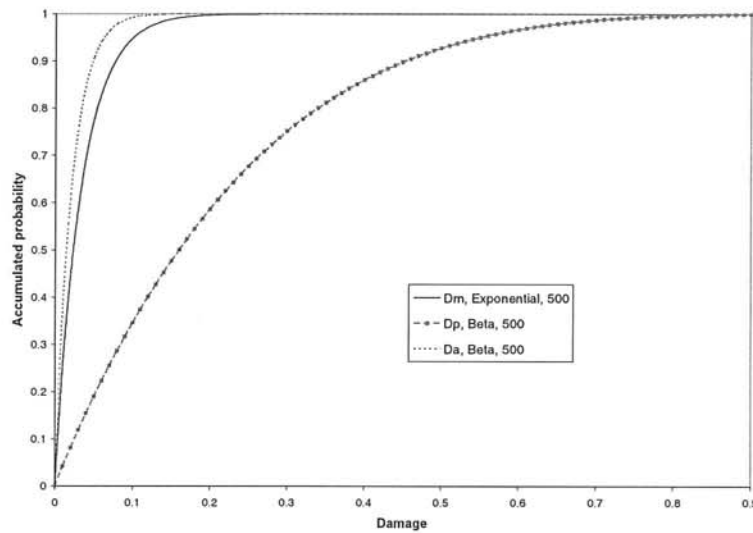


Figure 10.18 Fragility curves of global damage indices. Example 3

Moment	Damage						
	D <sub>m</sub>	D <sub>1</sub>	D <sub>2</sub>	D <sub>3</sub>	D <sub>4</sub>	D <sub>5</sub>	D <sub>6</sub>
$\bar{x}$	6.52E-02	8.79E-02	3.86E-02	5.27E-02	7.34E-02	1.37E-01	2.32E-03
$(\bar{x}_{low}, \bar{x}_{up})_{95\%}$	5.94E-02	6.87E-02	3.16E-02	4.34E-02	5.87E-02	1.21E-01	0.00E+00
	7.11E-02	1.07E-01	4.56E-02	6.21E-02	8.81E-02	1.53E-01	7.62E-03
Var( $x_1, \dots, x_N$ )	2.42E-03	2.57E-02	3.41E-03	6.12E-03	1.50E-02	1.79E-02	1.95E-03
$\sigma(x_1, \dots, x_N)$	4.92E-02	1.60E-01	5.84E-02	7.82E-02	1.23E-01	1.34E-01	4.42E-02
$(\sigma_{low}, \sigma_{up})_{95\%}$	4.50E-02	1.47E-01	5.35E-02	7.16E-02	1.12E-01	1.22E-01	4.05E-02
	5.33E-02	1.74E-01	6.34E-02	8.49E-02	1.33E-01	1.45E-01	4.79E-02
COV	75.4	182.2	151.5	148.3	167.1	97.9	1950.8
$x_{max}$	0.46	0.86	0.35	0.59	0.54	0.59	0.98

Table 10.12 Statistical moments of mean global damage and pier damage. Example 4

Damage							
Moment	D <sub>m</sub>	D <sub>p</sub>	D <sub>a</sub>	Moment	D <sub>m</sub>	D <sub>p</sub>	D <sub>a</sub>
$\bar{x}$	6.52E-02	3.31E-01	3.76E-02	$\sigma(x_1, \dots, x_N)$	4.92E-02	1.95E-01	3.33E-02
$(\bar{x}_{low}, \bar{x}_{up})_{95\%}$	5.94E-02 7.11E-02	3.08E-01 3.55E-01	3.36E-02 4.16E-02	$(\sigma_{low}, \sigma_{up})_{95\%}$	4.50E-02 5.33E-02	1.788E-01 2.11E-01	3.05E-02 3.62E-02
$\text{Var}(x_1, \dots, x_N)$	2.42E-03	3.79E-02	1.11E-03	COV	75.4	58.7	88.8
-	-	-	-	$x_{max}$	0.46	0.99	0.36

Table 10.13 Statistical moments of the global damage indices. Example 4

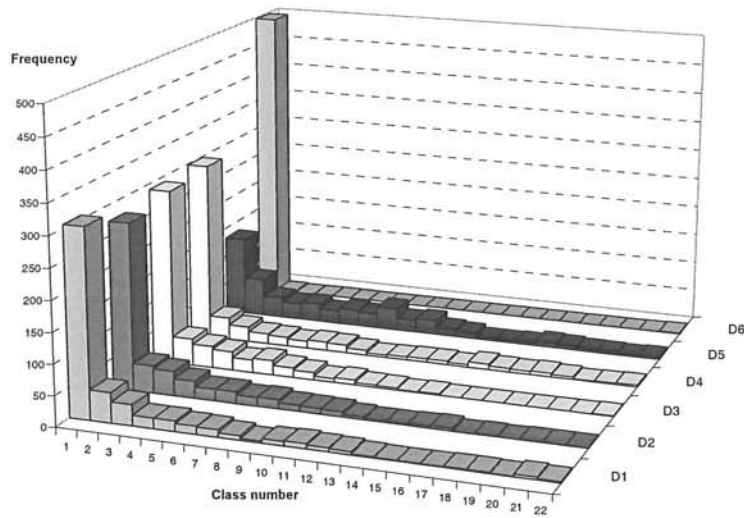


Figure 10.19 Histograms of pier damage and mean global damage indices. Example 4

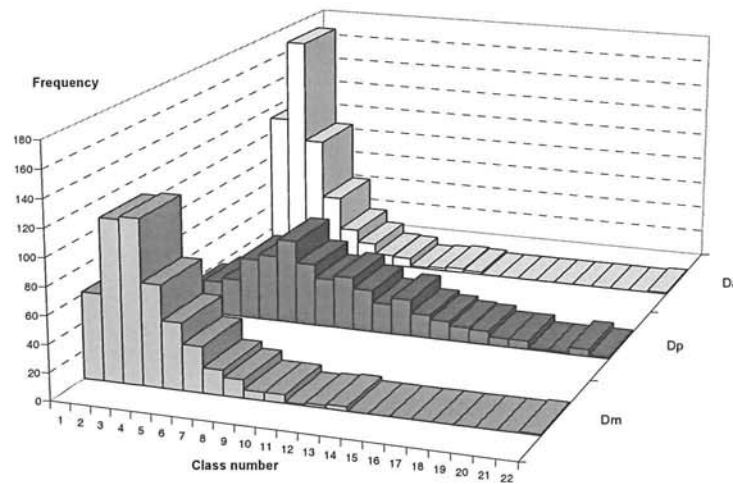


Figure 10.20 Histograms of global damage indices. Example 4

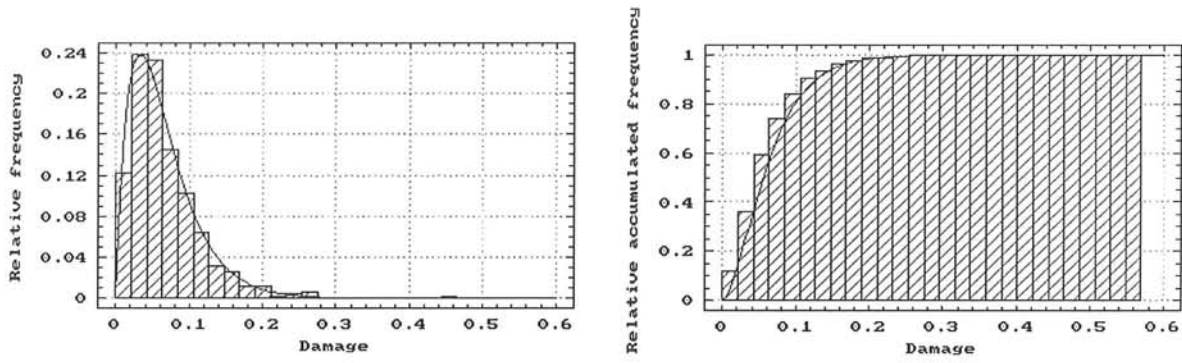


Figure 10.21 Gamma distribution function (left) and accumulated distribution (right).  
Global mean damage. Example 4

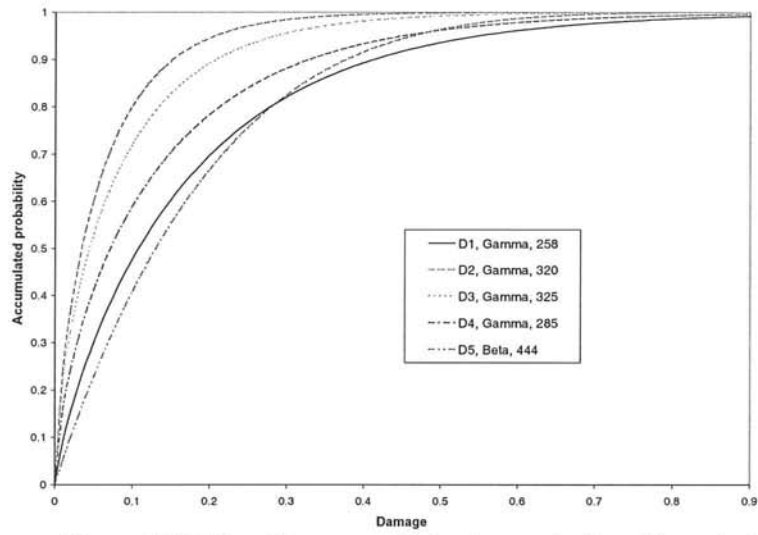


Figure 10.22 Fragility curves of pier damage indices. Example 4

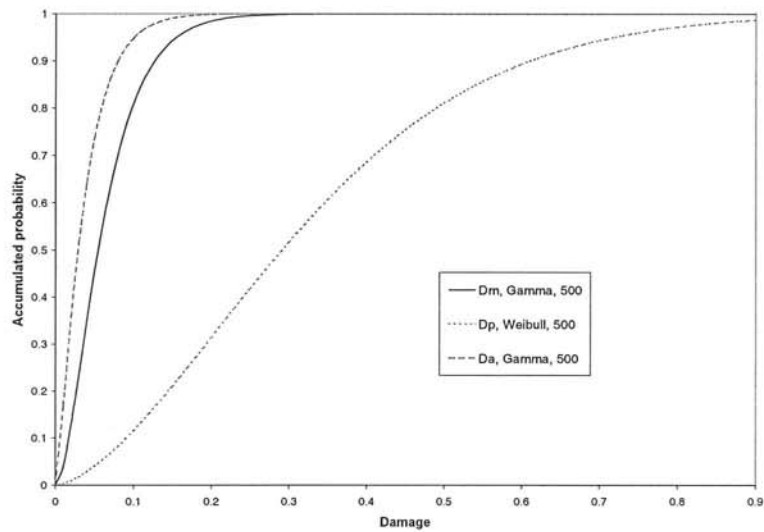


Figure 10.23 Fragility curves of global damage indices. Example 4



Moment	Damage						
	D <sub>m</sub>	D <sub>1</sub>	D <sub>2</sub>	D <sub>3</sub>	D <sub>4</sub>	D <sub>5</sub>	D <sub>6</sub>
$\bar{x}$	3.94E-02	5.31E-02	1.67E-02	2.50E-02	4.58E-02	9.60E-02	5.05E-05
$(\bar{x}_{low}, \bar{x}_{up})_{95\%}$	3.52E-02	3.90E-02	1.18E-02	1.95E-02	3.40E-02	8.24E-02	0.00E+00
	4.37E-02	6.71E-02	2.16E-02	3.04E-02	5.76E-02	1.10E-01	1.86E-03
Var(x <sub>1</sub> , ..., x <sub>N</sub> )	1.26E-03	1.37E-03	1.68E-03	2.04E-03	9.76E-03	1.28E-02	1.27E-06
$\sigma(x_1, \dots, x_N)$	3.55E-02	1.17E-02	4.09E-02	4.52E-02	9.88E-02	1.13E-01	1.13E-03
$(\sigma_{low}, \sigma_{up})_{95\%}$	3.25E-02	1.07E-02	3.75E-02	4.14E-02	9.04E-02	1.03E-01	1.03E-03
	3.85E-02	1.27E-01	4.40E-02	4.90E-02	1.07E-01	1.23E-01	1.22E-03
COV	90.0	220.8	244.9	181.1	215.7	117.85	2233.8
$x_{max}$	0.22	0.84	0.27	0.26	0.43	0.54	0.025

Table 10.14 Statistical moments of mean global damage and pier damage. Example 5

Damage							
Moment	D <sub>m</sub>	D <sub>p</sub>	D <sub>a</sub>	Moment	D <sub>m</sub>	D <sub>p</sub>	D <sub>a</sub>
$\bar{x}$	3.94E-02	2.14E-01	2.12E-02	$\sigma(x_1, \dots, x_N)$	3.55E-02	1.73E-01	2.18E-02
$(\bar{x}_{low}, \bar{x}_{up})_{95\%}$	3.52E-02	1.94E-01	1.86E-02	$(\sigma_{low}, \sigma_{up})_{95\%}$	3.25E-02	1.588E-01	1.99E-02
	4.37E-02	2.35E-01	2.38E-02		3.85E-02	1.88E-01	2.36E-02
Var(x <sub>1</sub> , ..., x <sub>N</sub> )	1.26E-03	3.00E-02	4.75E-04	COV	90.0	80.7	102.8
-	-	-	-	$x_{max}$	0.22	0.89	0.16

Table 10.15 Statistical moments of the global damage indices. Example 5

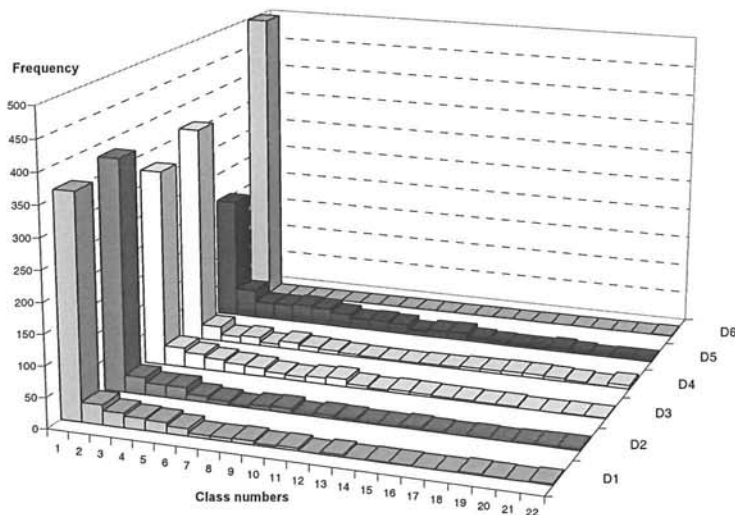


Figure 10.24 Histograms of pier damage and mean global damage indices. Example 5

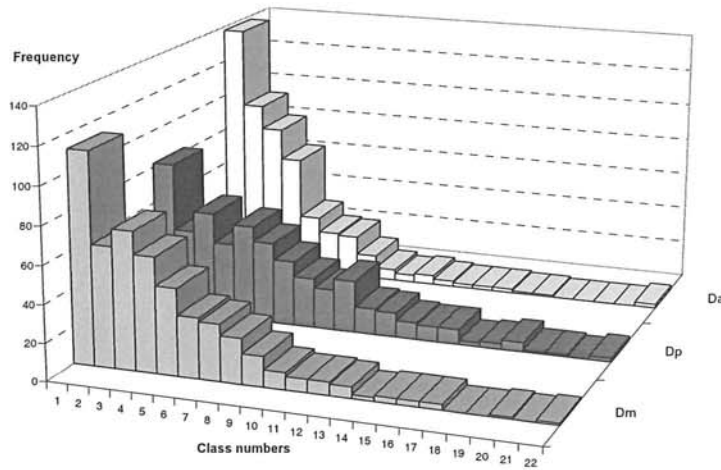


Figure 10.25 Histograms of global damage indices. Example 5

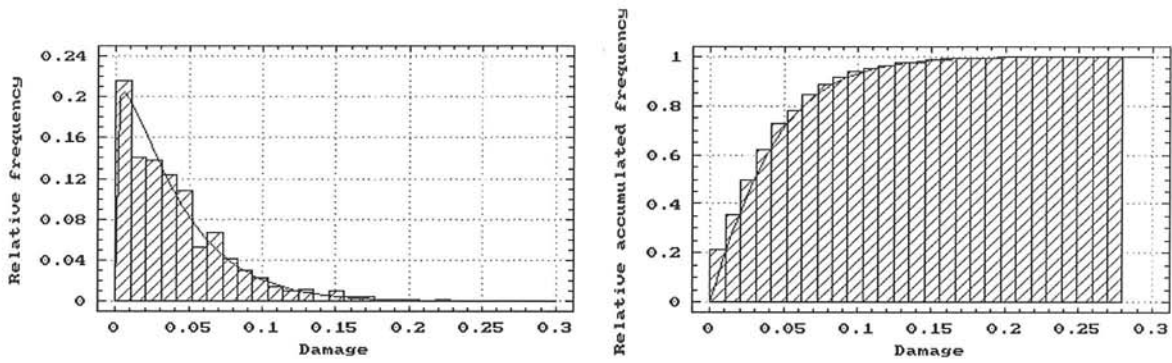


Figure 10.26 Beta distribution function (left) and accumulated distribution (right). Global mean damage. Example 5

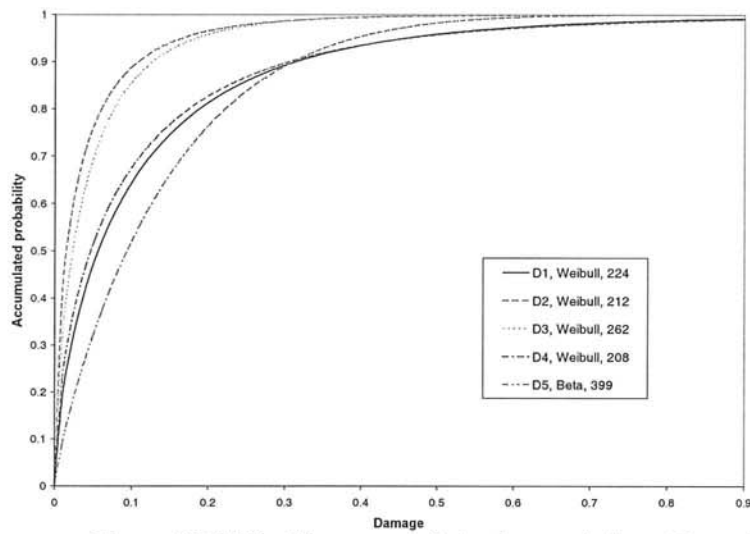


Figure 10.27 Fragility curves of pier damage indices. Example 5

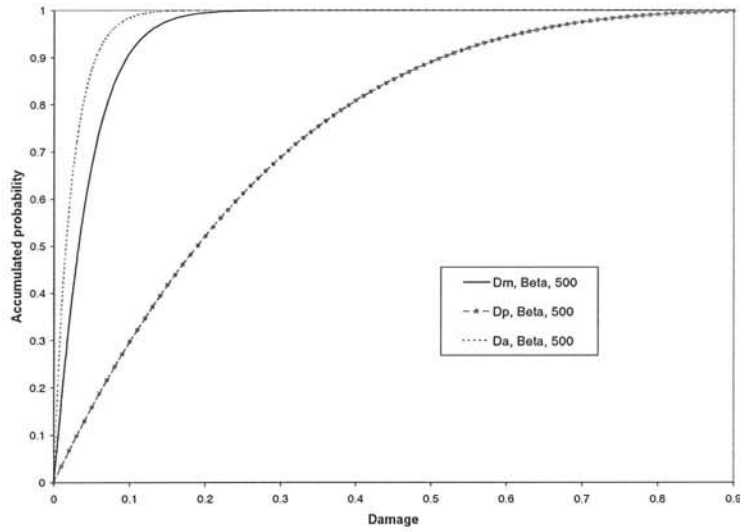


Figure 10.28 Fragility curves of global damage indices. Example 5

Moment	Damage						
	D <sub>m</sub>	D <sub>1</sub>	D <sub>2</sub>	D <sub>3</sub>	D <sub>4</sub>	D <sub>5</sub>	D <sub>6</sub>
$\bar{x}$	3.29E-01	5.85E-01	4.56E-01	3.45E-01	3.01E-01	2.07E-01	7.80E-02
$(\bar{x}_{low}, \bar{x}_{up})_{95\%}$	3.18E-01	5.66E-01	4.45E-01	3.33E-01	2.85E-01	1.83E-01	5.63E-02
	3.39E-01	6.03E-01	4.68E-01	3.57E-01	3.17E-01	2.31E-01	9.96E-02
Var( $x_1, \dots, x_N$ )	7.24E-03	2.26E-02	9.51E-03	9.44E-03	1.69E-02	3.91E-02	3.19E-02
$\sigma(x_1, \dots, x_N)$	8.51E-02	1.51E-01	9.75E-02	9.71E-02	1.30E-01	1.98E-01	1.79E-02
$(\sigma_{low}, \sigma_{up})_{95\%}$	7.78E-02	1.38E-01	8.92E-02	8.89E-02	1.19E-01	1.81E-01	1.63E-01
	9.24E-02	1.63E-01	1.06E-01	1.06E-01	1.41E-01	2.15E-01	1.94E-01
COV	25.9	25.7	21.4	28.1	43.2	95.7	229
$x_{min}$	0.199	0.160	0.138	0.014	0	0	0
$x_{max}$	0.722	0.896	0.786	0.698	0.802	0.866	0.961

Table 10.16 Statistical moments of global mean damage and pier damages. Example 6

Moment	Damage						
	D <sub>a</sub>	DP <sub>1</sub>	DP <sub>2</sub>	DP <sub>3</sub>	DP <sub>4</sub>	DP <sub>5</sub>	DP <sub>6</sub>
$\bar{x}$	1.97E-01	3.25E-01	2.55E-01	2.41E-01	1.96E-01	1.09E-01	5.78E-02
$(\bar{x}_{low}, \bar{x}_{up})_{95\%}$	1.91E-01	3.18E-01	2.47E-01	2.33E-01	1.89E-01	1.00E-01	4.20E-02
	2.04E-01	3.32E-01	2.63E-01	2.49E-01	2.03E-01	1.17E-01	7.36E-02
Var( $x_1, \dots, x_N$ )	3.08E-03	3.70E-03	3.93E-03	4.05E-03	3.47E-03	4.61E-03	1.72E-02
$\sigma(x_1, \dots, x_N)$	5.55E-02	6.08E-02	6.27E-02	6.36E-02	5.89E-02	6.79E-02	1.31E-01
$(\sigma_{low}, \sigma_{up})_{95\%}$	5.08E-02	5.56E-02	5.73E-02	5.82E-02	5.39E-02	6.21E-02	1.20E-01
	6.03E-02	6.60E-02	6.80E-01	6.92E-02	6.40E-02	7.37E-02	1.42E-01
COV	28.2	18.7	24.6	26.4	30.1	62.5	227
$x_{min}$	0.113	0.170	0.127	0.104	0.069	0.004	0
$x_{max}$	0.473	0.528	0.483	0.451	0.385	0.414	0.734

Table 10.17 Statistical moments of DiPasquale and Cakmak global and pier damages. Example 6

Damage							
Moment	$D_m$	$D_p$	$D_a$	Moment	$D_m$	$D_p$	$D_a$
$\bar{x}$	3.29E-01	9.20E-01	1.97E-01	$\sigma(x_1, \dots, x_N)$	8.51E-02	4.01E-02	5.55E-02
$(\bar{x}_{low}, \bar{x}_{up})_{95\%}$	3.18E-01 3.39E-01	9.15E-01 9.25E-01	1.91E-01 2.04E-01	$(\sigma_{low}, \sigma_{up})_{95\%}$	7.78E-02 9.24E-02	3.66E-02 4.35E-02	5.08E-02 6.03E-02
$\text{Var}(x_1, \dots, x_N)$	7.24E-03	1.61E-03	3.08E-03	COV	25.9	4.4	28.2
$x_{min}$	0.199	0.769	0.113	$x_{max}$	0.722	0.999	0.473

Table 10.18 Statistical moments of the global damage indices. Example 6

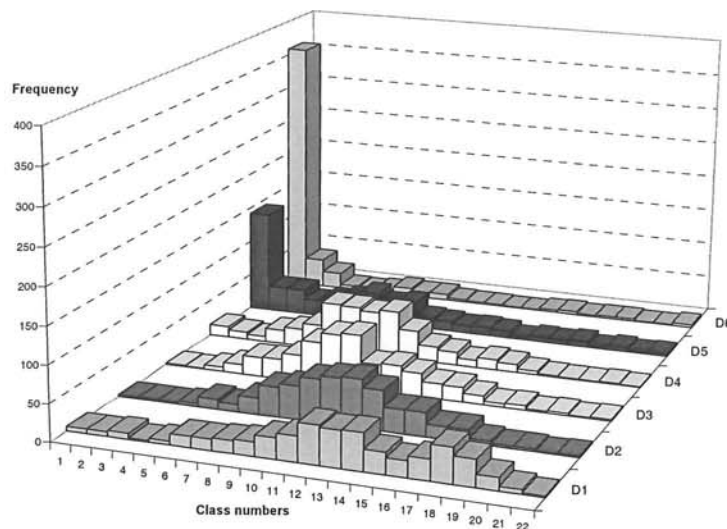


Figure 10.29 Histograms for pier damage indices. Example 6

The principal statistical moments of the pier and global damages are shown in tables 10.14 and 10.15. Means of the global damages of 4.0% ( $D_m$ ), 21.4% ( $D_p$ ), and 2.12% ( $D_a$ ) were obtained, with mean values of the pier damages between 0 and 9.6%.

Figures 10.24 to 10.28 show the histograms and fragility curves for the pier and global damages. The fragility curves of figure 10.27 are less pronounced than those of example 3, principally for pier  $P_5$ .

#### 10.2.3.6 Influence of random structural parameters and deterministic accelerograms. Second seismic scenario

For this simulation random structural parameters and deterministic geometrical variables were used. In this case, however, the external action was defined by the six deterministic accelerograms of the second seismic scenario, magnitude 6.5 and distance to the source of 30 km. The statistical moments of the pier damage and global damages of the bridge are presented in tables 10.16 to 10.18. In these tables is observed that the mean of the global damage of the bridge are of 32.9% ( $D_m$ ), 92.0% ( $D_p$ ) and 19.7% ( $D_a$ ), being the mean of the pier damage of bridge piers between the 7.8% for pier  $P_6$  and of 58.1% for pier  $P_1$ .

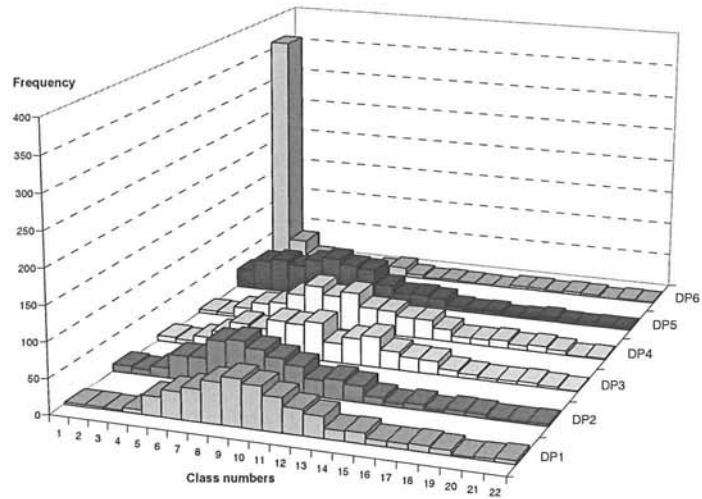


Figure 10.30 Histograms of DiPasquale and Cakmak pier damage indices. Example 6

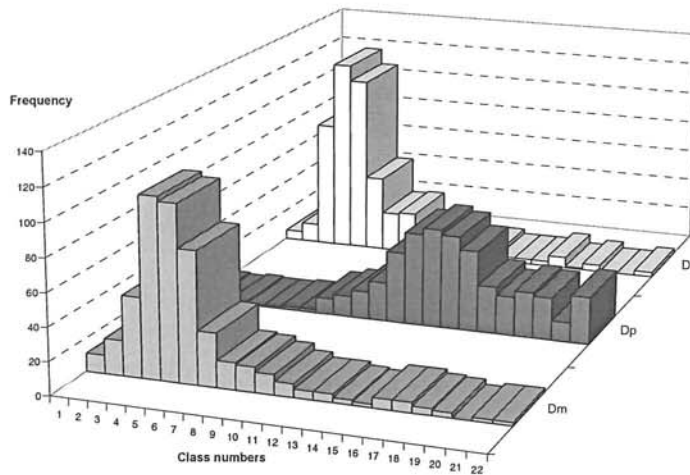


Figure 10.31 Histograms of global damage indices. Example 6

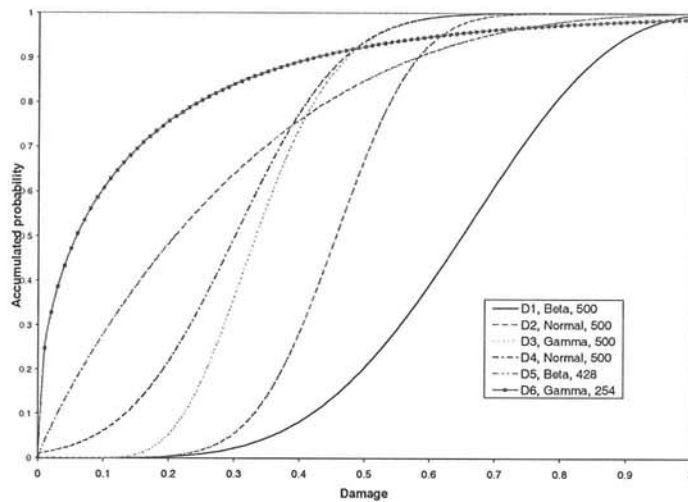


Figure 10.32 Fragility curves of pier damage indices. Example 6

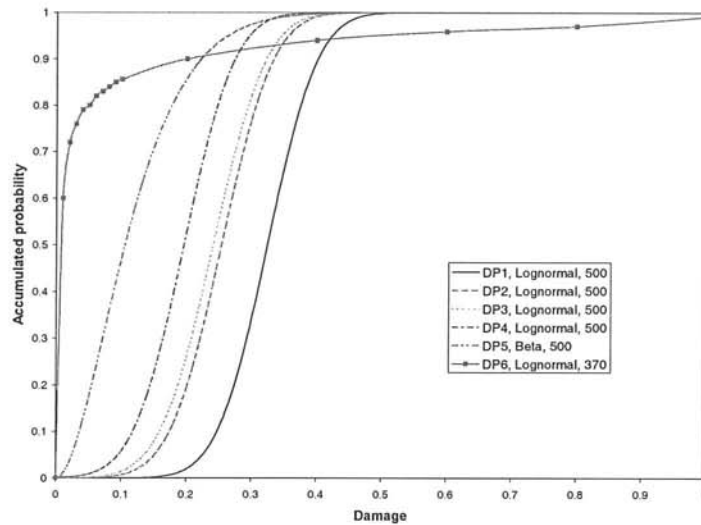


Figure 10.33 Fragility curves of DiPasquale and Cakmak pier damage indices. Example 6

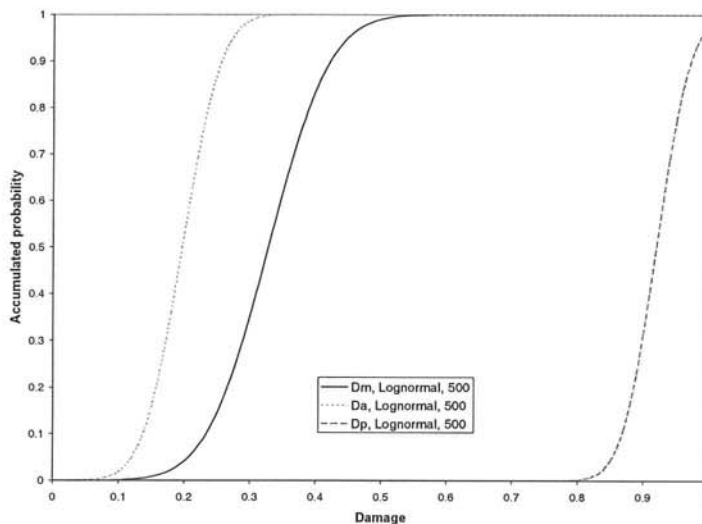


Figure 10.34 Fragility curves for global damage indices. Example 6

In this simulation, the obtained histograms for the damage variables are represented in figures 10.29 to 10.31. In addition, figures 10.32 to 10.34 show the theoretical distributions functions adjusted to the statistical results obtained for these variables. The adjusted curves for global damages  $D_m$  and  $D_a$  (figure 10.34) do not pass the chi-square and K-S goodness of fit tests for significance levels of 0.1 or 0.05. Other techniques to obtain a theoretical function can be developed for these variables. However, the theoretical curves of figure 10.35 have not greater difference to the empirical ones.

For the last simulation is observed that:

1. The second seismic scenario is more destructive for the analysed bridge.
2. The fragility curves of the damage variables are less pronounced, that is, the frequencies of damage intervals are more distributed. This can not occur with the pier damage of pier  $P_6$ , which can suffer mean damage lesser than 10%

3. For ground accelerations similar to the used in this example, the fragility curves of the DiPasquale and Cakmak pier damages show more difference than the curves obtained with earthquakes of the first seismic scenario.
4. The functional global damage index presents values greater than 90%. Thus, one can conclude that for levels of seismic action similar to the ones used in this example, the bridge may suffer important interruptions of its function service.

## Appendix A. Newark's algorithm

Starting from the mass, stiffness, and damping matrices of a structure, Newark's algorithm determines the displacement, velocity and acceleration. It is an implicit scheme for the solution of the equation of motion, which considers that the response at the instant  $t_{i+1}$  is a function of the responses at the instant  $t_i$  (Barbat and Canet 1998, Bathe 1996) and is unconditionally stable if its parameters are  $\alpha = 0.5$  y  $\beta = 0.25$ .

In a non-linear analysis, the solution of the equation the motion is obtained by using the Newark's time integration algorithm, an incremental formulation and an iterative solution procedure. Normally, the Newton-Rapshon scheme is used as an iterative process to reach the convergence at each time increment. In each iteration of the process, an out of balance load vector ( $\Delta \mathbf{F}_{i+1}^{(j)}$ ) that yields an increment in displacements ( $\delta \mathbf{v}_{i+1}^{(j)}$ ) is obtained. The iterative process continues until the out of balance load vector or the displacement increments are sufficiently small (see figure A.1 for a single degree of freedom case). Important aspects of the non-linear solution are the calculation of the load vector, the tangent stiffness matrix  $\mathbf{K}e_{i+1}$ , and the evaluation of the incremental displacement. A schematic representation of the global non-linear algorithm of Newmark is given in table A.1.

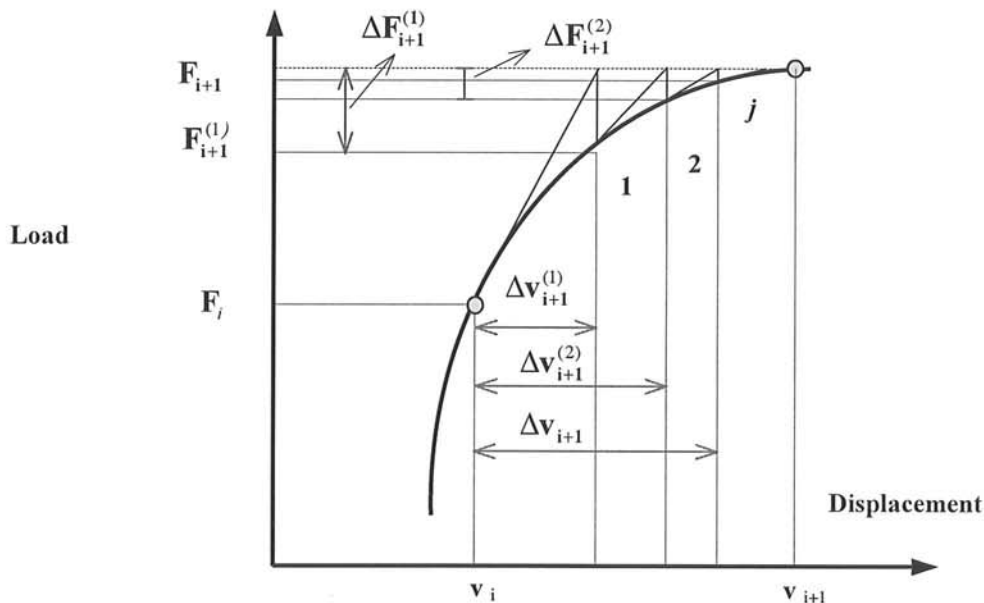


Figure A.1 Full Newton-Raphson iteration scheme. Single degree of freedom system



- Constants:

$$\beta = 0.25, \quad \gamma = 0.5, \quad \Delta t = t_{i+1} - t_i$$

- First iteration (instant  $t_i$  to instant  $t_{i+1}$ ):

Update the stiffness matrix  $\mathbf{K}$

Determine the effective force and the equivalent stiffness,  $\mathbf{fe}$  and  $\mathbf{Ke}$ :

$$\mathbf{Ke} = \frac{1}{\beta \Delta t^2} \mathbf{M} + \frac{\gamma}{\beta \Delta t} \mathbf{C} + \mathbf{K}$$

$$\mathbf{fe} = \mathbf{f}(t_{i+1}) + \mathbf{M} : \left[ \frac{1}{\beta \Delta t^2} \mathbf{v}_{i-1} + \frac{1}{\beta \Delta t} \dot{\mathbf{v}}_{i-1} + \left( \frac{1}{2\beta} - 1 \right) \ddot{\mathbf{v}}_{i-1} \right] +$$

$$\mathbf{C} : \left[ \left[ \frac{\gamma}{\beta \Delta t} \mathbf{v}_{i-1} + \left( \frac{\gamma}{\beta} - 1 \right) \dot{\mathbf{v}}_{i-1} + \left( \frac{\gamma}{2\beta} - 1 \right) \Delta t \mathbf{v}_{i-1} \right] \right]$$

Obtain the first approximation for instant  $i+1$ :

$$\mathbf{v}^{(1)} = \mathbf{Ke}^{-1} \mathbf{fe}_{i+1}^{(1)}$$

$$\ddot{\mathbf{v}}_i^{(1)} = \left( \frac{1}{\beta \Delta t^2} \right) (\mathbf{v}_i^{(1)} - \mathbf{v}_{i-1}) - \left( \frac{1}{\beta \Delta t} \right) \dot{\mathbf{v}}_{i-1} - \left( \frac{1}{2\beta} - 1 \right) \ddot{\mathbf{v}}_{i-1}$$

$$\dot{\mathbf{v}}_i^{(1)} = \dot{\mathbf{v}}_{i-1} + \Delta t (1 - \gamma) \ddot{\mathbf{v}}_{i-1} + (\gamma \Delta t) \ddot{\mathbf{v}}_i^{(1)}$$

- Second and subsequent iterations (equilibrium iterations for instants  $i+1$ ):

I. Update

$$\mathbf{Ke} = \frac{1}{\beta \Delta t^2} \mathbf{M} + \frac{\gamma}{\beta \Delta t} \mathbf{C} + \mathbf{K}$$

$$\mathbf{fe}^{(j+1)} = \mathbf{f}(t_{i+1}) + \mathbf{M} : \mathbf{v}_{i+1}^{(1)} + \mathbf{C} : \dot{\mathbf{v}}_i^{(1)}$$

II. If the effective force is not small enough, evaluate

$$\delta \mathbf{v}^{(j+1)} = \mathbf{Ke}^{-1} \mathbf{fe}^{(j+1)}$$

$$\ddot{\mathbf{v}}_i^{(j+1)} = \left( \frac{1}{\beta \Delta t^2} \right) \delta \mathbf{v}_i^{(j+1)} + \ddot{\mathbf{v}}_i^{(j)}$$

$$\dot{\mathbf{v}}_i^{(j+1)} = \left( \frac{\gamma}{\beta \Delta t} \right) \delta \mathbf{v}_i^{(j+1)} + \dot{\mathbf{v}}_i^{(j)}$$

$$\mathbf{v}_i^{(j+1)} = \delta \mathbf{v}_i^{(j+1)} + \mathbf{v}_i^{(j)}$$

III. Return to step I

**Table A.1** Non-linear algorithm of Newmark

## Appendix B. Isotropic damage model

In the isotropic damage model for concrete elements of Oliver et al. (1990) based on the continuum damage mechanics, the non-linear behaviour is monitored through a single internal variable, called damage,  $d$ , which ranges from 0 (no damage) to 1 (complete damage) and measures the loss of secant stiffness of the material.

The constitutive equation for an isotropic damage model is

$$\boldsymbol{\sigma} = (1 - d)\mathbf{D}_0 : \boldsymbol{\varepsilon} \quad (\text{B.1})$$

where  $\boldsymbol{\sigma}$  and  $\boldsymbol{\varepsilon}$  are the stress and strain tensors, respectively,  $d$  is the damage variable and  $\mathbf{D}_0$  is the elastic constitutive tensor. Starting from equation B.1 it is considered that: (1) the material stiffness is only affected by a scalar factor; (2) equation B.1 can be interpreted as a decomposition of the stress into elastic and inelastic parts

$$\boldsymbol{\sigma} = \mathbf{D}_0 : \boldsymbol{\varepsilon} - d\mathbf{D}_0 : \boldsymbol{\varepsilon} = \boldsymbol{\sigma}_0 - \boldsymbol{\sigma}_i \quad (\text{B.2})$$

where  $\boldsymbol{\sigma}_0$  is the undamaged stress tensor.

The model defined by equation B.1 is fully determined if the value of  $d$  can be evaluate at every time of the deformation process. So, one must define:

- A *suitable norm*,  $\tau$ , of the strain tensor, or alternatively, of the undamaged stress tensor. This norm, denominated the *equivalent strain*, is used to compare different states of deformation. The norm  $\tau$  is a positive scalar function, with zero value for the undeformed state.

For elements with degradation in tension and compression, like the reinforced concrete elements, the equivalent deformation is defined as:

$$\tau = \left( \theta + \frac{1-\theta}{n} \right) \sqrt{\boldsymbol{\sigma}_0 : \mathbf{D}_0^{-1} : \boldsymbol{\sigma}_0} \quad (\text{B.3})$$

where

$$\theta = \frac{\sum_{i=1}^3 \langle \boldsymbol{\sigma}_0^i \rangle}{\sum_{i=1}^3 |\boldsymbol{\sigma}_0^i|} \quad (\text{B.4})$$

is a weighting factor depending on the state of stress and  $n$  is the ratio of the compressive strength to the tensile strength, which takes a value approximately equal to 10 for concrete materials

$$n = \frac{f'_c}{f'_t} \approx 10 \quad (\text{B.5})$$

In the above two equations,  $f'_c$  and  $f'_t$  are the compressive and tensile strengths, respectively, and  $\sigma_0$  is the elastic stress vector. The values of  $\theta$  range from zero for triaxial compression to 1.0 for triaxial tension. For intermediate states  $0 < \theta < 1$ .

- A *damage criterion*,  $F(\tau, r) \leq 0$ , formulated in the strain or undamaged stress spaces. The simplest form of this criterion is

$$F(\tau^t, r^t) = G(\tau^t) - G(r^t) \leq 0 \quad \forall t \geq 0 \quad (\text{B.6})$$

where  $\tau^t$  is the norm at the current time  $t$ ,  $r^t$  is the damage threshold at the current time  $t$ , and  $G(x)$  is a suitable monotonic scalar function. Starting from results from uniaxial tension test, the initial threshold value,  $r^*$ , is defined as

$$r^* = \frac{f'_t}{\sqrt{E_0}} \quad (\text{B.7})$$

where  $E_0$  is Young's modulus and  $r^t \geq r^0 = r^*$ . Expression (B.6) represents a bonding surface in the strain or undamaged stress spaces. Figure B.1 shows the corresponding surface  $\tau - r^* = 0$  in the  $\sigma_0^t - \sigma_0^3$  plane and the uniaxial curve. In this figure, the approximation of the behaviour of the real material can be verified.

Damage occurs when the norm  $\tau$  exceeds the current threshold value. In particular, damage is initiated when the norm exceeds the value of  $r^*$ .

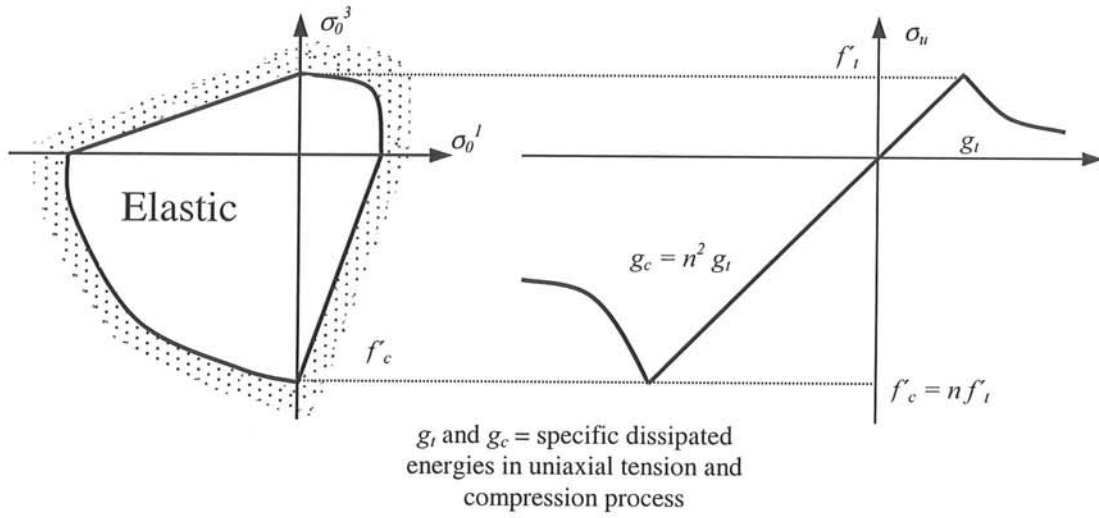
- *Evolution laws* for the damaged threshold and the damage variable. For the Kuhn-Tucker relations (Oliver et al. 1990) the evolution of the internal variables can be expressed as:

$$r^t = \max\{r^{s^0}, \max \tau^s\} \quad 0 < s < t \quad (\text{B.8})$$

$$d^t = G(r^t) \quad (\text{B.9})$$

which fully describes evolution of the internal variables for loading, unloading and reloading situations. The scalar function  $G(\bullet)$ , defining the evolution of the damage value, must be monotonic, and ranges from 0 to 1. Oliver et al. proposed the following expression for this scalar function:

$$G(r^t) = 1 - \frac{r^*}{r^t} \exp\left\{A \left(1 - \frac{r^t}{r^*}\right)\right\} \quad 0 < r^* < r^t \quad (\text{B.10})$$



**Figure B.1** Damage bounding surfaces and uniaxial curves for the Oliver et al. model

<p>Initial data for time <math>t+1</math>:</p> <ul style="list-style-type: none"> <li>• Material properties: <math>f_t, n, E_0, \nu, G_f</math></li> <li>• Initial threshold: <math>r^*</math> (equation B.7)</li> </ul> <p>Operations:</p> <ul style="list-style-type: none"> <li>• Determine <math>A</math> (equation B.11)</li> <li>• If <math>t = 0</math> initialise <math>r^0 = r^*</math></li> <li>• Evaluate undamaged stresses <math>\sigma_0^{t+1} = \mathbf{D}_0 : \boldsymbol{\varepsilon}^{t+1}</math></li> <li>• Evaluate <math>\tau^{t+1}</math> (equation B.3)</li> <li>• Update internal variables (equations B.8 and B.9)</li> <li>• Update stresses <math>\sigma^{t+1} = (1 - d^{t+1})\sigma_0^{t+1}</math></li> </ul>
---

**Table B.1** Algorithm of the Oliver et al. (1990)

where

$$A = \left( \frac{G_f E_0}{l^* (f_t')^2} - \frac{1}{2} \right)^{-1} \geq 0 \quad (\text{B.11})$$

is a parameter, obtained through energy approximations,  $G_f$  is the fracture energy per unit area (assumed to be a material property) and  $l^*$  is a characteristic length of the finite element. The values of  $A$  and  $n$  determine the shape of the uniaxial stress-strain curve. As  $A$  must be positive, the expression B.11 limits the maximum size of the element that may be used in a finite element mesh.

Table B.1 shows the simple algorithm used to evaluate damage with the Oliver et al. (1999) model.

## References

- "*ABAQUS. User Manual*" (1999). Hibbit Karlsson and Sorensen, HKS. Version 5.8.
- Aguiar, R. and A. H. Barbat (1997). "*Daño sísmico en estructuras de hormigón armado*". Universidad Politécnica del Ejército, Ecuador.
- Ala-Saadeghvaziri, M. (1996). "A case study from the Northridge earthquake". 11th World Conference on Earthquake Engineering, CD ROOM, (1990), Acapulco, México.
- Alarcón-Guzmán, A. (1997). "Microzonificación sísmica de Santa Fe de Bogotá". Ingeominas. Unidad de Prevención y Atención de Emergencias de Santa Fe de Bogotá, D. C. y Dirección Nacional para la Prevención y Atención de Desastres. Convenio Interadministrativo **01-93**.
- Aldrich, J. H. and F. D. Nelson (1984). "**Linear probability, logit, and probit models**". Series: Quantitative Applications in the Social Sciences. Sage University Papers: 48-65.
- Alvaredo A. M. and F. H. Wittmann (1998). "Shrinkage as influenced by strain softening and crack formation". *RILEM Creep and Shrinkage of Concrete*. (13). Edited by Z. P. Bazant and I. Carol. Centro Internacional de Métodos Numéricos en Ingeniería.
- Amin G. and G. Tadros (1997). "Bridge progressive collapse vulnerability". *Journal of Structural Engineering*, ASCE, **121** (2):227-231.
- Anicic, D. and D. Moric (1994). "Nonlinear dynamic analysis of a girder bridge". Proceedings of the 10th European Conference on Earthquake Engineering, 2:1811-1817, Vienna.
- Applied Technology Council (1981). "*Seismic design guidelines for highway bridges*". **ATC-6** Report. Redwood City, California, USA.
- Applied Technology Council (1983). "*Seismic retrofitting guidelines for highway bridges*". **ATC-6-2** Report. Palo Alto, California, USA.
- Applied Technology Council (1985). "*Earthquake damage evaluation data for California*". **ATC-13**, Redwood City, California, USA.
- Applied Technology Council (1991). "*Seismic vulnerability and impact of disruption of lifelines in the conterminous United States*". **ATC-25**. Redwood City, California, USA.

- Aschheim, M. (1997). "Seismic vulnerability, evaluation, retrofit and new design of California bridge – a general vision". Proceedings of the U.S.-Italian Workshop on Seismic Evaluation and Retrofit. National Center for Earthquake Engineering Research. Technical Report. **NCEER-97-0003:220-232**. Edited by: D. P. Abrams and G. M. Calvi.
- Augusti G. and M. Ciampoli (1994). "Seismic capacity assessment: The example of reinforced concrete bridges". Proceedings of the 10<sup>th</sup> European Conference on Earthquake Engineering, **4:2709-2714**, Vienna.
- Barbat, A. and J. M. Canet (1994). "*Estructuras sometidas a acciones sísmicas. Cálculo por ordenador*". Centro Internacional de Métodos Numéricos en Ingeniería, Segunda edición.
- Barbat, A. H., L. Orozco, J. E. Hurtado and M. Galindo (1994). "Definición de la acción sísmica". *Monografías de ingeniería Sísmica*, **CIMNE IS-10**.
- Bartlett, F. M. and J. G. MacGregor (1996). "Statistical analysis of the compressive strength of concrete structures". *ACI Materials Journal*, **93(2):158-168**.
- Basöz, N. and A. S. Kiremidjian (1995). "Use of Geographic Information Systems for bridge prioritization". Proceeding of the Fifth International Conference on Seismic Zonation, Nice, France, **I:17-24**.
- Basöz, N. and A. S. Kiremidjian (1998). "Evaluation of bridge damage data from the Loma Prieta and Northridge, California earthquakes". Multidisciplinary Centre of Earthquake Engineering Research. Technical Report **MCEER-98-0004**.
- Bathe, K. J. (1996). "*Finite Element procedures*". Prentice Hall, New Jersey.
- Bazant, Z. P. and K. L. Liu (1985). "Random creep and shrinkage in structures: sampling". *Journal of Structural Engineering*, **111(5):1113-1134**.
- Billings, I. J. and D. W. Kennedy. (1996). "Auckland harbour bridge seismic assessment". 11<sup>th</sup> World Conference on Earthquake Engineering, CD-ROOM (**2023**), Acapulco, México.
- Bourque, L. (1997). "Book review: the public health consequences of disasters". *Earthquake Spectra*. Theme Issue: Loss Estimation, **13 (4):851-856**.
- Brookshire, D. S., S. E. Chang, H. Cochrane, R. A. Olson, A. Rose and J. Steenson (1997). "Direct and indirect economic losses by earthquake damage". *Earthquake Spectra*. Theme Issue: Loss Estimation, **13 (4):683-702**.
- Calvi, G. M. and P. E. Pinto (1994). "Seismic design of bridges: experimental and analytical research". Proceedings of the 10<sup>th</sup> European Conference on Earthquake Engineering, **4:2899-2904**, Vienna.

- Calvi, G. M. and P. E. Pinto (1996). "Experimental and numerical investigations on the seismic response of bridges and recommendations for code provisions". European Consortium of Earthquake Shaking Tables. Pre-normative Research in Supp. of Eurocode 8, Report No. 4.
- Canavos, G. C. (1988). "Probabilidad y estadística. Aplicaciones y métodos". Ed. Mac Graw Hill.
- Can-Zülfikar A. and O. Yüzügüllü (1995). "Preliminary assessment of seismic vulnerability of highway bridges in Istanbul, Turkey". Proceedings of the 4<sup>th</sup> Conference of Lifeline Earthquake Engineering. Edited by Michael J. O'Rourke. American Society of Civil Engineers, pp. 477-484, San Francisco, U.S.A.
- Chang, T. S., S. Pezeshk, K. C. Yiak and H. T. Kung (1995). "Seismic vulnerability evaluation of essential facilities in Memphis and Shelby County, Tennessee". *Earthquake Spectra*, **11** (4): 527-544.
- Chang, S., A. Rose and M. Shinozuka (1998). "Infrastructure life cycle cost analysis: direct and indirect user costs of natural hazards". Multidisciplinary Center for Earthquake Engineering Research. Technical Report. **MCEER-98-0017**: 153-162.
- Ciampoli, M. (1994). "Upgrading R/C bridges for seismic risk reduction". Proceedings of the 10<sup>th</sup> European Conference on Earthquake Engineering, 3:2209-2214, Vienna.
- Clough, R. and J. Penzien (1975). "*Dynamics of structures*". MacGraw Hill.
- Corsanegro, A. "Recent trends in the field of earthquake damage interpretation". *Proceeding of the 10<sup>th</sup> European Conference on Earthquake Engineering*, Bakelma, Rotterdam.
- Craig, R. R. (1981). "*Structural dynamics. An introduction to computer methods*". John Wiley and Sons.
- D'Áyala, D., R. Spencer, C. Oliveira and A. Pomonis (1997). "Earthquake loss estimation for Europe's Historic Town Centres". *Earthquake Spectra*. Theme Issue: Loss Estimation, **13** (4): 773-794.
- DesRoches, R. and G. L. Fenves (1997). "Evaluation of recorder earthquake response of a curved highway bridge". *Earthquake Spectra*, **13** (3): 363-386.
- DeRoches, R. and G. L. Fenves (1998). "Design procedures for hinge restrainers and hinge seat width for multiple-frame bridges". Multidisciplinary Center for Earthquake Engineering Research. Technical report **MCEER-98-0013**.
- Díaz-Canales, M. and G. Hernández-Zepeda (1997). "Análisis y diseño estructural de un puente carretero en Ometepec, Guerrero". Memorias del XI Congreso Nacional de Ingeniería Sísmica, **II**: 977-986, Veracruz, México.

- Diniz, S. M. C. and D. M. Frangopol (1990). "Reliability bases for high-strength concrete columns". *Journal of Structural Engineering*, **123 (10)**:1375-1381.
- DiPasquale, E. and A. S. Cakmak (1990). "Seismic damage assessment using linear models". *Soil Dynamics and Earthquake Engineering*, **9 (4)**:194-197, Princeton, NJ, USA
- Dolce M., G. Zuccaro, A. Kappos and A. W. Colburn (1994). "Report of the EAEE Working Group 3: Vulnerability and risk analysis". Proceedings of the 10<sup>th</sup> European Conference on Earthquake Engineering, **4**: 3049-3077, Vienna.
- Dolce, M. (1997). "Seismic vulnerability evaluation and damage scenarios". Proceedings of the U.S.-Italian Workshop on Seismic Evaluation and Retrofit. National Center for Earthquake Engineering Research. Technical Report. **NCEER-97-0003**: 85-101. Edited by: D. P. Abrams and G. M. Calvi.
- Duma, G. and S. Seren (1998). "Determination of basic seismological parameters for the Warth Bridge site". Technical report **CIMG**. Department of Geophysics, Austria.
- E8. "Eurocódigo 8. Disposiciones para el proyecto de estructuras sismorresistentes. Parte 2: Puentes". Volumen **UNE-ENV 1998-2**. *Norma Europea Experimental*
- Eguchi, R. T., J. D. Goltz, H. A. Seligson, P. J. Flores, N. C. Blais, T. H. Heaton and E. Bortugno (1997). "Real-time loss estimation as an emergency response decision support system: the early post-earthquake damage assessment tool (EPEDAT)". *Earthquake Spectra*. Theme Issue: Loss Estimation, **13 (4)**: 815-832.
- Eguchi, T. (1998). "Integrated real-time disaster information systems. The application of new technologies". Multidisciplinary Center for Earthquake Engineering Research. Technical Report. **MCEER-98-0017**: 93-99.
- Ellingwood, B. and T. A. Reinhold (1980). "Reliability analysis of steel beam-columns". *Journal of Structural Engineering*, **106(ST12)**:2560-2564.
- Elnashai, A. S. (1996). "Inelastic analysis of RC bridges and applications to recent earthquake". 11<sup>th</sup> World Conference on Earthquake Engineering, CD ROOM, (1842), Acapulco, México.
- ELSA, Laboratory (1996). "Pseudo-dynamic testing of large-scale R/C bridges in ELSA". 11<sup>th</sup> World Conference on Earthquake Engineering, CD ROOM, (2046), Acapulco, México.
- Enright, M. P. and D. M. Frangopol (1998). "Probabilistic analysis of resistance degradation of reinforced-concrete bridge beams under corrosion". *Journal of Engineering Structures*.
- EQE International (1989). "The October 17, 1989 Loma Prieta Earthquake". WWW EQE International's home page.



- EQE International (1994). "The January 17, 1994 Northridge, CA Earthquake". WWW EQE International's home page.
- EQE International (1995). "The January 17, 1995 Kobe Earthquake". WWW EQE International's home page.
- Fishman, K. L. and R. Richards, Jr. (1997). "Seismic analysis design of bridge abutments considering sliding and rotation". National Centre for Earthquake Engineering Research. Technical report **NCEER-97-0009**.
- Fishman, K. L., R. Richards Jr. and R. C. Divito (1997). "Seismic analysis for design of retrofit of gravity bridge abutments". National Center for Earthquake Engineering Research . Technical report **NCEER-97-0011**.
- Flesch, R. G. and A. Klatzer (1994). "Earthquake resistant design of R/C bridges: state-of-the-art report". Proceedings of the 10<sup>th</sup> European Conference on Earthquake Engineering, 2:1787-1796, Vienna.
- Flesch, R. G., P. H. Kirkegaard, C. Kramer, M. Brughmans, G. P. Roberts and M. Gorozzo (1999). "Dynamic in situ test of bridge WARTH/Austria". *Technical report, TU-Graz, TUG TA 99/0125*.
- Flesch, R. G., E. M. Darin, R. Delgado, A. Pinto, F. Romanelli, A. Barbat and M. Kahan (2000). "Seismic risk assessment of motorway bridge WARTH/Austria". *Proceedings of the 12<sup>th</sup> World Conference on Earthquake Engineering, (0445)*.
- Florian, A. (1992). "An efficient sampling scheme: updated Latin Hypercube sampling". *Probabilistic Engineering Mechanics, (7)*: 123-130.
- Frangopol, D. M. and J. P. Curley (1986). "Effects of damage and redundancy of structural reliability". *Journal of Structural Engineering, 113(7)*:1533-1549.
- García, O., A. G. Ayala and U. Mena (1997). "Comportamiento sísmico de puentes con apoyos elastoméricos". XI Congreso Nacional de Ingeniería Sísmica, **II**: 997-1006, Veracruz, México.
- Gentile C. and F. Martínez y Cabrera (1997). "Dynamic investigation of a repaired cable-stayed bridge". *Earthquake Engineering and Structural Dynamics, 26 (1)*: 41-60.
- Gómez Soberón, C., A. Barbat and S. Oller (1999a). "Vulnerabilidad de puentes de autopista: un estado del arte". Monografía de Ingeniería Sísmica, **CIMNE IS-41**.
- Gómez Soberón, C., A. Barbat and S. Oller (1999b). "Estado del arte de la vulnerabilidad sísmica de puentes de autopista". Proceedings of the XII Congreso Nacional de Ingeniería Sísmica de México, **II**: 790-799.
- Gómez Soberón, C., S. Oller and A. Barbat ( 2000). "Simplified models for the Warth Bridge. VAB-Project". Technical Report **CIMNE IT-358**. Centro Internacional de Métodos Numéricos

- Gülkan P., M. A. Sozen, S. Demir and U. Ersoy (1996). "An alternative evaluation for determining seismic vulnerability of building structures". 11<sup>th</sup> World Conference on Earthquake Engineering, CD ROOM, (2109), Acapulco, México.
- Housner, G. W., and C. C. Thiel, Jr (1995). "The continuing challenge: report of the performance of state bridges in the Northridge Earthquake". *Earthquake Spectra*, **11** (4): 607-636.
- Hristovski, V. Y. and D. Ristic (1996). "New integrated concept for diagnosis of the state of RC bridges under service and earthquake loads based on progressive structural failure prediction". 11<sup>th</sup> World Conference on Earthquake Engineering, CD ROOM, (918), Acapulco, México.
- Hull, D. (1987). "*Materiales compuestos*". Editorial Reverté, España.
- Hurtado, J. E. (1998). "Stochastic dynamics of hysteretic structures". Monograph series in earthquake engineering, **CIMNE IS-25**.
- Hurtado, J. E. (1999). "Modelación estocástica de la acción sísmica". Monografías de Ingeniería Sísmica, **CIMNE IS-33**.
- Hurtado, J. E. and A. Barbat (1998). "Monte Carlo techniques in computational stochastic mechanics". *Archives of Computational Methods in Engineering. State of the art reviews*, **5**(1): 3-30.
- Hwang, H. H., and J. W. Jaw (1990). "Probabilistic damage analysis of structures". *Journal of Structural Engineering*, **116**(7):1992-2007.
- Hwang, H. H. M., H. Lin and J. R. Huo (1997). "Seismic performance evaluation of fire stations in Shelby County, Tennessee". *Earthquake Spectra*. Theme Issue: Loss Estimation, **13** (4): 759-772.
- Jauregui, D. V. and C. M. Farrar (1996). "Assessment of damage identification algorithms on experimental and numerical bridge data". Proceedings in Building and International Community of Structural Engineering, pp. 892-899, U.S.A.
- Jeong, G. D. and W. D. Iwan (1988). "The effect of earthquake duration on the damage of structures". *Earthquake Engineering and Structural Dynamics*, (16):1201-1211.
- King, S. A. (1996). "A comparison of earthquakes damage and loss estimation methodologies". 11<sup>th</sup> World Conference on Earthquake Engineering, CD ROOM, (1482), Acapulco, México.
- King, S. A., A. S. Kiremidjian, N. Basöz, K. Law, M. Vucetic, M. Doroudian, R. A. Olson, J. M. Eidinger, K. A. Goettel and G. Horner (1997). "Methodologies for evaluating the socio-economic consequences of large earthquakes". *Earthquake Spectra. Theme Issue: Loss Estimation*, **13** (4): 565-584.

- Kircher, C. A., A. A. Nassar, O. Kustu and W. T. Holmes (1997a). "Development of building damage function for earthquake loss estimation". *Earthquake Spectra*. Theme Issue: Loss Estimation, **13 (4)**: 663-682.
- Kircher, C. A., R. K. Reitherman, R. V. Whitman and C. Arnold (1997b). "Estimation of earthquake losses to buildings". *Earthquake Spectra*. Theme Issue: Loss Estimation, **13 (4)**: 703-720.
- Kiremidjian, A. S. and N. Basöz (1997). "Evaluation of bridge damage data from recent earthquakes". National Center for Earthquake Engineering Research. *NCEER Bulletin*, **11 (2)**: 1-7.
- Kiremidjian, A. S., J. Moore, Y. Fan, A. Hortacsu, K. Burnell, and J. LeGrue (2001). "Earthquake risk assessment for transportation systems: analysis of pre-retrofitted system". Pacific Earthquake Engineering Research Center PEER, **4(1)**:1-5
- Kramer, S. L. (1996). "**Geotechnical Earthquake Engineering**". First Edition, Prentice Hall Civil Engineering and Engineering Mechanics Series, United States of America, pp. 348-417
- Kristek, V. and Z P. Bazant (1987). "Shear lag effect and uncertainty in concrete box girder creep". *Journal of Structural Engineering*, **113(3)**:557-574.
- Kunnath, S. K., A. El-Bahy, A. Taylor and W. Stone (1997). "Cumulative seismic damage of reinforced concrete bridge piers". National Center for Earthquake Engineering Research . Technical Report **NCEER-97-0006**.
- Lee, J. and G. L. Fenves (1998). "Plastic-damage model for cyclic loading of concrete structures". *Journal of Engineering Mechanics*, **124(8)**:892-900.
- Lemaitre, J. (1992). "*A course on damage mechanics*". Springer. Second Edition.
- Lou, K. and F. Y. Cheng (1996). "Post-earthquake assessment of bridge collapse and design parameters". 11<sup>th</sup> World Conference on Earthquake Engineering, CD ROOM, **(1316)**, Acapulco, México.
- Luo, Y. K., A. Durrani and J. Conte (1996). "Seismic reliability assessment of casting R/C flat-slab buildings". *Journal of Structural Engineering*, **121(10)**:1522-1530.
- Maldonado, E., J. R. Casas and J. A. Canas (2000a). "Utilización de Conjuntos Difusos en modelos de vulnerabilidad sísmica". *Monografías de Ingeniería Sísmica*. **CIMNE IS-39**
- Maldonado, E., J. R. Casas and J. A. Canas (2000b). "Modelo de vulnerabilidad Sísmica de puentes basado en Conjuntos Difusos". *Monografías de Ingeniería Sísmica*. **CIMNE IS-40**.
- Mander, J. B., D. K. Kim, S. S. Chen and G. J. Premus (1996). "Response of steel bridge bearings to reversed cyclic loading". National Center for Earthquake Engineering Research. Technical report **NCEER-96-0014**.

- McCormack, T. C. and F. N. Rad (1997). "An earthquake loss estimation methodology for buildings based on ATC-13 and ATC-21". *Earthquake Spectra*. Theme Issue: Loss Estimation, **13** (4): 605-622.
- Miranda, E. (1993). "Evaluation of seismic design criteria for highway bridges". *Earthquake Spectral*, **9** (2): 233-250.
- Miranda E. (1996). "Assessment of the seismic vulnerability of existing buildings". 11th World Conference on Earthquake Engineering, CD ROOM, (513), Acapulco, México.
- Mirza, S. A., M. Hatzinikolas and J. G. MacGregor (1979). "Statistical descriptions of strength of concrete". *Journal of Structural Division*, **105**(6):1021-1037.
- Mirza, S. A. and J. G. MacGregor (1979). "Variations in dimensions of reinforced concrete members". *Journal of the Structural Division*, **105**(4):751-765.
- Mirza, S. A. (1996). "Reliability-based design of reinforced concrete columns". *Structural Safety*, **18**(2/3):179-194.
- Moehle, J. P. (1995). "Northridge earthquake of January 17, 1994: reconnaissance report. Volume 1 - Highway bridges and traffic management". *Earthquake Spectra*, **11**, suppl. c.
- Moghtaderi-Zadeh, M. and A. Der Kiureghian (1983). "Reliability upgrading of lifeline networks for post-earthquake serviceability". *Earthquake Engineering and Structural Dynamics*. **11**: 557-566.
- Mota-Arteaga, A. and G. Ayala-Milán (1993). "Comportamiento sísmico no lineal de puentes de concreto". X Congreso Nacional de Ingeniería Sísmica, pp. 81-88, Puerto Vallarta, México.
- Mullen, C. L. and A. S. Cakmak (1997). "Seismic fragility of existing conventional reinforced concrete highway bridges". National Center for Earthquake Engineering Research. Technical Report NCEER-97-0017.
- Nakajima H. (1996). "Seismic performance and repair of mayor steel bridges on the Hanshin Expressway, Japan". 11<sup>th</sup> World Conference on Earthquake Engineering, CD ROOM, (2024), Acapulco, México.
- Nigam, N. C. (1983). "Introduction to random vibrations". The MIT Press, Cambridge Massachussets.
- Nowak, A. S., A. S. Yamani and S. W. Tabsh (1994). "Probabilistic models for resistance of concrete bridge". *ACI Structural Journal*, **91**(3):269-276.
- Nowak, A. S. (1995). "Calibration of LRFD Bridge Code". *Journal of Structural Engineering*, **121**(8):1245-1251.

- O'Connor, J. M. and B. Ellingwood. "Reliability of nonlinear structures with seismic loading". *Journal of Structural Engineering*, **113(5)**:1011-1028.
- Oliver, J., M. Cervera, S. Oller and J. Lubliner (1990). "Isotropic damage models and smeared crack analysis of concrete". Second International Conference on *Computer Aided Analysis and Design of Concrete Structures*, **2**:945-958, Austria.
- Oller, S., A. H. Barbat, E. Oñate and A. Hanganu (1992). "A damage model for the seismic analysis of buildings structures". *10<sup>th</sup> World Conference on Earthquake Engineering*. 2593-2598.
- Oller, S., B. Luccioni and A. Barbat (1996). "Un método de evaluación del daño sísmico de estructuras de hormigón armado". *Revista Internacional de Métodos Numéricos para el Cálculo y Diseño en Ingeniería*, **12(2)**:215-238.
- Oller, S. (2001). "*Fractura mecánica. Un enfoque global*". Centro Internacional de Métodos Numéricos en Ingeniería, España.
- Olshansky, R. B. (1997). "The role of earthquake hazard maps in loss estimation: a study of the Northridge earthquake". *Earthquake Spectra*. Theme Issue: Loss Estimation, **13(4)**: 721-738.
- ÖNORM B4015-2 (1998). "Belastungsannahmen im bauwesen. Außergewöhnliche einwirkungen erdbebeneinwirkungen grundlagen. Código de diseño sísmico austriaco
- O'Rourke, T. D. (1996). "Lessons learned for lifeline engineering from mayor urban earthquake". *11<sup>th</sup> World Conference on Earthquake Engineering*. CD ROOM, **(2172)**. Acapulco, México.
- Panza, G. F., F. Romanelli and F. Vaccari (2001) "Effects on bridge seismic response of asynchronous motion at the base of the bridge piers". International Center of Theoretical Physics (ICTP), Report **5/1,2,3F**, Trieste, Italy.
- Park, Y. J., A. H. Ang. (1983) "Mechanistic seismic damage model for reinforced concrete". *Journal of Structural Engineering*, **111(4)**:722-739.
- Park, Y. J., A. H. Ang and Y. K. Wen (1985). "Seismic damage analysis of reinforced concrete buildings". *Journal of Structural Engineering*, **111(4)**:740-757.
- Pezeshk, S., T. S. Chang, K. C. Yiak and H. T. Kung (1993). "Seismic vulnerability evaluation of bridges in Memphis and Shelby County, Tennessee". *Earthquake Spectra*, **9(4)**: 803-816.
- Pinto, A. V., editor (1996). "Pseudo-dynamics and shaking tables test on R. C. bridges". European Consortium of Earthquake Shaking Tables, Prenormative Research in Support of Eurocode 8, **5**.
- Pinto, A. V. (1999). "The Kobe earthquake (January 17<sup>th</sup>, 1995). Damage to R/C structures". Semi-rigid Behaviour of Civil Engineering Structural Connections. COST-

- C1 Earthquake Performance of Civil Engineering Structures. Report **ISSN 1018-5593: 21-44**.
- Pinto, A. V., G. Verzeletti, P. Negro and J. Guedes (1995). "Cyclic testing of a squat bridge-pier". European Laboratory for Structural Assessment, ELSA. Report. **EUR 16247 EN**.
- Pinto, A. V., G. Verzeletti, G. Magonette, P. Pegon, P. Negro and J. Guedes (1996). "Pseudo-dynamics testing of large-scale R/C bridges in ELSA". 11<sup>th</sup> World Conference on Earthquake Engineering, CD ROOM, (2046), Acapulco, México.
- Pinto, P. E. and R. Giannini (1997). "An automatic procedure for analytical seismic assessment of the bridges in a highway system". Proceedings of the U.S.-Italian Workshop on Seismic Evaluation and Retrofit. National Center for Earthquake Engineering Research. Technical Report. **NCEER-97-0003: 17-44**. Edited by: D. P. Abrams and G. M. Calvi.
- Powell, G. A. and R. Allahabadi (1988). "Seismic damage prediction by deterministic methods: concepts and procedures". *Earthquake Engineering and Structural Dynamics*, **16(7):719-734**.
- Press, W. H., S. A. Teulosky, W. T. Vetterling and B. P. Flannery (1992). "*Numerical recipes in Fortran 77. The art of scientific computing. Volume I*". Cambridge University Press.
- Priestley, M. J. N.; F. Seible and C. M. Uang (1994). "The Northridge earthquake of January 17, 1994". Structural Systems Research Project, University of California at San Diego. Technical Report **SSRP-94/06**.
- Rahman, S. and M. Grigoriu (1994). "Markov model for local and global damage indices in seismic analysis". National Center for Earthquake Engineering Research. Technical report **NCEER-94-0003**,
- Ren, S. and M. P. Gaus (1996). "GIS Tools for regional bridge seismic risk assessment". Technical Report, Department of Civil Engineering **GIS-2**, State University of New York at Buffalo.
- Rodríguez Gómez, S. and E. DiPasquale (1990). "MUMOID user's guide. A program for the identification of modal parameters". National Center for Earthquake Engineering Research. Technical report **NCEER-90-0026**.
- Rojahn, C., S. A. King, R. E. Scholl, A. S. Kiremidjian, L. D. Reaveley and R. R. Wilson (1997). "Earthquake damage and loss estimation methodology and data for Salt Lake Country, Utah (ATC-36)". *Earthquake Spectra*. Theme Issue: Loss Estimation, **13 (4): 623-642**.
- Sánchez-Sánchez, H (1996). "Ductility demands of isolated reinforced concrete bridge piers placed in Mexico City". 11<sup>th</sup> World Conference on Earthquake Engineering, CD ROOM, (753), Acapulco, México.

- Shadi, N. A., M. Saïidi and D. Sanders (2000). "Seismic response of reinforced concrete bridge pier wall in the weak directions". Multidisciplinary Center on Earthquake Engineering, **MCEER-00-0006**.
- Shinozuka, M. and Y. Sato (1967). "Simulation of nonstationary random processes". *Journal of the Engineering Mechanics Division*, **(93)**:11-40.
- Shinozuka, M., S. E. Chang, R. T. Eguchi, D. P. Abrams, H. H. M. Hwang and A. Rose (1997). "Advances in earthquake loss estimation and application to Memphis, Tennessee". *Earthquake Spectra*. Theme Issue: Loss Estimation, **13 (4)**:739-758.
- Shinozuka, M. (1998). "Development of bridge fragility curves". Proceedings of the U.S.-Italian Workshop on Seismic Evaluation and Retrofit, Multidisciplinary Center for Earthquake Engineering Research. Technical Report **MCEER-98-0015** :249-256.
- Singhal, A. and A. S. Kiremidjian (1997). "A method for earthquake motion-damage relationships with application to reinforced concrete frames". National Center for Earthquake Engineering Research. Technical Report **NCEER-97-0008**.
- Sobol, I. M. (1976). "*Método de Monte Carlo*". Lecciones Populares de Matemáticas, Editorial MIR, Moscú
- STAC. "Análisis estocástico por computadora. Manual de usuario. Versión 1.06" (2001). CIMNE Centro Internacional de Métodos Numéricos en Ingeniería.
- Steinberg, E. P. (1997). "Reliability of structural steel haunch connections to pretressed concrete". *Journal of Structural Engineering*, **123(10)**:1382-1389.
- Tanaka, S., H. Kameda, N. Nojima and S. Ohnishi (2000). "Evaluation of seismic fragility for highway transportation systems". 12<sup>th</sup> World Conference on Earthquake Engineering **(0546)**, Auckland New Zealand.
- Trautner, J. J. and D. M. Frangopol (1991). "Safety sensitivity functions for reinforced concrete beams". *ACI Structural Journal*, **88(5)**:631-640.
- Thomas, A; S. Eshenaur and J. Kulicki (1998). "Methodologies for evaluating the importance of highway bridges". Multidisciplinary Center for Earthquake Engineering Research. Technical Report **MCEER-98-0002**.
- Udoeyo, F. F. and P. I. Ugbem (1995). "Dimensional variations in reinforced concrete members". *Journal of Structural Engineering*, **121(12)**:1865-1867.
- Vaz, C. T. (1994). "Behaviour coefficients and structural reliability of R/C bridges". 10<sup>th</sup> European Conference on Earthquake Engineering, **3**: 1797-1802, Vienna.
- Vaz, C. T. and R. Bairrao (1996). "Quantification of behaviour coefficients for curved RC bridges". 11th World Conference on Earthquake Engineering, CD ROOM, **(1557)**, Acapulco, México.

- Wagaman, S. J., J. L. Wilson and J. W. Fisher (1995). "Fatigue inspection and evaluation of bridges". Proceedings of the 13<sup>th</sup> Structures Congress, pp. 894-902, U.S.A.
- Werner, S. D., C. E. Taylor and J. E. Moore (1997). "Loss estimation due to seismic risks to highway systems". *Earthquake Spectra*. Theme Issue: Loss Estimation, **13 (4)**: 585-604.
- Whitman, R. V., T. Anagnos, C. Kircher, H. J. Lagorio, R. S. Lawson and P. Schneider (1997). "Development of a national earthquake loss estimation methodology". *Earthquake Spectra*. Theme Issue: Loss Estimation, **13 (4)**: 643-662.
- Woo, G. (1997). "The treatment of earthquake portfolio uncertainty: a focus on issues of asset distribution". *Earthquake Spectra*. Theme Issue: Loss Estimation, **13 (4)**: 833-850.
- Xueshen, J. and F. Shuming (1995). "The definition of vulnerability matrixes for transportation systems". Proceeding of the Fifth International Conference on Seismic Zonation, Nice, France, **II** :101-108.
- Yamazaki, F., H. Motomura and T. Hamada (2000). "Damage assessment of expressway networks in Japan based on seismic monitoring". 12<sup>th</sup> World Conference on Earthquake Engineering, (0551), Auckland, New Zealand.
- Yeh, C. H. and Y. K. Wen (1996). "Modelling of nonstationary ground motions and analysis of inelastic structural response". *Structural Safety*. (8):281-298.
- Yépez, F., A. H. Barbat and J. A. Canas (1995). "Riesgo, peligrosidad y vulnerabilidad sísmica de edificios de mampostería". Monografías CIMNE **IS-12**, editor A. H. Barbat, Barcelona, España.
- Yépez-Montoya, F. (1996). "Metodologías para la evaluación de la vulnerabilidad y riesgo sísmico de estructuras aplicando técnicas de simulación". Memoria de la Tesis Doctoral. Escuela Técnica Superior de Ingenieros en Caminos, Canales y Puertos, Universidad Politécnica de Cataluña, Barcelona, España.
- Youd, T. L. and C. J. Beckman (1996). "Highway culvert performance during past earthquakes". National Center for Earthquake Engineering Research. Technical Report **NCEER-96-0015**.
- Youd, T. L. (1998). "Screening guide for rapid assessment of liquefaction hazard at highway bridge sites" Multidisciplinary Centre for Earthquake Engineering Research. Technical Report. **MCEER-98-0005**.





CENTRO INTERNACIONAL DE METODOS NUMERICOS EN INGENIERIA  
**Lista de monografías publicadas en la Serie de Ingeniería Sísmica**

Las monografías pueden adquirirse dirigiéndose al Departamento de Publicaciones del Centro Internacional de Métodos Numéricos en Ingeniería, Edificio C1, Campus Norte UPC, c/ Gran Capitán s/n, 08034 Barcelona, teléfono: 93-401.60.37, Fax: 93-401-65-17.

- IS-1 *Qualitative Reasoning for Earthquake Resistant Buildings*, Luís M. Bozzo, 149 pp., ISBN 84-87867-36-7, 1993.
- IS-2 *Control predictivo en sistemas de protección sísmica de estructuras*, R. Andrade Cascante, J. Rodellar, F. López Almasa, 143 pp., ISBN 84-87867-37-5, 1993.
- IS-3 *Simulación numérica del comportamiento no lineal de presas de hormigón ante acciones sísmicas*, M. Galindo, J. Oliver, M. Cervera, 255 pp., ISBN 84-87867-38-3, 1994.
- IS-4 *Simulación del daño sísmico en edificios de hormigón armado*, A. Hanganu, A.H. Barbat, S. Oller, E. Oñate, 96 pp., ISBN 84-87867-40-5, 1994.
- IS-5 *Edificios con aislamiento de base no lineal*, N. Molinares, A.H. Barbat, 96 pp., ISBN: 84-87867-41-3, 1994.
- IS-6 *Vulnerabilidad sísmica de edificios*, C. Caicedo, A.H. Barbat, J.A. Canas, R. Aguiar, 100 pp., ISBN 84-87867-43-X, 1994.
- IS-7 *Análisis de terremotos históricos por sus efectos*, J. R. Arango Gonzalez, 119 pp., ISBN 84-87867-44-8, 1994.
- IS-8 *Control activo no lineal de edificios con aislamiento de base*, A.H. Barbat, N. Molinares, J. Rodellar, 124 pp., ISBN 84-87867-46-4, 1994.
- IS-9 *Análise estocástica da resposta sísmica nao-linear de estruturas*, A.M. F. Cunha, 199 pp., ISBN: 84-87867-47-2, 1994
- IS-10 *Definición de la acción sísmica*, A.H. Barbat, L. Orosco, J.E. Hurtado, M. Galindo, 122 pp., ISBN: 84-87867-448-0, 1994
- IS-11 *Sismología y peligrosidad sísmica*, J.A. Canas Torres, C. Pujades Beneit, E. Banda Tarradellas, 87 pp., ISBN: 84-87867-49-9, 1994

- IS-12 *Riesgo, peligrosidad y vulnerabilidad sísmica de edificios de mampostería*, F. Yépez, A.H. Barbat, J.A. Canas, 104 pp., ISBN: 84-87867-50-2, 1995
- IS-13 *Estudios de ingeniería sismológica y sísmica*, J.A. Canas, ISBN: 84-87867-57-X, 13 pp., 1995
- IS-14 *Simulación de escenarios de daño para estudios de riesgo sísmico*, F. Yépez, A.H. Barbat y J.A. Canas, ISBN: 84-87867-58-8, 103 pp., 1995
- IS-15 *Diseño sismorresistente de edificios de hormigón armado*, L. Bozzo, A.H. Barbat, ISBN: 84-87867-59-6, 185 pp., 1995
- IS-16 *Modelo tridimensional de atenuación anelástica de las ondas sísmicas en la Península Ibérica*, J.O. Caselles, J. A. Canas, Ll. G. Pujades, R.B. Herrmann, ISBN: 84-87867-60-X, 119 pp., 1995
- IS-17 *Índices de daño sísmico en edificios de hormigón armado*, R. Aguiar ISBN: 84-87867-43-X, 99 pp., 1996
- IS-18 *Experimental study of a reduced scale model seismically base isolated with Rubber-Layer Roller Bearings (RLRB)*, D. Foti, J.M. Kelly ISBN: 84-87867-82-0, 112 pp., 1996
- IS-19 *Modelos de evaluación del comportamiento sísmico no lineal de estructuras de hormigón armado*, F. Yépez Moya ISBN: 84-87867-80-4., 96pp., 1996
- IS-20 *Evaluación probabilista de la vulnerabilidad y riesgo sísmico de estructuras de hormigón armado por medio de simulación*, F. Yépez Moya, A.H. Barbat, J.A. Canas, ISBN: 84-87867-81-2, 1996
- IS-21 *Modelización de la peligrosidad sísmica. Aplicación a Cataluña*, J.A. Canas, J.J. Egozcue, J. Miquel Canet y A.H. Barbat, ISBN: 84-87867-83-9, 101pp., 1996
- IS-22 *Evaluación del daño sísmico global en edificios porticados de hormigón armado*, R. Aguiar, A.H. Barbat and J. Canas, ISBN: 84-87867-96-0, 173pp., 1997
- IS-23 *Daño sísmico global en edificios con muros de cortante*, R. Aguiar, ISBN: 84-89925-00-3, 101 pp., 1997

- IS-24 *Conceptos de cálculo de estructuras en las normativas de diseño sismorresistente*, A.H. Barbat y S. Oller, ISBN: 84-89925-10-0, 107pp., 1997
- IS-25 *Stochastic dynamics of hysteretic structures*, J.E. Hurtado, ISBN: 84-89925-09-7, 205pp., 1998
- IS-26 *Análisis de los acelerogramas de la serie de Adra (Almería). Diciembre 1993 a Enero 1994*, R. Blázquez, A. Suárez, E. Carreño y A.J. Martín, ISBN: 84-89925-11-9, 91pp., 1998
- IS-27 *Respuesta de puentes frente a acciones sísmicas*, E. Maldonado, J.A. Canas, J.R. Casas, L.G. Pujades, ISBN: 84-89925-23-2, 107pp., 1998
- IS-28 *Estudio de parámetros en la vulnerabilidad sísmica de puentes*, E. Maldonado, J.A. Canas y J.R. Casas, ISBN: 84-89925-16-X, 97pp., 1998
- IS-29 *Metodologias para o cálculo sísmico não-linear de barragens de betão*, R. Faria ISBN: 84-89925-25-9, 113pp., 1998
- IS-30 *Acciones para el diseño sísmico de estructuras*, R. Aguiar, ISBN: 84-89925-27-5, 122pp., 1998
- IS-31 *Avaliação do comportamento sísmico de barragens de betão*, R. Faria, ISBN: 84-89925-28-3, 88pp., 1998
- IS-32 *Vulnerabilidad sísmica de hospitales. Fundamentos para ingenieros y arquitectos*, O.D. Cardona, ISBN:84-89925-33-X, 165pp., 1999
- IS-33 *Modelación estocástica de la acción sísmica*, J. E. Hurtado, ISBN:84-8925-34-8, 93pp., 1999
- IS-34 *Earthquake simulator testing of a steel model seismically protected with friction energy dissipators*, D. Foti and J. Canas, ISBN: 84-89925-40-2, 110pp., 1999
- IS-35 *Plasticidad y fractura en estructuras aperticadas*, J. Flórez López, ISBN: 84-89925-46-1, 90pp., 1999
- IS-36 *Estimación de efectos locales con movimientos sísmicos y microtemblores*, V. Giraldo, A. Alfaro, L. G. Pujades, J. A. Canas, ISBN: 84-89925-54-2, 83pp., 1999